ABSTRACT

Title of Dissertation: A STUDY OF GROUND-LEVEL OZONE OVER THE BALTIMORE/WASHINGTON OZONE NONATTAINMENT AREA

Yu-Jin Choi, Doctor of Philosophy, 2004

Dissertation directed by: Associate Professor Sheryl H. Ehrman
Professor Richard V. Calabrese
Department of Chemical Engineering
Professor Russell R. Dickerson
Department of Meteorology

Surface ozone is a persistent problem in U.S.A. and Europe as well as developing countries. A key prerequisite to identifying effective approaches to meeting an ozone air quality standard is to understand the relationship between VOC and NOx, the significance of biogenic emissions, and the contribution of long-range transport.

The Baltimore/Washington area is an EPA-designated severe ozone non-attainment area. In this study, the characteristics of ozone events over this area were investigated to develop a possible control strategy. Both observational and computational modeling approaches were employed, and it was divided into three parts. The first part was to investigate sources of VOC emissions in the Baltimore area using highly time resolved measurements, and to investigate possible relationships between each VOC source category and episodes of elevated ozone concentrations.

The results showed that biogenic emissions contribute significantly to local ozone production in this area. The second part was emissions inventory evaluation, focused on VOC emissions inventory because VOC estimates are commonly assumed to be more uncertain than NOx estimates. The results indicated a possibility of overestimation of solvent VOC emissions. Photochemical simulations with reduction of solvent VOC emissions did not affect ozone prediction, but affected significantly secondary organic aerosol prediction. Lastly, photochemical ozone simulations were performed to find an effective control strategy for this area. The simulation results showed that long-range transport of ozone was responsible for 20-90 ppb of ozone concentration in the state of Maryland, Northern Virginia, and D.C. area, displaying a decreasing contribution as it approached to the Baltimore/Washington area. Local emissions contributed considerably to high ozone occurrences in this area. Moreover, the contribution of biogenic VOC emissions in this region was responsible for much of the local ozone production, which was a consistent result from the part one. Accordingly, the results indicated that NOx emissions reductions would probably mitigate high ozone occurrences in this area, and this was confirmed through several simulations with emissions reductions. However, our results suggested that control of only local NOx emissions might not be sufficient to comply with the 8 hr ozone standard because of the importance of long-range transported ozone.

A STUDY OF GROUND-LEVEL OZONE OVER THE BALTIMORE/WASHINGTON OZONE NONATTAINMENT AREA

by

Yu-Jin Choi

Dissertation submitted to the Faculty of the Graduate School of the
University of Maryland, College Park in partial fulfillment
of the requirements for the degree of
Doctor of Philosophy
2004

Advisory Committee:
Associate Professor Sheryl H. Ehrman, Chair/Advisor
Professor Richard V. Calabrese, Coadvisor
Professor Russell R. Dickerson, Coadvisor
Professor Robert D. Hudson
Assistant Professor Srinivasa R. Raghavan

Acknowledgements

I would like to greatly acknowledge the enthusiastic supervision of my advisors, Professor Sheryl H. Ehrman, Professor Richard V. Calabrese, and Professor Russell R. Dickerson, during this work. This work cannot be completed without their encouragement, invaluable advice, continuous support, and patience through the many years.

I am grateful to Dr. Jeffrey W. Stehr for sharing lots of good ideas, and providing many helpful comments and suggestions. I thank Michael Mitchell for his great efforts to teach me UNIX and SMOKE. Special thanks to all my friends for being the surrogate family during the many years I have stayed here.

I have been supported financially by the Maryland Department of Environment. For this assistance I am very grateful.

Lastly, and most importantly, I wish to thank my family, and especially my parents, for their love, support and absolute confidence in me.

Table of Contents

List of Tables

List of Figures

Chapter 1: Introduction

1.1 Objectives and organization

Human exposure to high concentrations of ozone continues to bother many areas of the United States, despite the implementation of government-mandated emissions control strategies (Roselle et al., 1991). Persistent ozone problems also exist in parts of Western Europe, Mexico, Brazil, and other developing countries (Winner and Cass, 2000).

The task of developing control strategies for ozone is more difficult than controlling primary pollutants emitted directly from emissions sources. In case of the primary pollutants, a reduction in emissions results in an approximately proportional reduction of pollutants. However, ozone, a secondary pollutant, which is formed from primary pollutants and other chemical species in the atmosphere, does not necessarily respond in a proportional manner to reductions in precursor emissions (Finlayson-Pitts and Pitts, 2000).

Key prerequisites to identifying effective approaches to meeting ozone air quality standards at a given area are to understand the relationship between VOC and NOx, the significance of biogenic emissions, and the contribution of long-range transport.

The Baltimore/Washington area is classified as a severe ozone non-attainment area by the U. S. EPA. In this study, the characteristics of ozone events in this area are investigated to develop a possible control strategy leading to ozone reduction. For that reason, both an observation-based approach and an emission-based air quality modeling approach are employed, and the study is divided into three parts (Chapters 3, 4, and 5). Chapter 2 addresses background information about ground-level ozone, air quality models, and observational approaches to the ozone study. In Chapter 3, we investigate sources of VOC emissions in the Baltimore area using highly time resolved measurements, and possible relationships between each VOC source category and episodes of elevated ozone concentrations. In particular, the contribution of biogenic VOC emissions to high ozone occurrences in this area is compared to that of anthropogenic VOC emissions.

Several studies have been performed to predict ozone concentrations over the eastern U.S with coarse grid resolutions (36 km x 36 km, 18.5 km x 18.5 km) using various modeling systems such as Urban Airshed Model with Variable Grid (UAM-V), San Joaquin Valley Air Quality Model (SAQM), Urban and Regional Model (URM), Regional Oxidant Model (ROM) (Sistla et al., 2001; Roselle et al., 1995; Milford et al., 1994; Possiel et al. 1993). Kumar et al. (1996) pointed out that, by using coarse resolution over the whole domain, one could lose detail of the pollutant dynamics that can only be captured by using finer scales. Even though there are several studies focusing on smaller regions in a finer grid (Arunachalam et al., 2001; Smith et al., 2001; Hanna et al., 1996; Kumar et al., 1996), there has been little research into ozone formation with a fine grid resolution for the Baltimore/Washington

ozone non-attainment area. Hence, the next two parts (Chapters 4 and 5) are related to modeling of this area with a fine grid resolution. Chapter 4 describes an emissions inventory evaluation before a further photochemical ozone modeling study is performed, for it has been pointed out that the uncertainty of emissions inventory greatly affects the performance of a photochemical modeling. The focus of the evaluation is placed on the VOC emissions inventory because VOC estimates are commonly assumed to be more uncertain than NOx estimates. Several methods of evaluation of emissions are implemented to come to solid conclusions.

Chapter 5 is a photochemical ozone modeling study to determine an effective control strategy for the Baltimore/Washington ozone non-attainment area. The first simulations are focused on investigating the relative impact of long-range transport of ozone and precursors versus local emissions on high ozone occurrences in the Baltimore/Washington ozone non-attainment area. Russell and Dennis (2000) reported in their work that most studies were first done for urban applications, but more recently studies are progressing to regional scales because of the significance of long distance transport of pollutants including ozone precursors. Also, several studies based on observations stressed a significant role of long-range transport of pollutants on ozone events (Ryan et al., 1998; 2000; Zhang and Rao, 1999). Hence, the relative contribution of transport and local emissions is investigated by controlling boundary conditions obtained from multi-nesting technique. In the second group of simulations, the relative role of anthropogenic VOC emissions versus biogenic VOC emissions in high ozone occurrences is studied. Lastly, several simulations with emissions

reductions are carried out in order to identify a possible ozone control strategy leading toward ozone mitigation for the Baltimore/Washington ozone non-attainment area.

Finally, a summary of results and overall conclusions obtained from this study, and recommendations for future work are presented in Chapter 6.

1.2 Implications and impacts of the study

In this study, using observation-based and emissions-based air quality modeling approaches, we tried to identify and quantify each contribution of long-range transport, local anthropogenic emissions, and local biogenic emissions to ozone occurrences. Here, the issues associated with biogenic and long-range transport contributions to ozone events have been critical subjects of debate. The findings presented in the following chapter suggest that local anthropogenic NOx and biogenic VOC emissions play a significant role in high ozone occurrences over the Baltimore/Washington ozone non-attainment area, while the role of anthropogenic VOC in ozone formation is not as critical. This conclusion about the role of biogenic VOC in high ozone formation was consistent in both observation-based and air quality modeling-based approaches, even though the observation-based approach was limited to a Baltimore observation site. Also, the results suggest that lowering anthropogenic NOx emissions may lead to a decrease in high ozone concentration occurrences over the Baltimore/Washington ozone non-attainment area. However, a considerable contribution of long-range transport was also observed when considering a wider area encompassing the Baltimore/Washington region, hence the need for regulation of

ozone at upwind areas to accompany local reductions in order to meet the 8 hr ozone standard over this study region.

Even though this study was focused on the Baltimore/Washington ozone non-attainment area, the procedure we used in order to identify the characteristics of high ozone events and to develop an optimal control strategy can be applied to other regions.

Chapter 2: Background

2.1 Ground level ozone

The earth's atmosphere is divided into four distinct layers based on the vertical temperature profile: the troposphere, stratosphere, mesosphere, and thermosphere. The tops of these layers are called the tropopause, stratopause, mesopause, and thermopause, respectively. The troposphere is the atmosphere between the earth's surface and 10 to 18 km in altitude, where the temperature normally decreases with increasing altitude. The troposphere accounts for more than 80% of the mass and nearly all of the water vapor, clouds, and precipitation in the earth's atmosphere. The portion of the atmosphere between the tropopause and approximately 50 km altitude is the stratosphere, whose temperature increases with altitude. Beyond the stratosphere are the mesosphere and thermosphere (Wallace and Hobbs, 1977; Jacobson, 2002).

Ozone, a reactive oxidant gas, is found in the lower two layers of the atmosphere. Most of the earth's atmospheric ozone is found in the stratosphere, and stratospheric ozone prevents the sun's harmful ultraviolet rays in the wavelength range of 200-300 nm from reaching the lower atmosphere and the earth's surface. On the other hand, ozone in the troposphere is an air pollutant and a major component of urban smog.

Increased ground level ozone concentrations can negatively affect human health as well as damage forest systems, reduce agricultural yields, and degrade

sensitive materials. Repeated exposures to ozone can make people more susceptible to respiratory infection, result in lung inflammation, and aggravate pre-existing respiratory diseases such as asthma. The U.S. Environmental Protection Agency (EPA) estimates that 5% to 20% of the total U.S. population is especially susceptible to the harmful effects of ozone air pollution. Ozone also affects vegetation and ecosystems, leading to reduced growth and survivability of tree seedlings, and increased plant susceptibility to disease, pests, and other environmental stresses (DNREC Division of Air & Waste Management, 2001; Jacobson, 2002).

Ozone is a secondary air pollutant. It is not emitted directly into the air, but rather formed by the reaction of volatile organic compounds (VOC) and nitrogen oxides (NOx) in the presence of sunlight. Ground level ozone has an atmospheric lifetime of the order of days to weeks, generally longer than its precursors, and then once formed, it can be transported over much wider regions. Moreover, the precursors emitted from elevated sources such as power plant stacks can be also transported great distances, and ozone is often found outside of major urban centers and rural areas (Baumann et al., 2000). Consequently, the ground level ozone problem is not only a concern at urban sites that are the center of emissions, but also rural locations because ozone is wide-ranging as well as persistent.

Anthropogenic emissions of NOx and VOC have decreased over the last decade in Europe and North America (Jonson et al., 2001). Elkins et al. (2000) report that over the past 20 years, ambient ozone levels decreased 20% based on 1-hour average measurements, and 12% based on 8-hour average measurements. According to U.S. EPA emissions estimates, between 1980 and 1999, the emissions of VOC have

decreased 33%, and the emissions of NOx have increased 1%. For the more recent 10-year period (1990-1999), urban sites showed decreases in ozone of approximately 6% and suburban sites showed 4% decreases of ozone. However, rural sites in the eastern United States showed increases in 8-hour ozone levels over the last 10 years (Elkins et al., 2000). Also, many regions in the eastern United States still exceed the 1-hour ozone National Ambient Air Quality Standard (0.12 ppm) (NAAQS) in summer time. In addition, the shift to the 8-hour ozone standard (0.08 ppm; USEPA, 1997) is expected to increase the number of non-attainment areas (Sistla et al., 2001). That is because the 8-hour ozone standard is in most cases stricter than the 1-hour standard, and ozone levels in Mid-Atlantic States exceeding the 8-hour standard are more widespread than the 1-hour standard (Wierman, 2003).

2.2 Ozone chemistry in troposphere

In 1950s, Haagen-Smit and co-workers discovered the key roles of NOx and VOCs in ground-level ozone formation (Haagen-Smit and Fox, 1954). The discovery was observed from a study of production of ozone with NOx and VOCs in the laboratory (NRC, 1991; Jacobson, 2002). Since then, the chemical mechanism of ozone formation has been improved, and well established.

Ozone is present in the natural, unpolluted troposphere. The sources of ozone in the natural troposphere are a downward transport of ozone from the stratosphere, and in-situ photochemical production from reactions of natural organic compounds (e.g., CH_4, CO, and other organic carbons), NOx, and sunlight. These sources of

tropospheric ozone are balanced by in-situ photochemical destruction and by dry deposition at the earth's surface. Ozone mixing ratios at clean remote sites at ground level are in the range of 10 to 40 ppb, and tend to increase with increasing altitude (NRC, 1991; Atkinson, 2000). However, as human activities accompanying emissions of ozone precursors are increased, the balance of destruction and formation of ozone becomes broken, and accordingly the accumulation of ozone takes place.

In the troposphere, the first step in ozone formation is the production of OH radicals by initiation reactions, primarily photolysis of ozone. Water vapor collides with an excited oxygen atom to produce OH radical, which reacts with most trace species in the atmosphere, and leads to cycles of reactions, resulting in the photochemical degradation of organic compounds of anthropogenic and biogenic origin, the enhanced formation of ozone, and the atmospheric formation of acidic compounds (NRC, 1991).

$$O_3 + h\nu \rightarrow O(^1D) + O_2 \ (\lambda < 335 \text{ nm})$$

$$O(^1D) + H_2O \rightarrow 2OH$$

The production of OH radicals through the reactions above is the major process in the lower troposphere where water vapor mixing ratios are high, but in some continental environments, other sources like peroxides, acetone, and formaldehyde may be sources of OH (Seinfeld and Pandis, 1998). The next step in the chemical process of ozone formation occurs through reaction sequences involving VOC, CO and NOx, which

result in the conversion of NO to NO_2 through reactions below. The hydrocarbons and intermediate organics emitted directly are collectively referred to as VOC. The reaction sequences are almost always initiated by the reactions of OH radicals with reactive hydrocarbons (RH) (Sillman, 1999).

$$RH + OH + O_2 + M \rightarrow RO_2 + H_2O + M \quad (1)$$

$$CO + OH + O_2 + M \rightarrow HO_2 + CO_2 + M \quad (2)$$

where M represents a third body such as N_2 or O_2, which removes the energy of the reaction and stabilizes O_3. This is followed by the reaction of RO_2 and HO_2 radicals with NO

$$RO_2 + NO + O_2 \rightarrow RCHO + HO_2 + NO_2 \quad (3)$$

$$HO_2 + NO \rightarrow OH + NO_2 \quad (4)$$

where RCHO represents intermediate organic species, typically carbonyl compounds.

$$NO_2 + h\nu \rightarrow NO + O(^3P) \; (\lambda < 420nm) \quad (5)$$

$$O_2 + O(^3P) + M \rightarrow O_3 + M \quad (6)$$

Apparently, the reaction sequence initiated by RH, equation (1), leads to greater ozone formation per OH radical than the reaction sequence initiated by CO, equation (2), which otherwise dominates in the remote troposphere (Sillman, 1999). That is, the

lifetime of CO against breakdown by reaction (2) in tropospheric air is 28-110 days, and so the rate of ozone production by this sequence is low (Jacobson, 1999). Additionally, methane (CH_4) has been traditionally precluded from the consideration as a precursor to regional O_3 pollution episodes because of its long lifetime (8 to 9 years). Therefore, in case of the urban or regional ozone problem the extent of contribution of CO and CH_4 is small. However, on the global scale, reactions of OH with CO and CH_4 become major source of tropospheric background. Furthermore, recent studies have shown an important role of these pollutants on regional O_3 episodes causing increase of hemispheric background O_3 concentrations (Fiore et al., 2003).

2.3 Organic compounds and oxides of nitrogen

NOx is released into troposphere from a variety of biogenic and anthropogenic sources. It is emitted from the combustion of fossil fuels such as vehicle emissions and fossil-fueled power plants, which leads to emission directly into the planetary boundary layer (PBL), mainly in the form of NO (Jenkin et al., 2000). The four major natural sources of NOx are soil in which nitrification, denitrification, and the decomposition of nitrite contribute to NO production, lightning, natural fires, and the oxidation of NH_3 by photochemical processes in oceans and by some terrestrial plants (Finlayson-Pitts and Pitts, 2000). The natural sources are reported to be 3 to 6% of the total (Trainer et al., 2000). The estimated US and worldwide emissions of NOx are 1 million tons/yr, and 10 million tons/yr, respectively, for natural sources. Also, NOx

emissions from anthropogenic sources for the US and worldwide are estimated to be around 6 million tons/yr, and 40 million tons/yr, correspondingly (Atkinson, 2000).

Organic compounds are also emitted from natural and anthropogenic sources. Vehicles and gasoline-burning engines are large anthropogenic sources of VOC. VOC also comes from consumer products such as paints, insecticides, and cleaners as well as industrial operations, solvent usage, landfills, and waste facilities, petroleum refining, and chemical manufacturing. The estimates of US and worldwide emissions of anthropogenic VOC amount to 20 million tons/yr, and 60-140 million tons/yr, respectively (Atkins, 2000). Additionally, large quantities of VOC are emitted from vegetation. About 98% of the estimated total natural VOC emissions are from vegetation. Other natural emission sources are soil and biomass burning. Many of these species from biogenic sources such as isoprene, and terpenes are extremely photochemically reactive. Hence, it is expected that they exert a strong influence upon photochemical ozone production in regions where their emissions are localized (Trainer et al., 2000; Guenther et al., 2000). Isoprene is emitted typically from deciduous trees, and its emissions are ambient temperature and light dependent. On the other hand, terpenes such as α-pinene and β-pinene, whose emissions vary with ambient temperature, are emitted from conifers (Seinfeld and Pandis, 1998). Literature estimates of US and worldwide emissions of biogenic VOC are 29 million tons/yr, and 1150 million tons/yr, respectively (Atkins, 2000).

2.4 Air quality modeling

The U.S. EPA requires that areas not meeting the ozone NAAQS demonstrate an appropriate planning process showing that adequate steps, such as reductions in anthropogenic emissions of ozone precursors, will be undertaken to reduce the ozone problem (Sistla et al, 2001). Many studies have been conducted to understand the physicochemical characteristics of ozone formation, in order to determine adequate steps for mitigating the ozone problem. These include how pollutants are produced, what kinds of processes are most important, and how pollutant interactions occur. As a tool to perform these studies, air quality modeling has been used. That is, photochemical models can simulate the complex physical and chemical processes associated with the production and removal of ozone.

Air quality models are used mainly for two purposes. The first is for making regulatory or policy decisions. Model simulations are needed to identify the sources of a problem, contributing factors, and methods of controlling or alleviating pollutant emissions, in order to understand the causes of air pollution and alternative means of reducing it. Models are necessary to test the relative effectiveness of different controls and potential effects of the proposed strategies. Typically, an air quality model would be used to simulate a variety of alternative scenarios in a comparative manner to help the regulatory user arrive at recommendations. The second purpose is for improving our understanding of the physicochemical system, how pollutants are produced, what processes are most important, and how pollutant interactions occur. The models help

scientists understand how human and natural activities cause pollution problems in both rural and urban environments (Dennis et al., 1996).

Modern air quality models are actually a system of models or submodels. Each submodel performs a function when needed. A meteorological model, which in and of itself is a collection of models, characterizes the mean and turbulent physical properties of the atmosphere. A dispersion model estimates how a cloud of emissions expands as it moves downwind. A chemistry model simulates chemical transformations. A wet deposition model estimates removal by rainfall, and a dry deposition model estimates removal to the ground and vegetation. Most of the current air quality models are formulated in the Eulerian reference frame. In particular, multidimensional grid-based air quality models with several vertical layers are potentially the most powerful, and involve the least restrictive assumptions, but are also the most computationally intensive (Russell and Dennis, 2000).

First-generation models have first-order chemistry with only a few primary reactions simulated. The transport and dispersion calculations are based upon steady-state approximations in time and space. Second-generation models typically add removal processes, increase the level of sophistication in the parameterizations and chemistry simulations, and allow transport and dispersion to vary as a function of time and space. Third-generation models, called "next-generation" models, consist of select processes coupled together so that interactions and feedbacks can be investigated (Irwin, 2003).

A variety of air quality models have been applied to both urban and regional scales, and they have been improved and updated with the rapid development of

computer systems, and with continued research into the chemistry and meteorology related to air pollution. The Urban Airshed Model-version IV (UAM-IV), California Air Resources Board Grid model (CALGRID), California/Carnegie Institute of Technology model (CIT) and the Gas and Aerosol Transport and Reaction model (GATOR) are examples of urban scale photochemical air quality models. The Regional Acid Deposition Model (RADM), Regional Oxidant Model (ROM), European Air Dispersion Model (EURAD) and the Long Term Ozone Simulation model (LOTOS) are known as regional scale photochemical air quality models. As multiscale/nested models, providing the needed boundary conditions to the smaller model, SARMAP Air Quality Model (SAQM), Multiscale Air Quality Simulation Program (MAQSIP), European Air Dispersion Model (EURAD), Urban Airshed Model-Variable (UAM-V), and Community Multiscale Air Quality model (CMAQ) are used (Russell and Dennis, 2000). They have many things in common, but depending on the formulation of meteorological fields, numerical algorithms, and parameterization schemes used in simulating the ozone formation process, these models could give different results for modeled ozone concentrations that may affect the efficacy of emission control strategies based on model results (Sistla et al., 2001).

As shown in Figure 2.1, air quality modeling is composed of three main parts: chemistry and transport, meteorology, and emissions. The chemistry and transport model (CTM) simulates the chemical reactions that take place among chemical species in the atmosphere, and the movement of these components. To drive this, a meteorology model is needed to predict atmospheric conditions such as the wind fields, humidity, temperature and pressure. An emissions component of the model

should provide the information regarding sources of pollution, derived from inventories of known emissions sources of both manmade and natural origins.

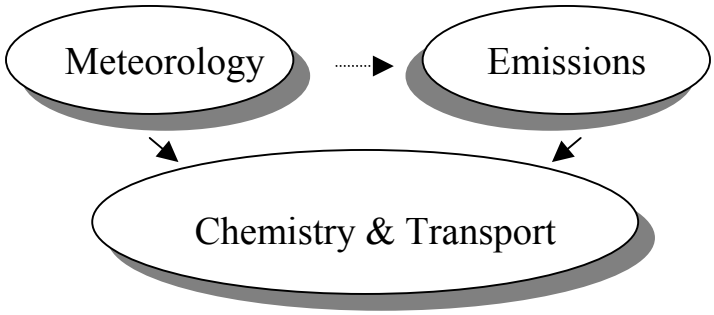

Figure 2.1: Air quality modeling system.

In this study, CMAQ, which has been developed to investigate scientific and regulatory concerns related to acid deposition, tropospheric ozone, and particulate matter over scales ranging from urban to intercontinental by the U.S. EPA, was used to simulate ozone formation on a regional scale (Ching and Byun, 1999). The CMAQ modeling system is composed of the CMAQ Chemical Transport Modeling system (CCTM) as a chemistry and transport model, the Pennsylvania State University-National Center for Atmospheric Research Mesoscale Model Version 5 (MM5) as a meteorology model, the Sparse Matrix Operator Kernel Emissions (SMOKE) as an emission preprocessing model, and interface processors to incorporate the outputs of the meteorology processors and to prepare the requisite information for initial conditions, boundary conditions and photolysis rates for the CCTM. Figure 2.2 illustrates the relationship to show the flow of data through the modeling system.

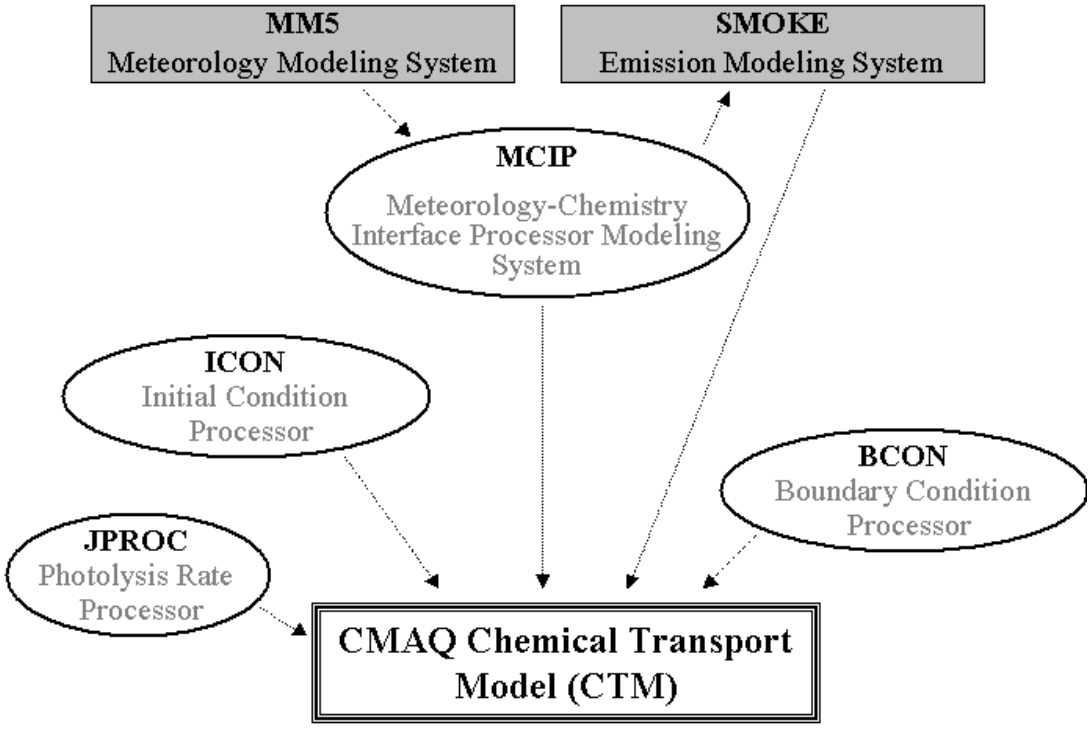

Figure 2.2: CMAQ modeling system. Schematic is based on the CMAQ manual (EPA-III, 1999).

2.4.1 MM5

MM5 has been developed in cooperation with Penn State and the University Corporation for Atmospheric Research (UCAR), and is continuously being improved by contributions from users at several universities and government laboratories. It was evolved from the model used by Anthes and Warner in the early 1970s. The model is a limited-area, nonhydrostatic (or hydrostatic), terrain-following sigma-coordinate model designed to simulate or predict mesoscale and regional-scale atmospheric circulation. In the hydrostatic model, the variables are explicitly predicted. In the

non-hydrostatic model, pressure, temperature and density are defined in terms of a reference state and perturbations from the reference state. MM5 is non-mass conserving in the non-hydrostatic mode (UCAR, 2003; Otte, 1999).

The model is supported by several auxiliary programs, which are referred to collectively as the MM5 modeling system. Terrestrial and isobaric meteorological data are horizontally interpolated from a latitude-longitude grid to a variable high-resolution domain on either a Mercator, Lambert conformal, or polar stereographic projection (programs TERRAIN and REGRID). Since the interpolation does not provide mesoscale detail, the interpolated data may be enhanced with observations from the standard network of surface and rawinsonde stations (program LITTLE_R/RAWINS). A subprogram performs the vertical interpolation from pressure levels to the sigma coordinate system of MM5 (program INTERF). The vertical coordinate is terrain following meaning that the lower grid levels follow the terrain while the upper surface is flat. Intermediate levels progressively flatten as the pressure decreases toward the chosen top pressure (UCAR, 2003).

MM5 is used to calculate the wind speed, which is especially critical for determining transport and residence times of pollutants, and estimates the turbulent diffusion coefficients and dry deposition velocities. Also, it provides temperature, relative humidity, mixing depth, and UV radiation (Seinfeld and Pandis, 1998).

2.4.2 SMOKE

SMOKE (Version 1.4), which employs matrix-vector multiplication for efficient emissions processing, has been developed by the North Carolina Supercomputing Center (NCSC). The main goal of an emission pre-processing model is to convert the source-level emissions (county total emissions) reported on a yearly basis to spatially resolved, hourly emissions, with detailed speciation information. Such conversions consist of multiplying emissions of various sources by several factors in steps called temporalization, speciation, and gridding. These steps are the main components of emissions pre-processing, and they are typically performed separately for point, area, mobile, and biogenic sources. At each step, a processing model uses profile tables and cross-reference tables to convert the emissions from county wide, yearly emissions to hourly emissions with finer spatial resolution. The cross-reference tables assign the profiles to each source (Houyoux et al., 2000). Figure 2.3 shows the SMOKE main programs and data flow.

In the temporalization step (TEMPORAL), SMOKE creates an hourly pollutant emissions inventory by applying the monthly, weekly, and diurnal profiles based on the source characteristics, using the cross-reference table to match the profile to the source type. If there is no temporal profile given in the cross-reference table for a particular source, the user must define a temporal profile for that source. In the speciation step (SPCMAT), it creates a speciation matrix containing conversion factors, used to convert total VOC concentration to the concentrations of specific compounds. In the same manner as in the temporal processing step, if the speciation matrix for a

particular source is not specified in the cross-reference table, the user must define the speciation matrix to be used by that source. In the gridding or spatial allocation step (GRDMAT), SMOKE uses a gridding surrogate to create a matrix containing conversion factors, used to transform county level aggregate emissions to emissions in each grid cell. A gridding surrogate is a dataset developed from geographic information (e.g. population or land use) at a finer spatial gridding resolution than the initial emissions data, and it is used to spatially allocate the emissions to the grid cells.

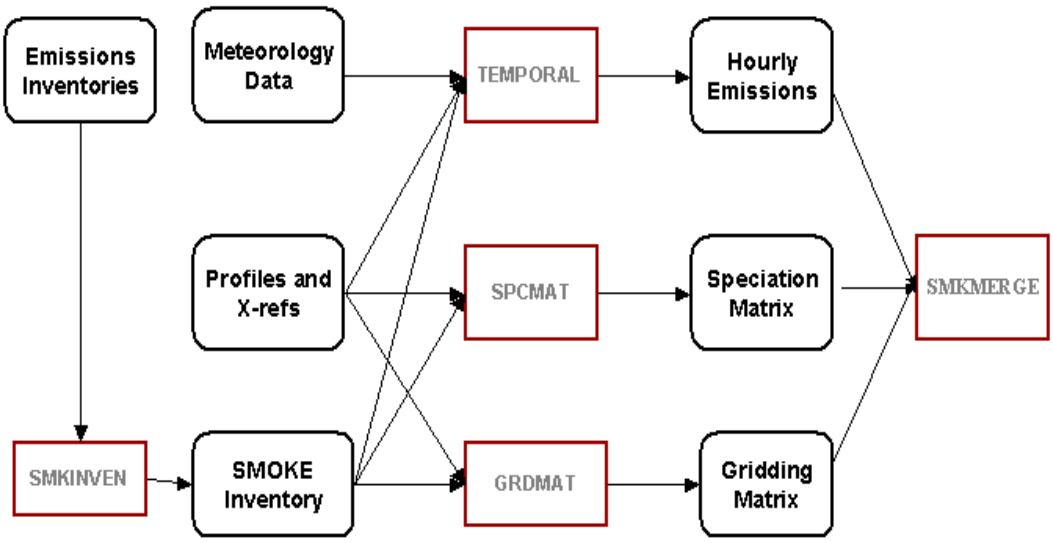

Figure 2.3: SMOKE main programs and dataflow.

The following surrogates are used for SMOKE processing: county area, population, urban, rural, and major highways. Surrogates based on the density of households, agriculture land use and forest type can also be used. After the spatial allocation step, if the spatial gridding surrogate contains zero values for an entire county, the default spatial gridding surrogate will be assigned to that source. The spatial allocation step is then repeated, and if the default spatial gridding surrogate for the source is still zero, this source is dropped from the final inventory.

SMOKE processes each source category slightly differently. For area source emissions, after importing the raw inventory, SMOKE allocates the county-level emissions to each grid cell using spatial surrogate files. Then SMOKE splits inventoried pollutants into model species using speciation profiles that contain the assumed pollutant-to-species factors. Following speciation, SMOKE assigns monthly, weekly, and diurnal temporal profiles to each source. Through these procedures SMOKE generates speciated, gridded, and hourly emissions data.

For mobile sources, SMOKE applies different procedures and requires different supplementary data depending on type of raw inventory: pollutant emissions or daily vehicle miles traveled (VMT). If pollutant emissions data are available, SMOKE processes mobile source data in the same manner as area source information. Otherwise, SMOKE converts VMT data into emissions data using the internal module MOBILE5b. The subsequent steps of speciation, gridding, and temporalization are the same as for area source processing.

SMOKE also applies the speciation and temporal profiles to process point source emissions. The gridding surrogates are not required since point sources contain

the latitude and longitude information that allow the direct allocation of emissions to each grid cell. While SMOKE treats area and mobile source emissions as occurring at the surface (2-D data), it calculates plume rise, which depends on ambient temperature, boundary layer height, pressure, and wind direction and speed. Those meteorological parameters were generated with the MM5 model and reformatted before inputting into SMOKE using the Meteorology-Chemistry Interface Processor (MCIP).

SMOKE determines biogenic source emissions based on emission factors and land-use data reflecting the types and quantities of vegetation represented in each grid cell. Specifically, the Biogenic Emissions Inventory System 2 (BEIS2), contained in SMOKE, converts land-use data into standard emissions by applying emissions factors. SMOKE then conducts the gridding process in the same manner as for area and mobile sources. Biogenic emissions are functions of temperature and solar radiation. SMOKE accounts for this by incorporating meteorological information in the emission estimation. Finally, SMOKE merges area, biogenic, mobile, and point source emissions to generate the three-dimensional total emissions for each grid cell (SMKMERGE) (Tao et al., 2003).

2.4.3 CMAQ CTM (CCTM)

The formation and transport of chemically reacting atmospheric species is described by the mass conservation equation.

$$\frac{\partial C_i}{\partial t} = -\nabla \bullet (\mathbf{u}C_i) + \nabla \bullet (K_e \nabla C) + R_i + E_i - S_i$$

where C is the concentration of the species of interest; **u** is the velocity vector at each grid point within the model domain; K_e is the eddy diffusivity used to parameterize the subscale turbulent fluxes of species; R is the net rate of chemical production; E is the emissions rate; and S represents removal fluxes from processes such as dry deposition and cloud scavenging (Ching and Byun, 1999; Seinfeld and Pandis, 1998; Tao et al., 2003). Generally, K-theory is used to determine the K_e values, which are expressed as a function of atmospheric stability and mixing height following some parameterization (Russell and Dennis, 2000).

The equation is a set of time-dependent, nonlinear, coupled partial differential equations. Several methods have been proposed to solve the full equation. The most popular technique for the solution is the operator splitting technique. The basic idea is to solve independently the pieces of the problem corresponding to the various processes and then couple the various changes resulting from the separate partial calculations, instead of solving the full equation at once. Hence, the chemical transport model solves chemical species equations in the general form

$$\frac{\partial C_i}{\partial t} = \left(\frac{\partial C_i}{\partial t}\right)_{adv} + \left(\frac{\partial C_i}{\partial t}\right)_{diff} + \left(\frac{\partial C_i}{\partial t}\right)_{cloud} + \left(\frac{\partial C_i}{\partial t}\right)_{dry} + \left(\frac{\partial C_i}{\partial t}\right)_{aeros} + E_i + R_i$$

where $(\partial C_i/\partial t)_{adv}$, $(\partial C_i/\partial t)_{diff}$, $(\partial C_i/\partial t)_{cloud}$, $(\partial C_i/\partial t)_{dry}$, and $(\partial C_i/\partial t)_{aeros}$ are the rates of change of C_i due to advection, diffusion, cloud processes (cloud scavenging,

evaporation of cloud droplets, aqueous-phase reactions, wet deposition, etc.), dry deposition, and aerosol processes (transport between gas and aerosol phases, aerosol dynamics, etc), respectively (Seinfeld and Pandis, 1998). As the equation above indicates, the CCTM contains modules representing advection, eddy diffusion, air chemistry, aerosol physics, in-cloud, precipitation processes, and sources and sinks such as dry deposition and emission. Thus, chemical transport models are characterized by the following science process classes (Seinfeld and Pandis, 1998; Ching and Byun, 1999):

HADV : Horizontal advection operator

VADV : vertical advection operator

HDIFF : Horizontal diffusion operator

VDIFF : Vertical diffusions operator

CHEM : Gas-phase chemistry operator

CLOUD : Cloud operator

AERO : Aerosol operator

S : Source and sink operator

If $\mathbf{C}(x,y,z;t)$ is the concentration vector at time t, then its value at the next time step ($t + \Delta t$) will be the net result of the simultaneous applications of all operators

$$\mathbf{C}(x,y,z;t + \Delta t) = \mathbf{C}(x,y,z;t) + [\ HADV(\Delta t) + VADV(\Delta t) + HDIFF(\Delta t) + VDIFF(\Delta t) + CEHM(\Delta t) + CLOUD(\Delta t) + AERO(\Delta t) + S(\Delta t)\ ]\ \mathbf{C}(x,y,z;t)$$

This method greatly shortens solution times and improves numerical accuracy because more accurate and efficient numerical algorithms are used to treat the different processes (Russell and Dennis, 2000). For example, in order to calculate the rate of advection, finite difference, finite element, or finite volume techniques can be employed. As for gas-phase chemistry, the Euler method, Tayler series, or Gear method can be introduced.

One of the major components of a photochemical model is its description of atmospheric chemistry. Interactions in the gas-phase are represented by means of chemical mechanisms, which are a collection of reactions that transform reactants into products, including important intermediates. Since a number of reactions take place in the atmosphere, and the chemistry of even relatively simple organics can be quite complex, it is impossible for a photochemical model to accommodate the complete reactions and species. Hence, chemical mechanisms developed for air quality modeling are highly condensed to substantially reduce the number of organic reactions, and these are parameterized representations of a true chemical mechanism. The manner in which the grouping of organic compounds is carried out typically distinguishes one mechanism from another. There are several chemical mechanisms commonly used: the Carbon Bond IV (CB-IV) mechanism, the Regional Acid Deposition Mechanism 2 (RADM2), and the SAPRC mechanism (Ching and Byun, 1999).

The CB-IV mechanism described by Gery et al. (1989) is a lumped structure type, and the CMAQ implementation of the CB-IV mechanism includes 46 species and 96 reactions, including aerosol and aqueous chemistry. Table 2.1 shows the 46 species

including ten primary organic species emitted directly to the atmosphere, used in the CB-IV mechanism. The ten primary organic species includes three single compounds, ETH (ethene), ISOP (isoprene), and FORM (formaldehyde), and six aggregated compounds, PAR (single carbon bond), OLE (double carbon bond), TOL (seven carbon aromatics), XYL (eight carbon aromatics), ALD2 (higher molecular weight aldehydes), TERP (terpenes), and NR (non-reactive carbon atom) (Ching and Byun, 1999).

The RADM2 mechanism described by Stockwell (1990) is a lumped species type that uses a reactivity-weighting scheme to adjust for lumping. It contains 65 modeling species and 161 reactions. In the RADM2, the primary organics are represented by 15 mechanism species with five single compounds, methane, ethane, ethen, isoprene, and formaldehyde, and ten aggregated compounds based on their reactivity with the hydroxyl radical (OH) and their molecular weights (Ching and Byun, 1999).

The latest version of the SAPRC mechanism designated as the SAPRC99 (Carter, 2000) represents a complete update of the SAPRC90 mechanism. The mechanism has assignments for 400 types of VOCs, and can be used to estimate reactivities for 550 VOC categories. A total of 24 model species are used to represent the reactive organic product species. The SAPRC99 mechanism used in the CMAQ consists of 72 species in 198 reactions (Jimenez et al., 2003).

The CB-IV mechanism is widely used in research and regulatory air quality models, and it is the mechanism used in this study.

Table 2.1: CB-IV mechanism species list

	Symbol	Description
Nitrogen Species	NO	Nitric oxide
	NO2	Nitrogen dioxide
	HONO	Nitrous acid
	NO3	Nitrogen trioxide
	N2O5	Nitrogen pentoxide
	HNO3	Nitric acid
	PNA	Peroxynitric acid
Oxidants	O3	Ozone
	H2O2	Hydrogen peroxide
Sulfur species	SO2	Sulfur dioxide
	SULF	Sulfuric acid
Atomic species	O	Oxygen atom (triple)
	O1D	Oxygen atom (singlet)
Odd hydrogen species	OH	Hydroxyl radical
	HO2	Hydroperoxy radical
Carbon oxides	CO	Carbon monoxide
Hydrocarbons	PAR	Paraffin carbon bond (C-C)
	ETH	Ethene (CH_2=CH_2)
	OLE	Olefine carbon bond (C=C)
	TOL	7 carbon aromatics
	XYL	8 carbon aromatics
	ISOP	Isoprene
Carbonyls and phenols	FORM	Formaldehyde
	ALD2	Acetaldehyde and higher aldehydes
	MGLY	Methyl glyoxal ($CH_3C(O)C(O)H$)
	CRES	Cresol and higher molecular weight phenol
Organic nitrogen	PAN	Peroxyacyl nitrate ($CH_3C(O)OONO_2$)
	NTR	Organic nitrate
Organic radicals	C2O3	Peroxyacyl radical ($CH_3C(O)OO\cdot$)
	ROR	Secondary organic oxy radical
	CRO	Methylphenoxy radical
Operators	XO2	NO-to-NO2 operation
	XO2N	NO-to-nitrate operation
Products of organics	TO2	Toluene-hydroxyl radical adduct
	OPEN	High molecular weight aromatic oxidation ring fragment
	ISPD	Products of isoprene reactions

Table 2.1 (continued)

	Symbol	Description
Species for aerosol	SULAER	Counter species for H_2SO_4 production
	TOLAER	Counter species for toluene reaction
	XYLAER	Counter species for xylene reaction
	CSLAER	Counter species for cresol reaction
	TERPA	Counter species for terpene reaction
	TERP	Monoterpenes
Species for aqueous chemistry	FACD	Formic acid
	AACD	Acetic and higher acids
	PACD	Peroxy acetic acid
	UMHP	Upper limit of methylhydroperoxide

2.4.4 CMAQ Interface Processors

The CMAQ modeling system includes several interface processors to incorporate the outputs of the meteorology processor and to prepare the required information for initial and boundary conditions and photolysis rates to the CCTM. Since most meteorological models including MM5 are not built for air quality modeling purposes, the outputs cannot be implemented directly to air quality models. The MCIP program translates and processes model output from the MM5 model for the CCTM and the SMOKE processor. The MCIP handles data format transformation, conversions of units of parameters, extraction of data for appropriate window domains, collapsing of metrological profile data if coarse vertical resolution data are required, computation of clouds parameters, surface and PBL parameters, and species-specific dry deposition velocities. The programs Initial Condition (ICON) and Boundary Condition (BCON) provide the concentration fields for individual chemical species for the beginning of a simulation and for the grids surrounding the modeling domain,

respectively. The photolysis processor (JPROC) creates look-up table of clear-sky photolysis rates depending on the chemical scheme, latitude, altitude, and hour angles. Then, a module in CCTM interpolates and adjusts the photolysis rates for each grid cell location and modeling time considering the presence of clouds. For example, the below cloud photolysis rate will be lower than the clear-sky value due to the reduced transmission of radiation through cloud. The above cloud values will be enhanced, and within cloud photolysis rates will be interpolated from the below cloud values and above cloud values (Ching and Byun, 1999).

2.5 Observation-based approaches to understanding the ozone problem

Emission-based approaches such as CMAQ air quality models, which use emissions inventories and a numerical representation for transport and photochemistry, play a central role in determining relationship between ozone precursors and the production and accumulation of ozone within a given area, and in developing a strategy for ozone abatement within the area. However, there can be significant uncertainties in the many aspects of emission-based models associated with emissions inventories, meteorological fields and parameterization (Cardelino and Chameides, 1995, 2000). For this reason, observation-based approaches have been developed to provide complimentary method for assessing ozone precursor relationships. Since they are based on observations, inaccurate and incomplete observations can result in misleading conclusions as well. Also, they are a diagnostic rather than prognostic and cannot be used in predicting ozone to determine the exact amount of precursor

reduction needed to bring an area into attainment. Hence, the observation-based approaches should be viewed as a complement to more sophisticated gridded, emission-based models (Cardelino and Chameides, 1995; 2000).

Observation-based methods can be divided into two broad categories: methods based on ambient VOC, NOx and CO; and methods based on secondary reaction products, usually involving reactive nitrogen and peroxides (Sillman, 1999). Chameides et al. (1992) and Rappengluck et al. (1998) used reactivity-weighted ambient VOC/NOx ratios to obtain information about NOx-VOC sensitivity to ozone occurrences for area of interest. Some examples for the latter case are O_3/NOy (NOy = NOx + PAN + HNO_3 + N_2O_5 + other nitrates), O_3/NOz (NOz = NOy – NOx), H_2O_2/HNO_3, etc (Sillman, 1999). That is, ambient measurements of those ratios can be used to interpret NOx-VOC sensitivity.

In this study, we attempted to interpret characteristics of high ozone occurrences over an area of interest, using ambient VOC and NOx measurements and implementing a receptor model. The results obtained from the observation-based approach were compared with that of emissions-based air quality model to corroborate our conclusions. Here, receptor models are focused on elucidating sources and source contributions to pollution in the ambient environment from analysis of measurements at the point of impact (Hopke, 1991). Receptor models have been applied to air quality data, providing useful insight into sources of gaseous hydrocarbons and speciated aerosols since the late 1960's (Thurston and Spengler, 1985; Miller et al., 1972; Billford and Meeker, 1967). The details about the receptor model implemented in this study are described in Chapter 3.

Chapter 3: Investigation of Sources of Volatile Organic Carbon in the Baltimore Area Using Highly Time Resolved Measurements

3.1 Introduction

Since nitrogen oxides (NOx) and volatile organic compounds (VOCs) were uncovered as key precursors of ground level ozone formation by Haagen-Smit, and co-worker in the1950s (Haagen-Smit and Fox, 1954), many studies have been focused on determining effective strategies for ozone reduction. The complex relationship between ozone and its precursors, and the strong dependence of ozone formation on meteorological conditions are the major difficulties associated with the study of ground-level ozone. Though meteorological conditions and transport are important variables for ozone formation and accumulation, anthropogenic VOC and NOx emissions are the primary focus of ozone reduction programs in that only they are controllable.

Most NOx emissions are from combustion related sources such as motor vehicles and fossil-fueled power plants in urban and suburban areas. On the other hand, VOCs are emitted from wide variety of sources, both anthropogenic and biogenic. In the United States, it is estimated that the amount of VOC emissions from biogenic sources is of the same order of magnitude as the total emissions of anthropogenic VOCs (Watson et al., 2001; Atkinson, 2000; Trainer et al., 2000).

Guenther et al. (2000) concluded that over 98% of total biogenic VOCs in North America are from vegetation. Biogenic VOCs are composed primarily of isoprene (35%), terpenoid compounds (25%) and non-terpenoid compounds (40%).

Lagrangian and Eulerian models have been used extensively to predict the change of ozone to controls of NOx and VOC. Several modeling studies have shown that, in general, VOC controls may be effective in reducing the ozone levels in urban and suburban areas, which are most strongly impacted by anthropogenic emissions (Hanna et al., 1996; Possiel and Cox, 1993; McKeen et al., 1991). In addition, a simple rule, based on a modeling study, that morning VOC (ppbC) /NOx (ppb) ratios less than 10 indicate VOC-sensitive peak ozone, and morning VOC/NOx ratios more than 20 indicate NOx-sensitive peak ozone has been used to justify NOx-VOC sensitivity prediction and policies (Sillman, 1999). Therefore, a reduction of VOC emissions in VOC-sensitive regions may be effective in reducing ozone, while a reduction of NOx emissions in NOx-sensitive regions may lead to ozone reduction. However, the emissions from biogenic sources have been reported to be most likely underestimated in past modeling studies, and several analyses of observed measurements have suggested a significant role of biogenic hydrocarbon emissions in many urban and suburban locations in ozone formation (Chameides et al., 1992, 1988; Cardelino and Chameides, 2000, 1995). Thus, it cannot easily be determined whether reducing VOC emissions or NOx emissions or both is the most effective strategy for ozone reduction for a given area, using a simple rule based on modeling studies conducted for only a few specific areas (Sillman, 1999).

The development of an effective ozone reduction strategy in a given urban or suburban area requires an accurate understanding of three key ozone precursor relationships: the relative concentrations of NOx and VOC in the area, the importance of natural VOC relative to anthropogenic VOC in the atmosphere (Piety et al., 2003, Trainer et al. 2000, Cardelino and Chameides, 1995), and the significance of long range transport as compared to local emissions of ozone precursors. While the importance of long range transport versus local emissions can only be resolved using photochemical and meteorological modeling, source apportionment of VOC can be expected to give insight into the importance of natural VOC relative to anthrogenic VOC in the atmosphere for a given area.

In this work, hourly ambient surface measurements of the concentrations of 55 VOC species, taken from a Photochemical Assessment Monitoring Stations (PAMS) site in Baltimore County in the state of Maryland during the summer months of 1996 ~ 1999, are used to investigate the relationships between ozone and its natural and anthropogenic precursors. To identify and apportion VOC sources, the UNMIX receptor model is used. Specific focus is placed on analysis of the observed diurnal variation in concentrations as well as source contributions. These phenomena have been investigated for VOC in other geographical regions, for example, Seoul, Korea (Na et al., 2003) and the Paso del Norte region of the Texas – Mexico border (Fujita, 2001). VOC emissions can vary greatly from region to region, and in contrast to the above-mentioned regions, biogenic emissions at the location under study here are significant. With the receptor modeling results, a study of the contribution of the identified source categories to episodes of high ozone concentrations is conducted.

The results of this study will be useful in the development of effective ozone control strategies in this and similar regions.

3.2 VOC source identification and apportionment using a receptor model

3.2.1 Receptor models

There are several different approaches to receptor model analysis that have been successfully applied including the chemical mass balance (CMB) and multivariate receptor models.

CMB models require that the compositions of emissions from all the contributing source types be known. That is, the source profile (the mass fraction of a chemical in the emissions from each source type) must be known before the analysis. Several libraries of VOC source profiles have been assembled from original measurements at sources and a combination of published and unpublished laboratory test results. Even though CMB is widely accepted, the need for accurate profiles is a limitation associated with its usage; available profiles represent older technology and fuels that may be different today, and some of profiles may be regionally specific. An alternative is the use of multivariate receptor models, which do not require *a priori* knowledge of detailed source profiles, requiring only ambient measurement data and known source tracers to interpret the factors (Kavouras et al., 2001; Kumar et al., 2001; Dillon and Goldstein, 1984).

Several multivariate receptor models have been applied to air pollution studies including absolute principal component analysis (PCA), target transformation factor

analysis, and factor analysis followed by multiple linear regression (Hopke, 1991). However, interpreting results from traditional factor analysis is problematic. Use of traditional factor analysis can produce many different solutions, which are statistically sound, but which may be physically invalid (Poirot et al., 2001; Henry, 2001). There have been some improvements in multivariate receptor models such as positive matrix factorization (PMF) and UNMIX. These models have recently been introduced to air pollution source apportionment and their utility for this purpose has been evaluated (Miller et al., 2002; Chen et al., 2002; Larson et al., 2002;Wu and Pratt, 2002; Poirot et al., 2001).

In this study, the UNMIX version 2.4 receptor model developed by Henry (2001) was used to determine possible sources and source contributions to ambient concentrations of VOC. The UNMIX process starts with the normalization of data to a mean of one by dividing each measurement for a given species by the mean of all measurements of that species, in order to put all measurements on the same scale. In UNMIX, unlike other factor analysis routines, a centering about the mean, or z-score transformation, is not done because there is no appropriate method to un-center the results. The normalized data is analyzed in order to reduce the dimensionality, or the number of sources, of the data space using the singular value decomposition (SVD) matrix operation. The SVD operation produces an abstract mathematical solution. Factor analysis routines such as PCA typically use either a transformation method such as an orthogonal transformation that keeps the statistical independence of the factors, or an oblique transformation that allows the factors to be co-dependent, in order to derive meaningful factors (Hopke, 1991), but those solutions may still contain many

negative loadings and lead to negative concentrations. In contrast, UNMIX incorporates user specified non-negativity constraints and edge finding algorithms in order to derive a single, physically reasonable solution from the abstract mathematical solution (Wu and Pratt, 2002; Poirot et al., 2001; Henry, 2001, 2002). Further details regarding the model can be found in Henry (2001, 2002). The final outputs of the UNMIX model are the estimates of the number of sources, the source composition, the average source contribution, and source contribution to each sample.

3.2.2 Ambient monitoring measurements

In accordance with the 1990 Clean Air Act Amendments, the U.S. EPA initiated the Photochemical Assessment Monitoring Stations (PAMS) program for 1hr ozone nonattainment areas with persistently high ozone levels (mostly large metropolitan areas). The objective of the PAMS program is to develop a large database of ambient air measurements for important pollutants associated with ozone, which will be used to test complicated photochemical air quality models (Lewis et al., 1998).

The U.S. EPA has determined that the network should consist of five different site types to provide information sufficient to satisfy important monitoring objectives. Type 1 sites are located in the predominant morning upwind direction, with the purpose of characterizing upwind background and transported ozone and its precursor concentrations entering the area. Type 2 sites are located immediately downwind of areas with significant ozone precursor emissions. Type 2A sites may be required

depending on the size of the area, and are placed in the downwind area of the second-most predominant morning wind direction. Type 3 sites are located 10 to 30 miles from the boundary of the urban area. These sites are intended to monitor maximum ozone concentrations occurring downwind from the area of maximum precursor emissions. Type 4 sites are used for extreme downwind monitoring of transported ozone and for measurements of its precursor concentrations exiting the area (Demerjian, 2000).

The sampling frequency varies among regions, states, and sites. Of the five PAMS sites located in the state of Maryland, only the Essex site, located in a parking lot northeast of downtown Baltimore as shown in Figure 3.1, belongs in the Type 2 site category. The samples are collected and analyzed hourly using an on site gas chromatograph equipped with a flame ionization detector. See EPA-I (1998) for further details about the analysis method.

The Essex site is surrounded by residential and commercial areas with several gas station facilities within 500 m of this site, and several industrial point sources distributed around this site within a few kms.

The concentrations of 55 hydrocarbons, total nonmethane organic carbon species (TNMOC), ozone, oxides of nitrogen, as well as meteorological conditions such as temperature, wind direction, wind speed, and radiation are monitored at the Essex site. Using these continuous hourly measurements gathered by Maryland Department of Environment (MDE) personnel, we investigated source and receptor relationships of VOCs during the summer months of 1996, 1997, 1998 (June to September), and 1999 (June to July). The summary is shown in Table 3.1.

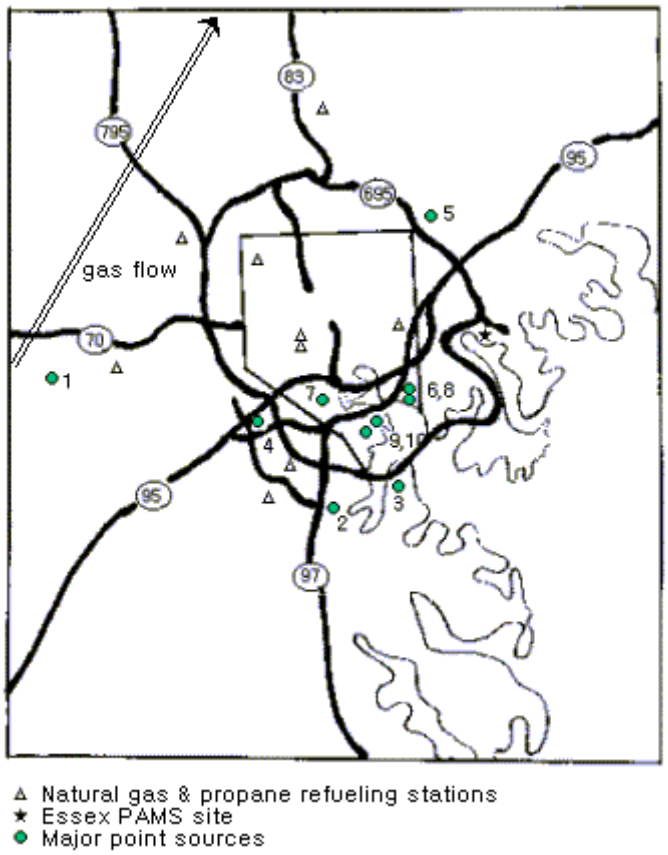

	Description of major point sources	VOC (tons/yr)
1	Natural gas transmission	228
2	Commercial printing	330
3	Electric services	104
4	Food manufacture (distilled & blended liquors)	186
5	Food manufacture (bread)	172
6	Food manufacture	249
7	Paint manufacture	237
8	Automobile surface coating operations	816
9	Petroleum bulk stations and terminals	123
10	Prepared feeds	172

Figure 3.1: Map of region surrounding the PAMS measurement site, Essex, MD (Point sources information based on the1996 EPA National emission trends database).

Table 3.1: Summary of measurement data used in the study

Year	1996	1997	1998	1999
Period of measurement	June 6 to September 30	June 6 to September 30	June 4 to September 14	June 1to July 31
Number of measurements	2683	2833	2206	1284

3.2.3 Methods

Figure 3.2 shows the box plots for several compounds selected to provide a representative summary of the variation in the observed concentrations. For comparison purposes, concentrations or mixing ratios are reported in units of ppb on a carbon basis. The black line across the box denotes the mean, and the median is shown as a gray line across the box. The lower and upper boundaries of box are defined as the 25^{th} percentile and the 75^{th} percentile, respectively. The bottom and top lines extending from box denote the 10^{th} and 90^{th} percentiles, respectively. Isoprene, which is expected to be a marker of biogenic emissions, shows much larger variation during daytime than during nighttime, while the other species show the reverse behavior.

Source apportionment of hydrocarbons was conducted using measurement data from all four years. 37 chemical species were selected from the 55 measured species based upon several considerations; either they made up the majority of the TNMOC mass emissions (Hopke, 1991), their lifetimes were greater than that of toluene (Fujita,

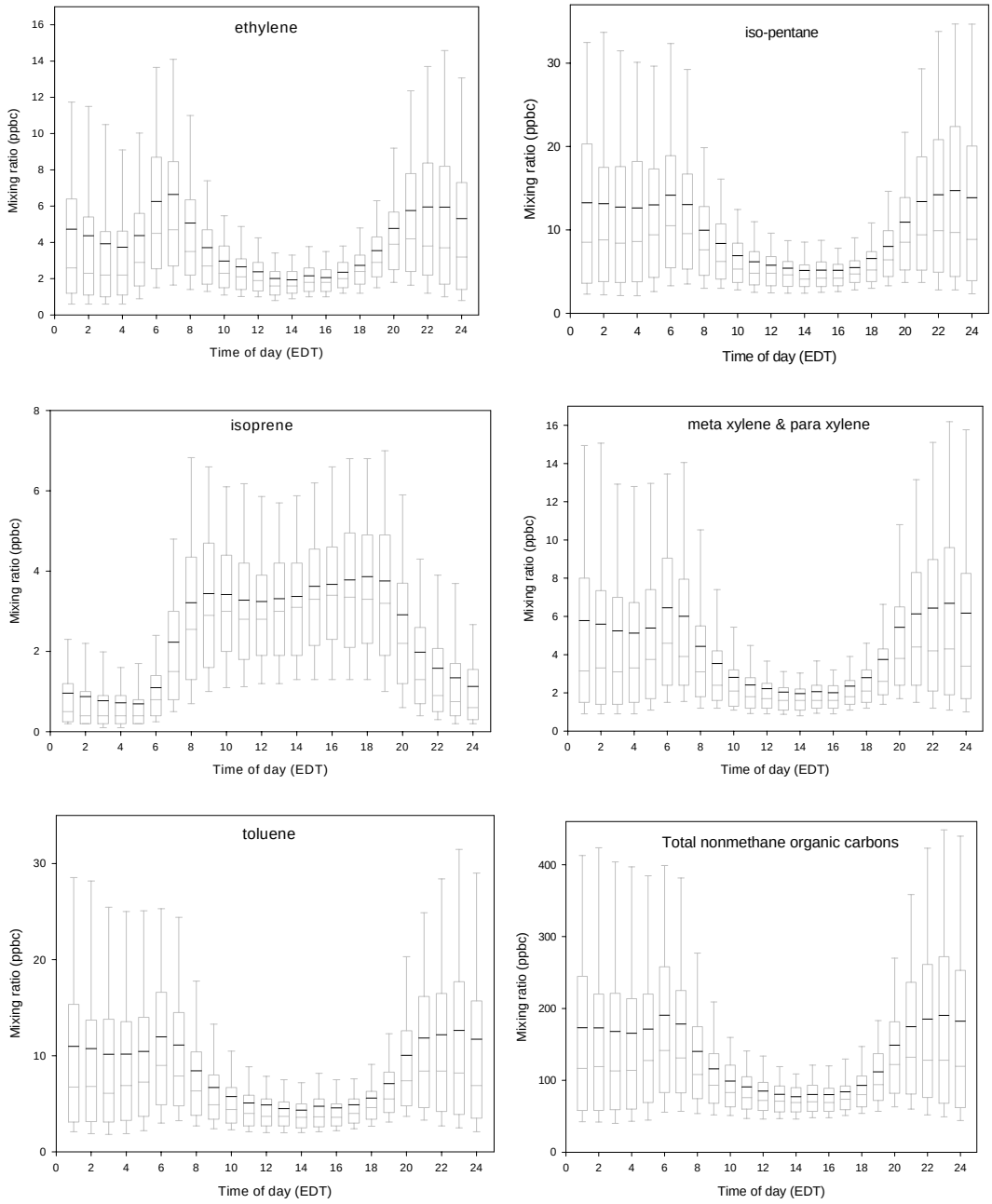

Figure 3.2: Box plots of selected species to show distribution of observed concentrations by hour of day. The black line across the box denotes the mean value, and the gray line across the box denotes the median value. The lower and upper boundaries of box are defined as the 25th percentile and the 75th percentile, respectively. The bottom and top lines extending from box denote the 10th and 90th percentiles, respectively. The EDT represents eastern daylight time.

2001), or these species have been used as tracer species in previous studies. The number of species was reduced using the UNMIX overnight option, in which multiple numbers of possible combinations of input variables are tried with the goals of maximizing the number of input variables and of generating physically reasonable and interpretable results (Poirot et al., 2001). After this optimization, 23 species and 8975 observations were employed by UNMIX to identify sources of total hydrocarbons. The 23 species are given in Table 3.2.

To investigate yearly trends of hydrocarbon sources, we applied the UNMIX model to each year of 1996, 1997 and 1998. The year 1999 was not used to investigate yearly trends because only June and July measurements were available. 25 species and 2673 observations for 1996, 25 species and 2812 observations for 1997, and 25 species and 2203 observations for 1998 were employed by UNMIX. Refer to Appendix 2.

3.2.4 UNMIX receptor model results

Six possible source categories of hydrocarbons for the 1996-1999 combined set of measurements were identified using the UNMIX receptor model. Table 3.2 gives the mean contributions and compositions of each source category, and their one-sigma errors as estimated by the so-called 'bootstrap method' (Henry, 2001). Isoprene is predominantly associated with the first source category, suggesting the source is biogenic in origin. The mass fraction of iso-pentane in this source is a little over 0.05, with ethane and toluene showing mass fractions just under 0.05. Considering that

Table 3.2: Source compositions (mass fraction) and apportionment results for the combined set, 1996~1999, of measurements

Estimated source category	Source 1 biogenic	Source 2 liquid gasoline	Source 3 Surface coatings	Source 4 natural gas	Source 5 vehicle exhaust	Source 6 Gasoline vapor
Species						
Ethane	0.038 ± 0.003	0.038 ± 0.005	0.009 ± 0.007	**0.270** ± 0.061	**0.056** ± 0.002	0.037 ± 0.005
Ethylene	0.015 ± 0.001	0.023 ± 0.002	0.018 ± 0.002	0.010 ± 0.005	**0.059** ± 0.001	0.022 ± 0.001
Propane	0.030 ± 0.004	**0.057** ± 0.005	0.018 ± 0.003	**0.259** ± 0.074	0.048 ± 0.003	-0.002 ± 0.004
Propylene	0.010 ± 0.001	0.013 ± 0.001	0.009 ± 0.001	0.014 ± 0.002	0.029 ± 0.001	0.008 ± 0.001
Acetylene	0.010 ± 0.001	0.005 ± 0.002	0.003 ± 0.002	0.015 ± 0.003	0.038 ± 0.001	0.008 ± 0.001
n-butane	0.029 ± 0.001	0.018 ± 0.002	0.020 ± 0.003	**0.079** ± 0.018	0.024 ± 0.001	0.025 ± 0.003
iso-butane	0.009 ± 0.001	0.014 ± 0.001	0.009 ± 0.001	**0.055** ± 0.011	0.019 ± 0.001	0.013 ± 0.001
n-pentane	0.017 ± 0.001	**0.220** ± 0.018	0.011 ± 0.001	0.022 ± 0.002	0.024 ± 0.001	0.023 ± 0.001
iso-pentane	**0.056** ± 0.004	**0.071** ± 0.003	0.042 ± 0.005	**0.071** ± 0.010	**0.070** ± 0.002	**0.107** ± 0.004
3-methylpentane	0.008 ± 0.001	0.017 ± 0.001	0.008 ± 0.001	0.006 ± 0.004	0.016 ± 0.000	0.023 ± 0.001
n-hexane	0.008 ± 0.002	0.018 ± 0.001	0.013 ± 0.001	0.003 ± 0.007	0.018 ± 0.001	0.030 ± 0.001
Isoprene	**0.153** ± 0.012	0.003 ± 0.000	0.000 ± 0.000	-0.002 ± 0.001	0.004 ± 0.000	0.002 ± 0.000
3-methylhexane	0.008 ± 0.001	0.010 ± 0.001	0.011 ± 0.001	-0.002 ± 0.005	0.011 ± 0.000	0.018 ± 0.001
2,2,4-trimethylpentane	0.010 ± 0.002	0.016 ± 0.001	0.011 ± 0.002	-0.011 ± 0.011	0.024 ± 0.001	0.037 ± 0.002
2,3,4-trimethylpentane	0.003 ± 0.001	0.007 ± 0.000	0.005 ± 0.001	-0.005 ± 0.005	0.010 ± 0.000	0.015 ± 0.001
2-methylhexane	0.005 ± 0.001	0.008 ± 0.000	0.009 ± 0.001	-0.003 ± 0.005	0.009 ± 0.000	0.016 ± 0.001
2,3-dimethylbutane	0.008 ± 0.000	0.007 ± 0.000	0.002 ± 0.001	0.006 ± 0.001	0.010 ± 0.000	0.013 ± 0.000
2-methylpentane	0.013 ± 0.002	0.023 ± 0.001	0.010 ± 0.002	0.012 ± 0.006	0.027 ± 0.001	0.036 ± 0.001
M&p xylene	0.010 ± 0.002	0.025 ± 0.002	**0.117** ± 0.013	0.007 ± 0.007	0.028 ± 0.001	0.025 ± 0.001
Benzene	0.012 ± 0.001	0.014 ± 0.001	0.012 ± 0.001	0.009 ± 0.003	0.028 ± 0.001	0.018 ± 0.001
Toluene	0.042 ± 0.004	**0.052** ± 0.003	**0.084** ± 0.007	0.018 ± 0.018	**0.065** ± 0.002	**0.086** ± 0.003
Ethylbenzene	0.007 ± 0.000	0.007 ± 0.001	0.034 ± 0.004	0.003 ± 0.002	0.008 ± 0.000	0.008 ± 0.000
o-xylene	0.006 ± 0.001	0.010 ± 0.001	0.035 ± 0.003	0.001 ± 0.003	0.011 ± 0.000	0.011 ± 0.000
Total NMOC(ppbc)	14.4 ± 0.8	11.5 ± 0.9	15.9 ± 2.1	17.0 ± 3.1	39.0 ± 1.7	35.5 ± 2.6
% of total NMOC	11	9	12	13	29	26

Bold values indicate mass fractions > 0.05. The errors are based on one sigma.

isoprene is likely underestimated because of its high reactivity, the mass fraction of isoprene in reality may be much higher. Therefore, the relative importance of the other compounds would be reduced. However, it should be noted that some studies report that alkanes are emitted from vegetation, and that aromatics are emitted from microbial decomposition of leaves litter (Guenther et al., 2000; Isidorov et al., 2002). Moreover, as shown in Figure 3.3, Source 1 follows very different diurnal patterns from the other sources. During nighttime when photosynthesis ceases, the concentration of Source 1 falls to a much lower value, and a rapid increase in concentration is observed with sunrise. This pattern is typical of isoprene, the principal biogenic VOC (Trainer et al., 2000). Thus, this source category is identified as biogenic in origin. Even though highly reactive species are not typically included to perform source apportionment, isoprene is included as a modeling species because it is a marker of biogenic emissions and a major precursor to ozone. Hence, the source contribution estimate is likely to be low compared to actual biogenic contributions, as noted by other researchers (Fujita, 2001; Lawrimore and Aneja, 1997; Fujita et al., 1995).

According to several previously reported source profiles, sources related to gasoline such as vehicle exhaust, liquid gasoline and gasoline vapor show high loadings of iso-pentane, n-pentane and toluene (Lawrimore and Aneja, 1997; Fujita et al., 1994). Here, the gasoline vapor category stands for headspace emissions from service stations and bulk terminals, and some evaporative emissions from vehicles such as diurnal emissions, and resting loss, characterized by an enrichment of high

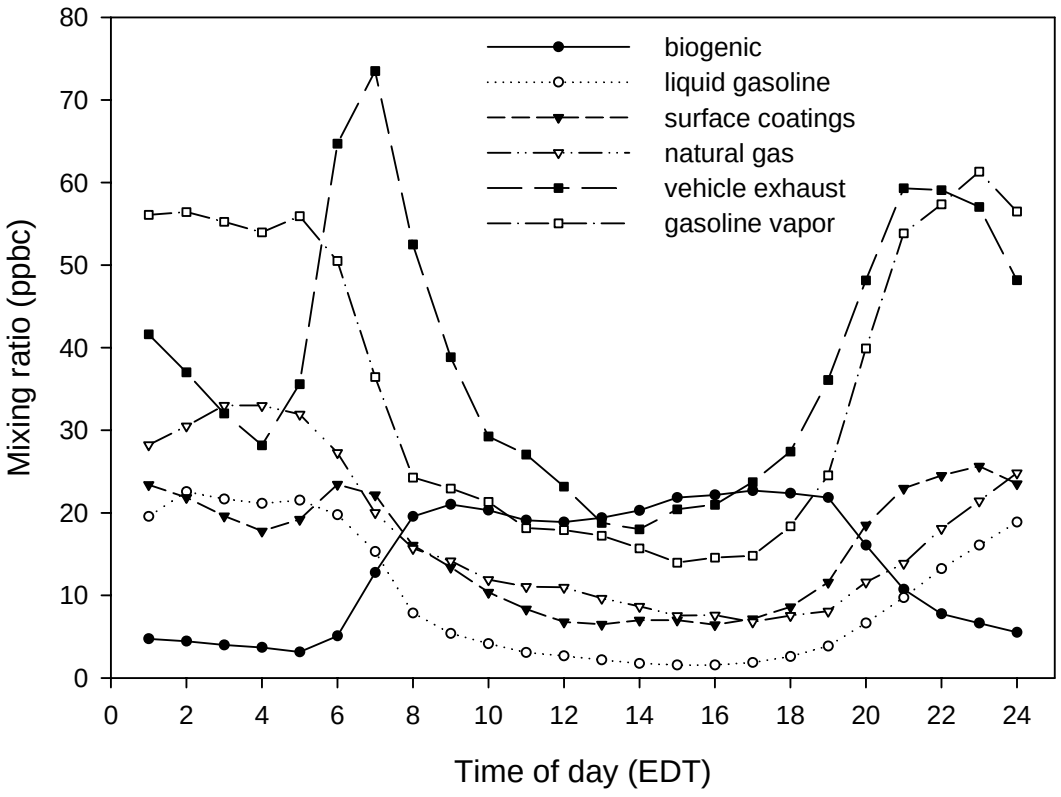

Figure 3.3: Average diurnal patterns of each source type of VOC, estimated from hourly source apportionment using summer measurements taken over four years from 1996 to 1999.

volatility species. The liquid gasoline category represents whole gasoline emissions having a composition resembling liquid gasoline itself, which can arise from spillage, leakage, and vehicle operations such as running loss and hot soak (Scheff et al., 1996). Hence, the origins of Source 2, Source 5, and Source 6 were regarded as gasoline-related sources, and each of them was interpreted based upon previously reported source profiles.

Source 5 shows higher loadings of ethene and acetylene than the other two sources. Source profiles reported in several studies indicated that high ethene and acetylene loadings were associated with automotive emissions (Vega et al., 2000; Lawrimore and Aneja, 1997; Scheff et al., 1996; Kenski et al., 1995; Fujita et al., 1994; Wadden et al., 1994). Also, as shown in Figure 3.4, Source 5 exhibits significantly different weekday and weekend diurnal behaviors; during weekdays the peak in VOC concentration resulting from Source 5 takes place at around 7 am, during heavy commuting traffic time, while on weekends this sharp peak around 7 am is not observed. This is consistent with different diurnal activity levels for automotive sources on weekends versus weekdays. Therefore, Source 5 is recognized as a vehicle exhaust source category. As far as Source 6 and Source 2 are concerned, their diurnal patterns do not show significant differences between weekends versus weekdays. Even though the liquid gasoline and gasoline vapor source categories include contributions from motor vehicle activity, they include other contributions that may not be directly related to commuter traffic patterns such as losses during handling of bulk gasoline. The only difference was that Source 6 had slightly higher loadings of iso-pentane and toluene while Source 2 had a higher loading of n-pentane. Several

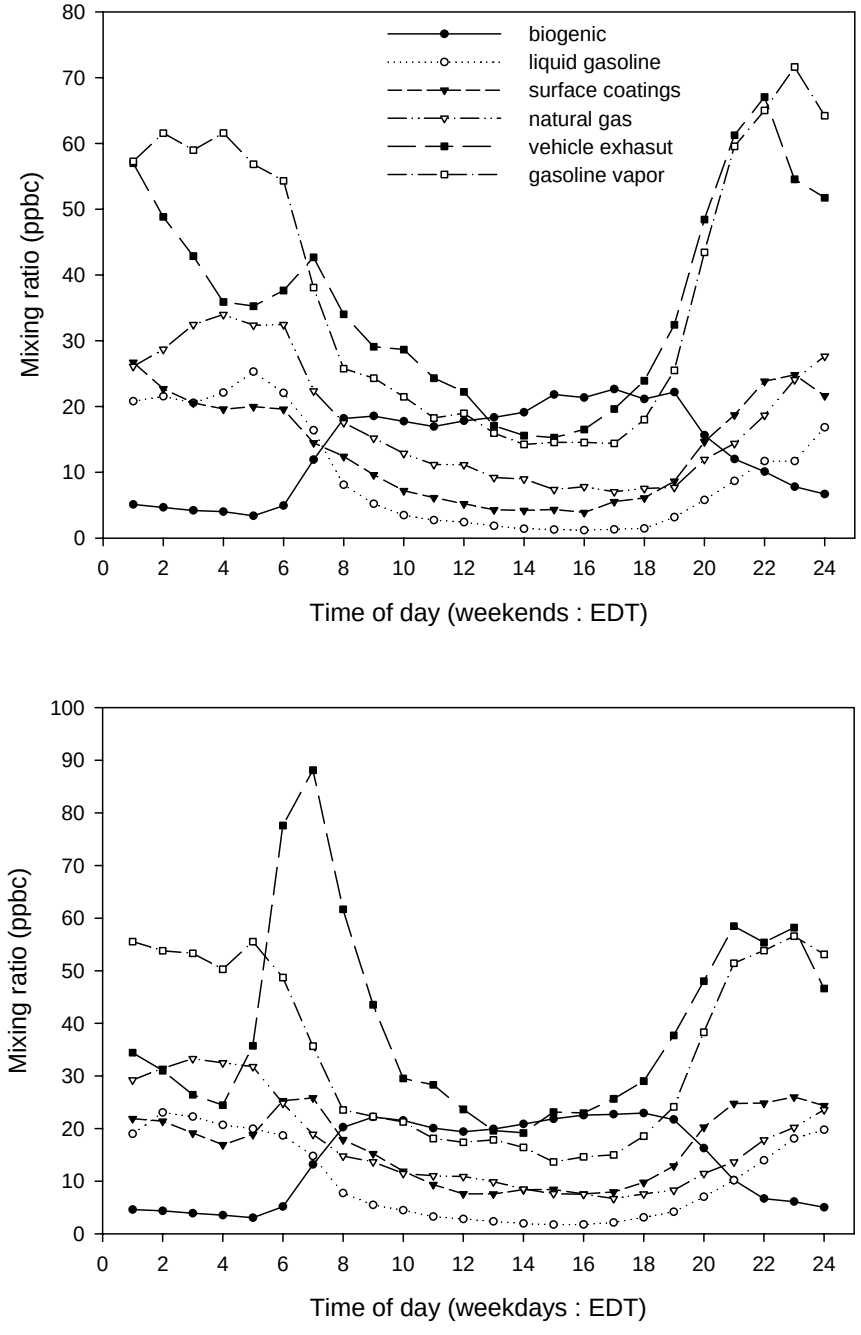

Figure 3.4: Comparison of average diurnal pattern of weekdays with that of weekends, estimated from hourly source apportionment using the summer measurements taken over four years from 1996 to 1999.

studies showed that iso-pentane is especially abundant in gasoline vapor, and iso-pentane has higher vapor pressure than n-pentane. Thus, Source 6 and Source 2 were regarded as gasoline vapor and liquid gasoline source categories, respectively (Watson et al., 2001; Lawrimore and Aneja, 1997; Scheff et al., 1996; Fujita et al., 1994).

The greater proportion of the lower molecular weight paraffin hydrocarbons such as ethane and propane in Source 4 suggests a natural gas source category. The natural gas source may result from possible leakage in the transmission system, or refueling stations of natural gas and propane around the sampling site as the Figure 3.1 shows (Mukund et al., 1996; Derwent et al., 1995; Fujita et al., 1994). Source 3 was considered to be related to surface coating sources because it was primarily composed of xylene and toluene (Fujita, 2001; Lawrimore and Aneja, 1997; Mukund et al., 1996), and local point sources such as paint manufacture and automobile surface coating operations were located around the measurement site as shown in Figure 3.1.

The relationship between surface wind direction and source category concentrations was examined for each source category, in order to try to further resolve specific sources. However, no correlations were observed, likely because of the significant hour-to-hour variation in surface wind direction observed at the sampling location.

Figure 3.5 shows the overall mean hourly absolute source contributions and percentage source contributions for each year and for four years, respectively. In the single year analyses, 6 source categories for 1996 and 1997, and 5 source categories for 1998 were identified using UNMIX (Appendix 2). Source compositions for each

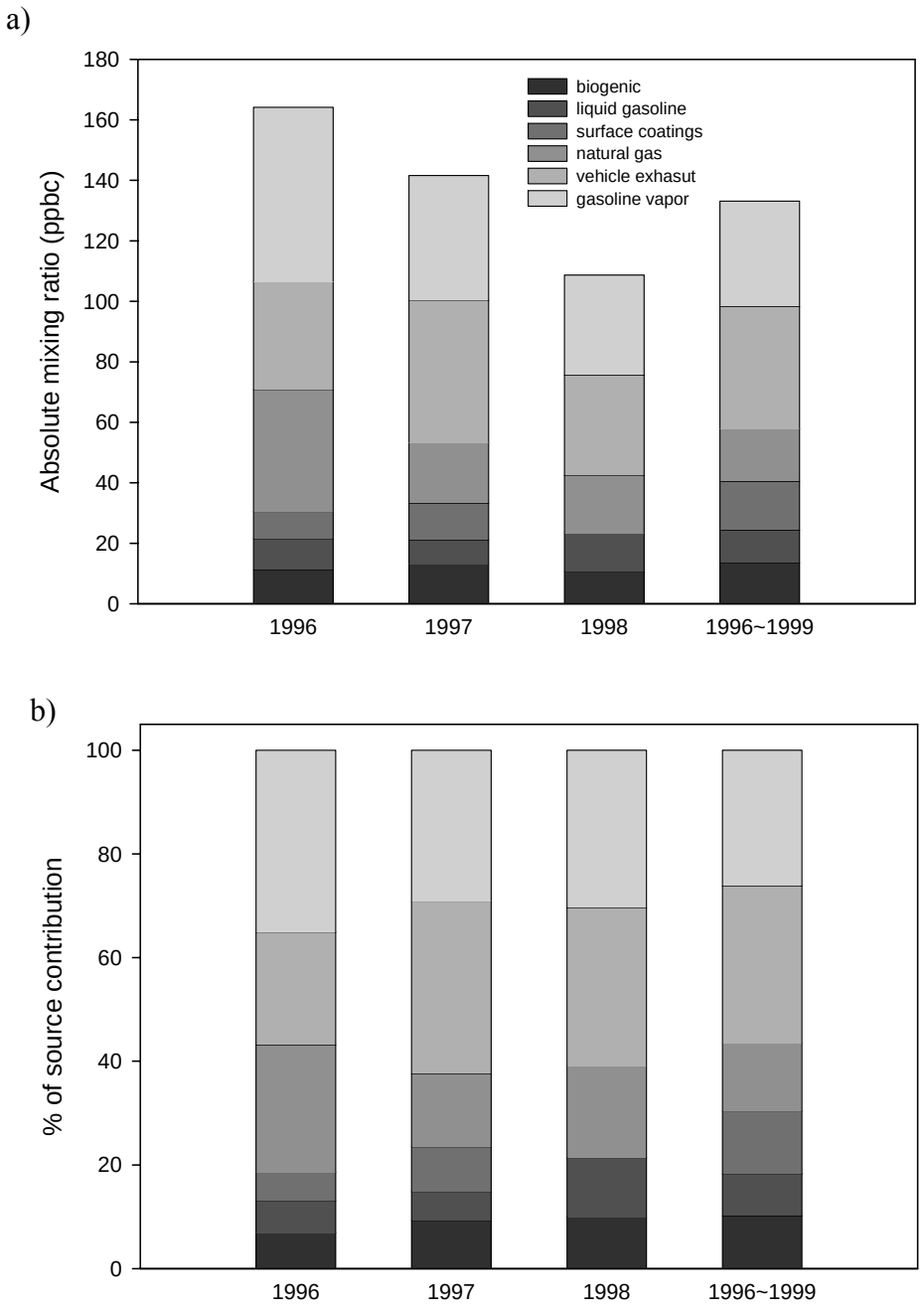

Figure 3.5: Yearly trend of each source contribution to average hourly total VOC in terms of a) both absolute mixing ratio in ppbC as well as b) percent contribution.

year showed the same characteristics as those of four-year data analysis, and thus each source category was identified in the same way as explained above. The surface coating source category was not identified as a distinct source for 1998, but high loadings of xylene and toluene were seen in the vehicle exhaust and gasoline vapor source categories.

The contribution of the natural gas source category in terms of absolute concentration is significantly greater in 1996 than in subsequent years. The possible cause of the difference may be increased handling of natural gas, particularly injection and release from underground storage wells, reported for 1996 as compared to subsequent years (DOE, 2001).

Generally, gasoline vapor and vehicle exhaust source categories explain more than half of contributions to total hydrocarbons for all cases. Also, a downward trend in total VOC concentrations is observed.

As mentioned by Watson et al. (2001) in a recent review of VOC source apportionment by the chemical mass balance receptor model approach, gasoline vehicle exhaust, liquid gasoline, and gasoline vapor typically contribute more than 50% of ambient VOC in urban areas in the United States. Results presented for VOC source apportionment using the UNMIX receptor model in the Baltimore area suggest that around 60% of total hydrocarbons came from gasoline-related source categories such as vehicle exhaust, gasoline vapor and liquid gasoline. Biogenic emissions, natural gas and surface coating source categories explained the remaining 40% of total hydrocarbons. Considering that the sampling site is located in a parking lot close to

the city of Baltimore, near heavily traveled roads and several industrial/commercial sites as shown in Figure 3.1, the source apportionment results seem reasonable.

3.3 Identification of characteristics of source patterns during high ozone episodes

During the time period of the PAMS measurements between 1996 and 1999, ozone levels at Essex, Maryland exceeded the 8-hour ozone standard of 80 ppb on 47 out of a total of 400 days according to hourly ozone measurements. NOx, meteorological variables such as wind speed, and temperature as well as the hourly contribution of each source category were split into high ozone days and low ozone days based on this criteria.

Figure 3.6 shows the diurnal patterns of hourly mean mixing ratios on high ozone days and low ozone days for total hydrocarbons and NOx. The horizontal arrow bars in the figures indicate the times which can be considered as having significantly different mean mixing ratios based upon a two-tailed t-test at the 95% confidence interval. As shown in Figure 3.6, the mean mixing ratios of total hydrocarbons during afternoon of both high and low ozone days are not significantly different, while the difference during nighttime between both days is distinct. UNMIX apportions total hydrocarbons to each source category, and Figure 3.7 shows the diurnal patterns of hourly mean mixing ratios on high ozone days and low ozone days for each source category obtained from the UNMIX outputs. We can see only the biogenic source category has a significant difference in mean mixing ratios between high and low

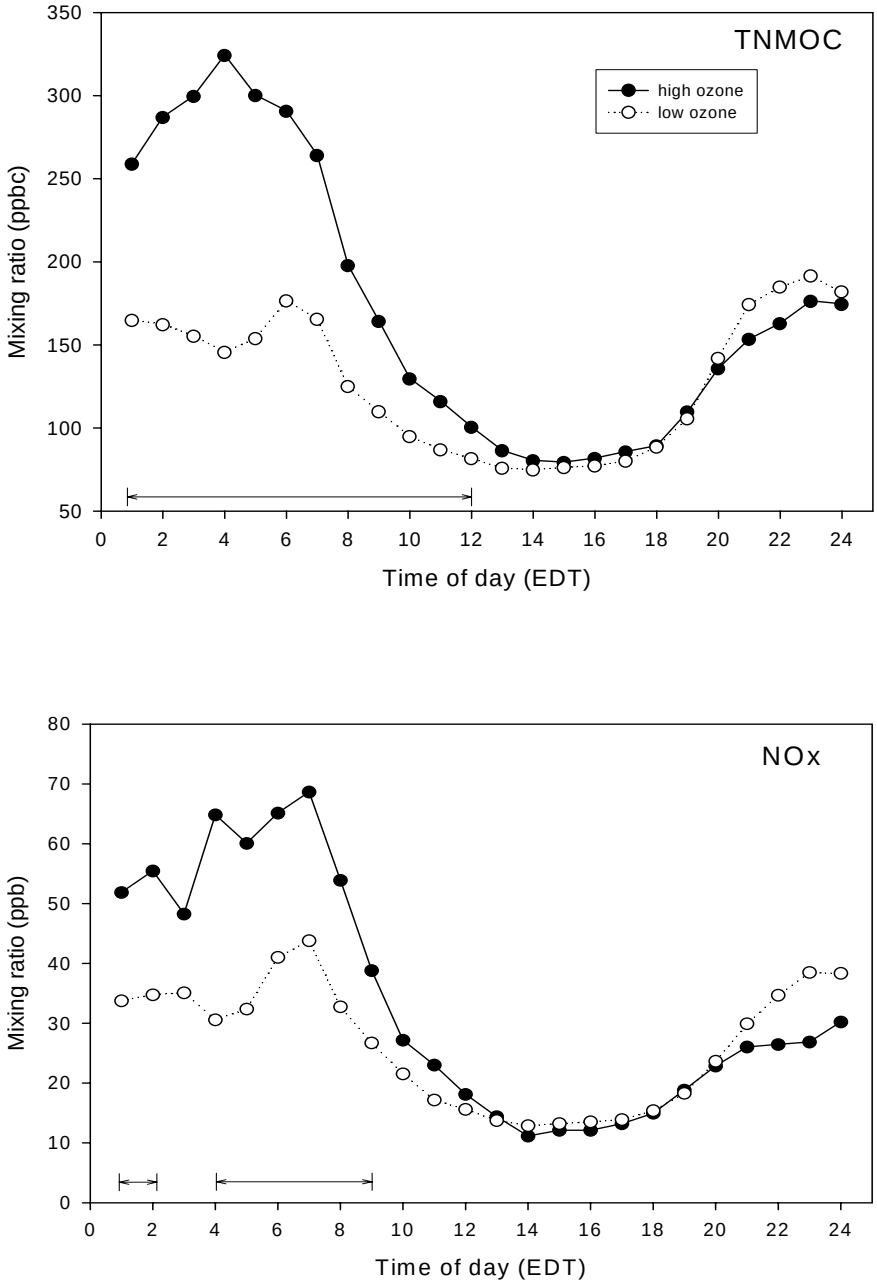

Figure 3.6: Comparisons of diurnal pattern of average mixing ratios of NOx and total nonmethane organic carbon (TNMOC) between high ozone days and low ozone days. The bars indicate the times that can be considered as having significantly different mean mixing ratios between both days based upon a two-tailed t-test at the 95% confidence interval.

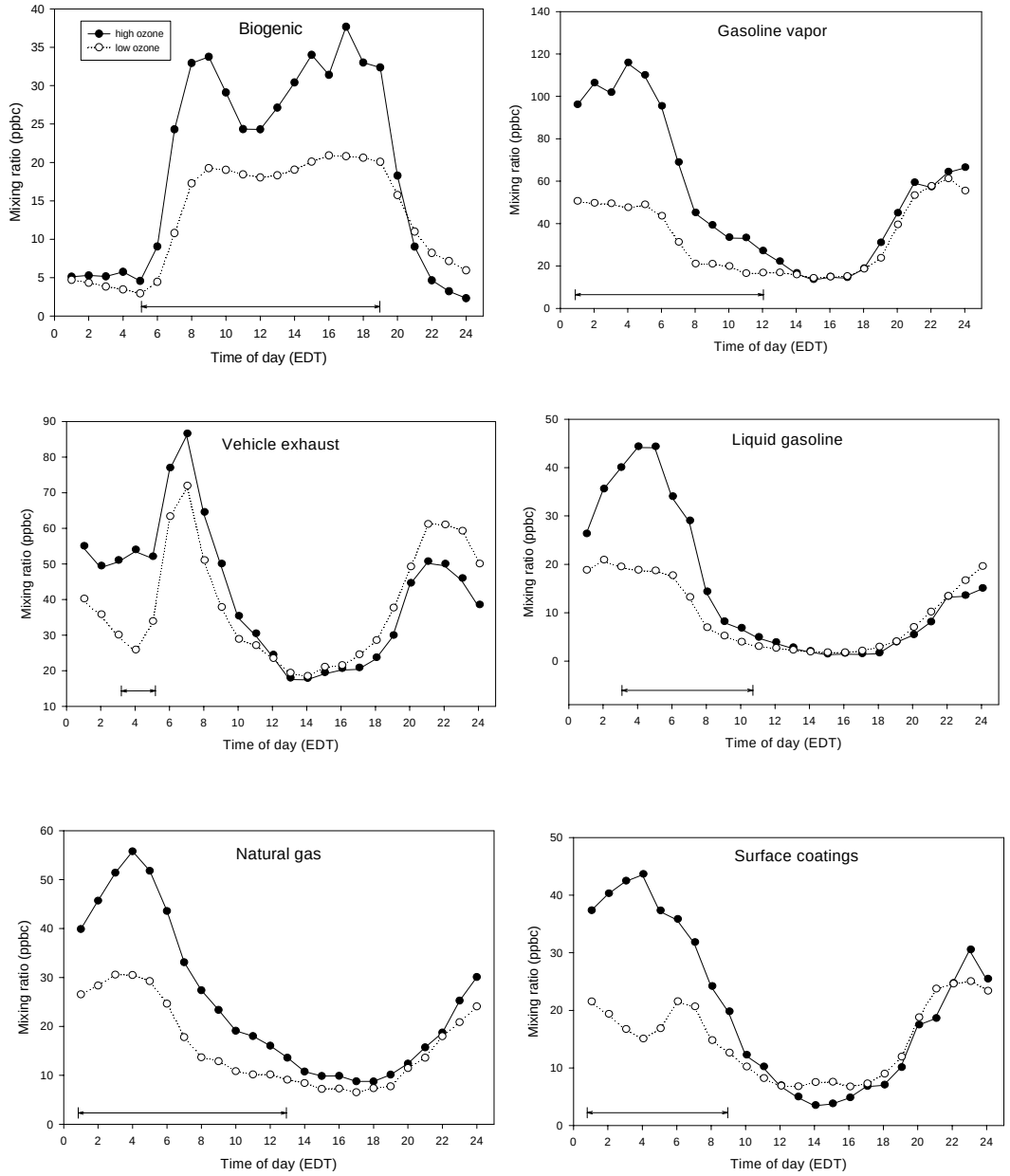

Figure 3.7: Comparisons of diurnal pattern of average mixing ratio of each VOC emission source between high ozone days and low ozone days. The bars indicate the times that can be considered as having significantly different mean mixing ratios between both days based upon a two-tailed t-test at the 95% confidence interval.

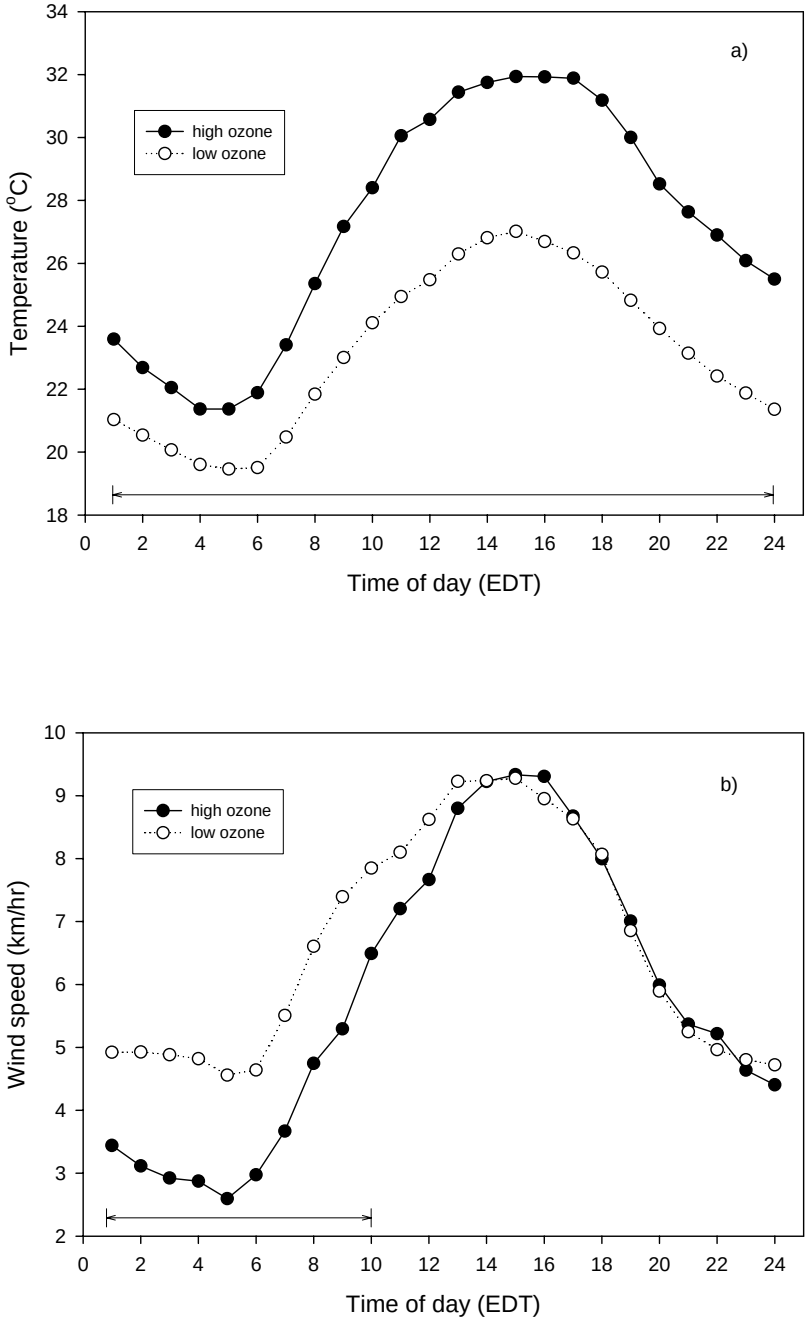

Figure 3.8: Comparisons of diurnal patterns of a) average temperature and b) average wind speed between high ozone days and low ozone days. The bar indicates the times which can be considered as having significantly different mean temperatures and wind speeds between both days based upon a two-tailed t-test at the 95% confidence interval.

ozone days during the afternoon. During the afternoon on high ozone days, the contribution of the biogenic source category to the total hydrocarbon mixing ratio is twice as high as that during the afternoon of low ozone days, while other source categories show no significantly different mixing ratios for both days. As shown in Figure 3.8a, higher contributions from biogenic sources during high ozone episodes may have resulted from higher temperatures (by 4~5 ^{o}C) during daytime, as the emission activity of biogenic sources tends to increase exponentially with temperature (Guenther et al., 2000).

On the other hand, during nighttime, the VOC mixing ratios resulting from anthropogenic source categories during high ozone days show similar patterns, about 1.5 ~2 times as high as those during low ozone days. Generally, the natural gas source is expected to show a constant emissions rate, and so differences in the mixing ratio associated with the source categories are most likely from variations of the mixing height in the atmosphere with time (Derwent et al., 1995). At night, the air is stably stratified because of the warmer air above the colder ground, and the effect of shear stress becomes dominant in maintaining turbulent flow, leading to mixing of pollutants from surface sources. During daytime the effect of buoyancy is predominant resulting in relatively vigorous and rapid vertical mixing. Under circumstances corresponding to very low wind speeds at night, shear is minimal and stratification becomes dominant, leading to poor mixing of pollutants from surface sources (Seinfeld and Pandis, 1998). As a result, the mixing height becomes relatively thin, and emissions from surface sources are concentrated. As shown Figure 3.7, the difference of natural gas mixing

ratios by a factor of two between both types of days likely suggests a difference in mixing height in the late evening and early morning between the two types of days.

To determine if the differences between two types of days during nighttime result from different emissions from sources or from poor atmospheric mixing during nighttime, we took a closer look at meteorological variables for both types of days. Figure 3.8b gives the diurnal patterns of average wind speed for both types of days, and during nighttime on high ozone days the average wind speed was less than that during nighttime on low ozone days by about 1.5 km/hr. A scatter plot of wind speed vs. total hydrocarbons and NOx from 1 am to 6 am shown in Figure 3.9, illustrates the inverse relationship between them. Also, hourly average temperatures, as shown in Figure 3.8a, were significantly higher on high ozone days. Therefore, we can explain the higher mixing ratios of anthropogenic sources on high ozone days at night by increased stratification caused by higher temperatures, and weaker shear stress caused by weaker wind speed rather than an increase in emissions from surface sources.

Accordingly, our focus is on the daytime differences. As mentioned earlier, the only difference during daytime between two types of days is seen in the biogenic source category, which shows the highest afternoon mixing ratios among source categories during high ozone days as shown in Figure 3.7. In the Baltimore region, a reactivity weighted source apportionment analysis of VOC for the summer time of 1993 and 1995 revealed biogenic sources to be the most significant source category with respect to ozone formation (Morales-Morales, 1998). Additionally, Cardelino and Chameides (2000), in a study of hydrocarbons measured at PAMS sites in Washington, DC and Bronx, NY in the summer of 1995, showed that during some

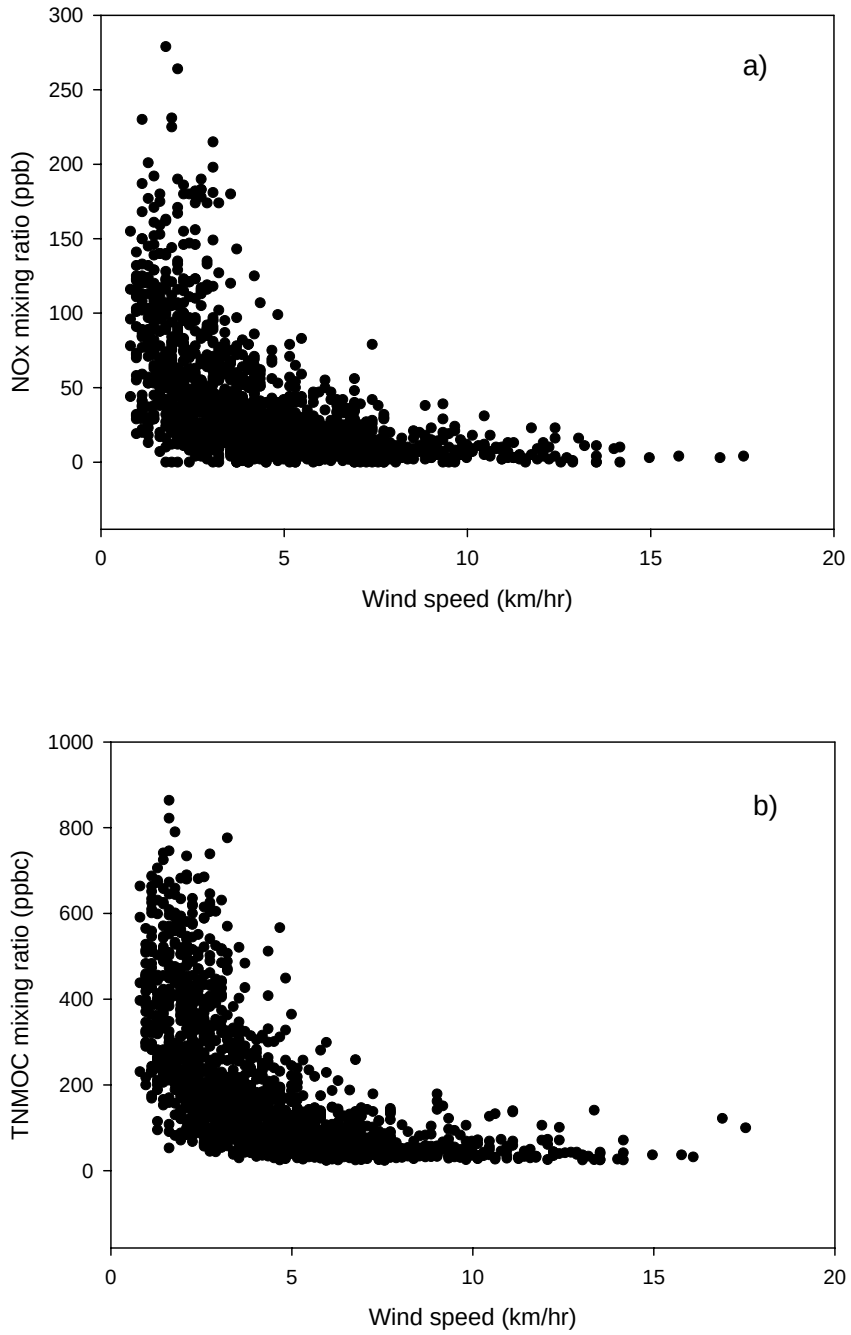

Figure 3.9: Scatter plots of wind speed vs. a) NOx and b) TNMOC for observations between 1 am to 6 am.

ozone episodes, the reactivity-based average concentrations of natural hydrocarbons from 7 am to 7 pm were greater than those of anthropogenic hydrocarbons. Even at these two sites, which are categorized as urban/central city commercial, natural hydrocarbons appear to be an important emission source in ozone formation.

To investigate contributions of each source category based on reactivity, we assumed that the 23 chemical species, shown in Table 3.2, account for 100 % of the mass fraction of each source category, and we estimated source contributions during daytime from 7 am to 7 pm. The reactivity-weighted mixing ratios of each source category were calculated by multiplying mixing ratios of each species by the maximum incremental relativities (MIR) scale (moles O_3 formed/moles C). The MIR scale developed by Carter et al. (1989) is defined as the change in ozone caused by adding a small amount of a VOC species, and has been used to quantify a species ability to produce ozone (Carter et al., 1994). It should be noted that this rough estimate of reactivity-weighted source contribution contains substantial uncertainty because of the assumption that emissions from each source category are composed solely of the 23 species.

Table 3.3 shows the reactivity–based comparison of mixing ratios for each source category. As indicated in Table 3.3, the reactivity-weighted mixing ratio of the biogenic source category shows the same order of reactivity-weighted mixing ratio of vehicle exhaust source category. Also, the biogenic and surface coating source categories are likely to be more reactive towards ozone production than the other four source categories because the mixing ratios of the former two categories show similar values for both reactivity based and absolute mass based contributions, while those of

the latter source categories show significantly reduced contributions in the reactivity-weighted scale.

Table 3.3: Source mixing ratios (ppbc) based on reactivity and on absolute mass, obtained from daytime (7 am to 7 pm) source contributions

	Absolute mixing ratio	Reactivity-weighted mixing ratio
Biogenic emissions	20.1	23.7
Liquid gasoline	4.3	2.3
Surface coatings	10.3	10.8
Natural gas	10.9	3.1
Vehicle exhaust	32.2	23.5
Gasoline Vapor	20.2	12.4
Total TNMOC	98.0	75.8

In addition, in terms of the morning VOC/NOx ratio used to justify NOx-VOC sensitivity to peak ozone in the past, this area would fall into the VOC-sensitive category, for which VOC reduction results in a decrease of ozone formation. However, the method of determining VOC or NOx sensitivity using the morning VOC/NOx ratio does not incorporate the impact of the biogenic source identified as a significant source in this study and other studies (Sillman, 1999; Milford et al., 1994). As indicated in Figure 3.10, the average ratios of VOC/NOx during 6 am to 9 am are the same for both types of days, and are much lower than 10, the criteria for VOC sensitivity. High ozone episodes in this area took place when the biogenic contribution was elevated, while average NOx mixing ratios as well as the average mixing ratios of other emission sources remained at the same levels.

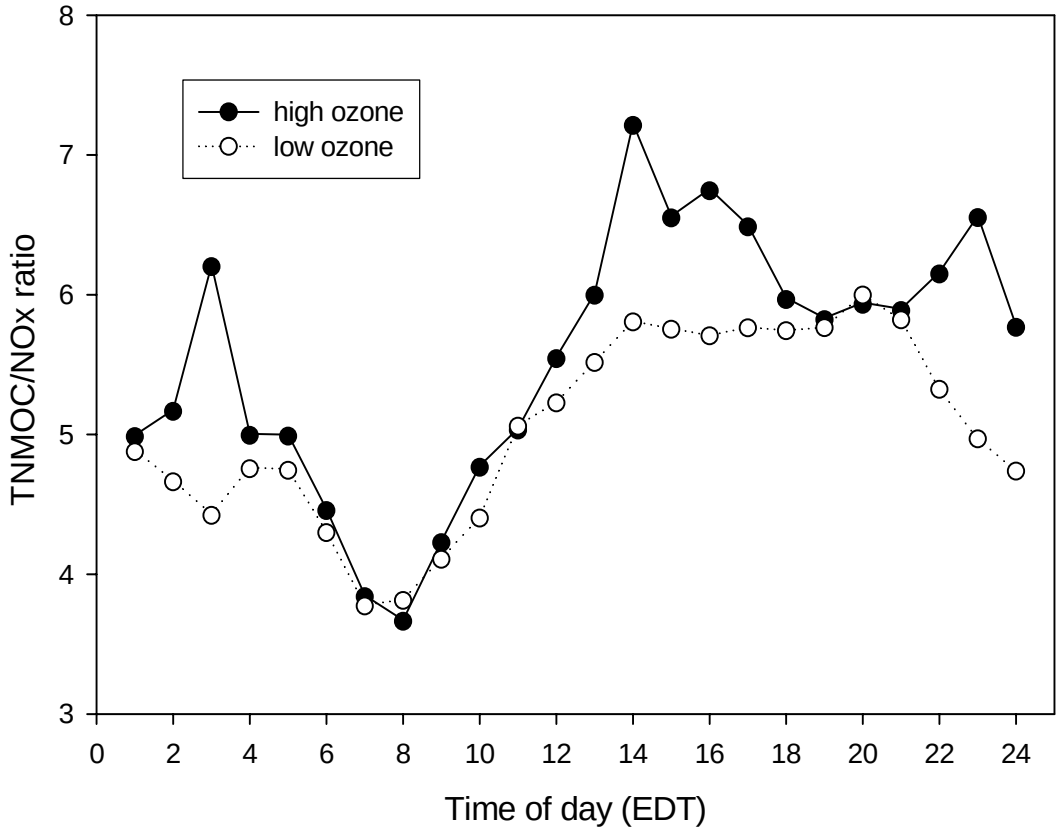

Figure 3.10: Comparison of diurnal pattern of average ratio of TNMOC to NOx between high ozone days and low ozone days.

As Ryan et al. (1998) indicated, the most severe ozone events in the Baltimore/Washington area occurred when the regional-scale transport of ozone and its precursors was significant. Thus, long-range transport of ozone and its precursors is likely an important contributor to ozone episodes in this area. With receptor models, techniques developed to assess contributions from various sources based on observations at receptor sites, the impacts of long-range transport on the contributions of a particular source cannot be resolved without additional meteorological input. For this reason, it is not possible to gauge the impact of regional transport and local ozone production on ozone episodes, including mild ozone events, in this area. Considering the short lifetime of compounds of biogenic origin such as isoprene, compared to compounds from other sources, the results presented here suggest that biogenic emissions play an important role in local ozone production in this area. Hence, if only local ozone production is considered, simply decreasing the emission of anthropogenic VOC by a small amount may not result in local ozone reduction in this area if weather conditions are conducive to high levels of biogenic emissions.

3.4 Summary and conclusions

Hourly hydrocarbon mixing ratios measured at Essex, Maryland, for the summers of 1996 to 1999 were analyzed to identify possible VOC sources using the UNMIX receptor model. Gasoline-related sources such as vehicle exhaust, gasoline vapor, and liquid gasoline explained more than half of total VOC mixing ratio, which is typical for VOC found in urban/suburban areas in United States. Natural gas,

surface coatings, and biogenic source categories each accounted for 13, 12 and 11 % of the total VOC, respectively, when all measurements were considered.

Even though the hourly average contribution of biogenic sources in quantity did not appear to be significant, the comparisons of diurnal patterns of high-ozone days with those of low-ozone days and rough reactivity-weighted daytime source apportionment results suggested that biogenic emissions contribute significantly to local ozone production for high ozone episodes at this site.

At this point, without a help of air quality modeling, we cannot conclude whether VOC control or NOx control or both controls will be effective in reducing violations of National Ambient Air Quality Standard (NAAQS) for ozone in this area. However, if the focus is on the reduction of high ozone occurrences coming from local ozone production in which weather conditions are conducive to high biogenic emissions, NOx reduction, which must be significant enough to offset increased biogenics, may be more effective, because NOx reduction creates NOx limited conditions, and highly reactive biogenic VOCs cannot proceed to react to form ozone. However, the NOx reduction may not lead to ozone reduction under weather conditions unfavorable to increased biogenic emissions. On the other hand, if the focus is on the general reduction of ozone for all summer days, a substantial reduction of anthropogenic VOC sources such as automobile exhaust may lead to ozone reduction. These strategies can be resolved through the use of a well-evaluated photochemical air quality model taking into account long-range transport of ozone and its precursors, deposition of pollutants, and chemical reactions. This practice using an air quality model was performed, and the results were described in the Chapter 5.

Chapter 4: Evaluation of a VOC Emissions Inventory by Comparison to Ambient Measurements

4.1 Introduction

Air quality models, composed of meteorology, chemistry and emissions, have been widely implemented to simulate the chemistry and physics of the atmosphere, and to understand the cause-effect relationships between pollutants and their precursors. Potential control measures for target air pollutants have been determined, based on those modeling results. Hence, inaccurate results from air quality modeling can lead to negative impacts both economic and environmental in nature. The usefulness of the output of air quality models is largely dependent on the quality of their inputs. Hanna et al. (1998), Placet et al. (2000), and Solomon et al. (2000) indicate that the uncertainties in atmospheric model results may originate mainly from the uncertainties in the emission inventories.

Previous studies described in detail the limitations and difficulties associated with evaluation of emission inventories resulting from the intrinsically different nature of inventory estimates and ambient monitoring measurements (Fujita et al., 1992; Harley et al., 1992; Funk et al., 2001; Mannschreck et al., 2002; Slemr et al., 2002; Houyoux et al., 2000; EPA-II, 1996; LADCO, 1998; Stoeckenius et al., 2000). Such comparisons are limited to ratios of VOC species or VOC species groups (abundance

of a given species or species group relative to that of another species group) since the emissions estimates in units of mass flux per area cannot be converted directly into concentrations without the application of a suitable dispersion model or a chemical transport model. In addition, the chemical mechanisms commonly used in photochemical models aggregate chemical species, and this constrains the comparisons to a few individual species and species groups. Furthermore, since estimates from emissions processing models do not demonstrate the impact of chemical reactions and transport, the comparison is often limited to the early morning hours of the day when these impacts tend to be minimal.

Because of the above limitations, two approaches in terms of ratio comparisons have been employed to evaluate emissions inventories. In one approach, VOC/NOx or CO/NOx ratios and weight fractions of individual VOC species are compared to ambient measurements during the early morning (6:00 a.m.-10:00 a.m.) (Fujita et al., 1992; Funk et al., 2001; Houyoux et al., 2000; LADCO, 1998; Stoeckenius et al., 2000). In another approach, receptor-modeling techniques are used to compare emissions estimates for specific source categories (Harley et al., 1992; EPA-II, 1996; Hidy, 2000). Receptor models take ambient measurements of speciated organic compounds and allocate VOCs to various source categories through complex statistical manipulations.

Even though the ratio comparisons can give some insight into the uncertainty in an emissions inventory, care is needed to avoid reaching misrepresentative and possibly misleading conclusions. For example, the same values modeled and observed VOC/NOx ratios do not indicate that the absolute amounts of VOC and NOx are the

same in both the simulation and the observation. For that reason, a dispersion model has been employed in several studies. Fujita et al. showed the comparisons of measured CO/NOx and NMOG (non-methane organic gas)/NOx and CO, NMOG, and NOx concentrations with air quality model prediction using the UAM model (Fujita et al., 1992). Recently, Mannschreck et al. and Kuhlwein et al. adopted a Gaussian dispersion model to calculate pollutant concentrations of individual hydrocarbons for comparison with measured concentration ratios (Mannschreck et al., 2002; Kuhlwein et al., 2002). Slemr et al. (2002) performed a comparison of the results from a CTM (chemistry and transport model) with observations as a part of their study.

This study focuses on emissions inventory evaluation. As NOx is a direct product of combustion, while VOCs are emitted by both combustion and non-combustion sources, NOx emission estimates are generally assumed to be more accurate than VOC estimates (Funk et al., 1992; Watson et al., 2001). In addition, Hanna et al. (1998) concluded, in a study of estimates of uncertainties in predictions by a photochemical grid model, that anthropogenic VOC area source emissions had the most influence on the variations in the 50% of peak ozone concentrations. Therefore, the evaluation of the emissions inventory here is mainly focused on VOC.

Since the use of several evaluation methods and inter-comparison between the results from each method will lead to more solid conclusions, we investigate both ratio comparisons of each VOC source contribution from a source apportionment model and CB-IV VOC groups relative to NOx or CO at the emissions modeling level (EPA-II, 1996). Furthermore, the CMAQ model, a photochemical air quality model including the effects of chemistry and transport, is employed to compare the ratios of CB-IV

VOC groups to NOx or CO, and effectively to put values from the emissions inventory into concentration units so they may be compared with observations.

4.2 Modeling and monitoring data

4.2.1 Overview of emissions inventory and modeling

An aggregated emissions inventory was obtained from the Mid-Atlantic Regional Air Management Association (MARAMA). This is an improved emission inventory for 1997 to support studies of regional ozone in the Mid-Atlantic and Northeastern states. Average daily VOC, NOx, and CO emissions for area and point sources and average daily Vehicle Mileage Traveled (VMT) were compiled at the county level. It was based upon EPA's 1996 National Emission Trends (NET) inventory.

Additionally, a gridded land use assessment, prepared by the New York State Department of Environmental Conservation (NYDEC), was used for biogenic source processing. Even though the focus of our evaluation is on the anthropogenic emissions inventory, it is necessary to process biogenic emissions in conjunction with anthropogenic emissions since the ambient measurements include the contributions from biogenic sources and biogenics lead to ozone.

We employed the SMOKE version 1.4, an emissions pre-processing model, to convert the source-level emissions (county total emissions) to gridded, speciated, and temporally allocated emissions.

As described in Chapter 2, the temporal allocation step creates an hourly pollutant emissions inventory based on the characteristics of each source. In the spatial allocation step, a gridding surrogate is used to create a matrix containing conversion factors, used to transform county level aggregate emissions into emissions in each grid cell. For example, emissions from major on-road mobile sources are allocated in each grid cell according to the distribution of roads. In the speciation step, SMOKE creates a speciation matrix containing conversion factors, to convert VOC emissions into emissions of specific compounds. In this study, the speciation is based on the CB-IV chemical mechanism (Gery et al., 1989). Actual VOCs are converted to 10 modeling species: ETH (ethene), ISOP (isoprene), PAR (paraffin group, molecules containing single carbon bond groups), OLE (olefin group, molecules containing double carbon bond groups), TOL (toluene group, 7-carbon rings), XYL (xylene group, 8-carbon rings), ALD (aldehyde group), FORM (formaldehyde), NR (non reactive VOC group), and TERP (terpene group). The final gridded, chemically speciated hourly emission estimates are produced by multiplication of the matrices developed in the main processing steps. For biogenic sources, in order to convert land use information to normalized emissions values, the BEIS2 is embedded in SMOKE. For mobile sources, MOBILE5b, also embedded in SMOKE, generates emission factors, which are multiplied by VMT in order to get emissions values (Houyoux et al., 2000).

CMAQ version 4.3 used in this study has been designed to approach air quality as a whole by including state-of-the-science capabilities for modeling multiple air quality subjects. The CMAQ modeling system simulates various chemical and physical processes that are thought to be important for understanding atmospheric

trace gas transformation and distribution such as dispersion, chemical reactions, and surface deposition (EPA-III, 1999). More details are described in Chapter 2.

Meteorological variables, required to process biogenic, mobile, and point sources in SMOKE, and CMAQ, were simulated using the MM5 by the Department of Meteorology, University of Maryland. The simulations were performed with a modified Blackadar PBL scheme and a standard nudging process (Sistla et al., 2002; Zhang and Zheng, 2004). The meteorological variables for 4 km grid resolution were extracted and interpolated from the meteorological variables for 12 km grid resolution using the MCIP version 2.2.

The simulation was performed for the period July 5-July 20 of 1997 using multi-nesting techniques for boundary conditions. As shown in Figure 4.1, the detailed 4 km study domain, nested within the outer domains, covers the whole state of Maryland, and parts of Virginia, West Virginia, Delaware, New Jersey, and Pennsylvania. The innermost domain has 108 columns by 78 rows with 4 km horizontal grid cell resolution, and 16 vertical layers. The outer domains have horizontal grid cell resolutions of 36 km, and 12 km, respectively. The comparison to observations was done from July 8-July 20 of 1997, allowing for three days of spin-up time to minimize the impact of initial conditions on the CMAQ simulation.

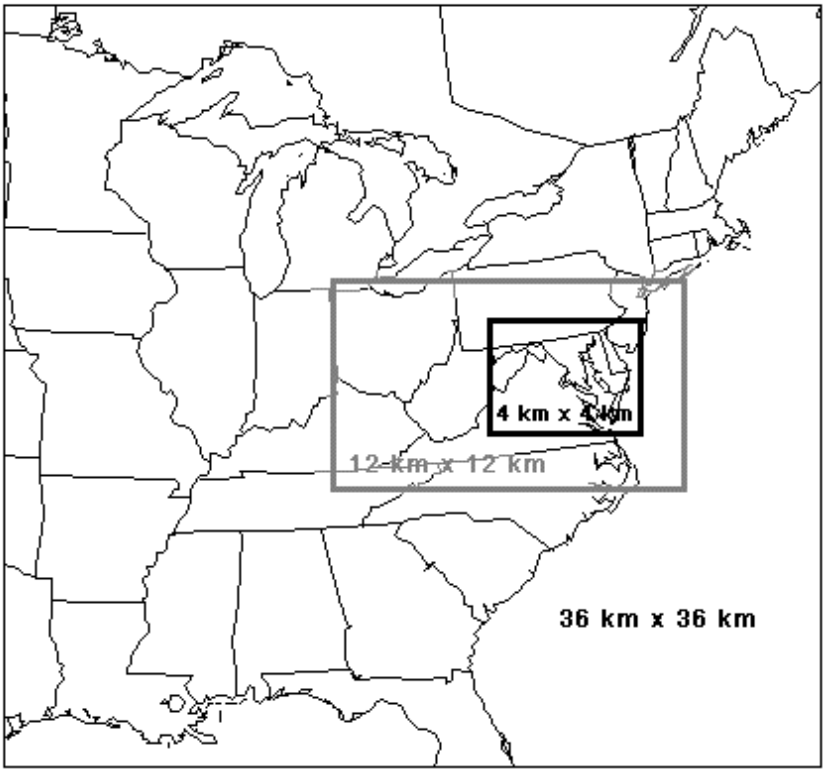

Figure 4.1: Map of CMAQ modeling domain.

4.2.2 Overview of ambient measurements

The PAMS network consists of five different site types to provide information sufficient to satisfy important monitoring objectives. Type 2 sites are located immediately downwind of areas with significant ozone precursor emissions. It is reasonable to compare ambient measurements and emissions estimates only in situations where the local ozone precursor concentrations are dominated by local sources because emissions estimates and ambient measurements are two fundamentally different quantities. Emissions estimates represent the amount of a given pollutant released by a particular source. Ambient measurements represent the concentration of these pollutants in the atmosphere at a particular location and time. It is best to use monitoring measurements from sites where local emissions dominate such as PAMS type 2 sites (LADCO, 1998; Stoeckenius et al., 2000). We obtained the measurements for three PAMS sites (McMillan reservoir in DC, Essex in MD, Camden in NJ), categorized as type 2 sites. Table 4.1 contains a summary of the PAMS measurements and Figure 4.2 shows the site locations. The concentrations of 55 hydrocarbons, total nonmethane organic carbon (TNMOC), ozone, oxides of nitrogen, as well as surface meteorological conditions such as temperature, wind direction, wind speed, and radiation are monitored at the sites. At the Camden site, CO was measured instead of NOx.

Table 4.1: Summary of PAMS observations

	Essex, MD	McMillan Reservoir, DC	Camden, NJ
Period of obs.	Jun. 1 -Sep. 30,1997	Jun. 1 -Sep. 24,1997	Jun. 1 -Aug. 31,1997
# of hourly obs. for 6:00 am-9:00 am	387	359	269
Total # of hourly obs.	2812	2152	1680

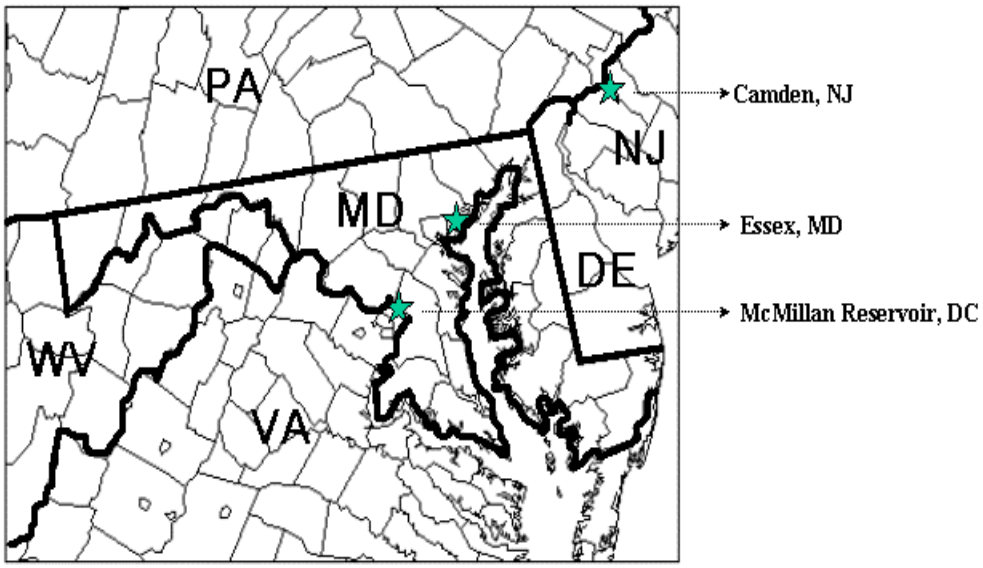

Figure 4.2: Map of PAMS locations used in this study. DE (Delaware), MD (Maryland), NJ (New Jersey), PA (Pennsylvania), VA (Virginia), WV (West Virginia).

The 55 individual hydrocarbons observed by PAMS were lumped into categories for comparison with emissions estimates using the VOC categories in the CB-IV chemical mechanism. There is a limitation associated with this conversion. TERP, FORM, and ALD2 are not included in the 55 PAMS species. ETH and ISOP in the CB-IV mechanism are the only single species measured by PAMS. Also, the 55 PAMS hydrocarbons accounted for only 70-90% of the TNMOC for the three sites, with the remainder unidentified. The unidentified portion of TNMOC might be volatile hydrocarbons of C2 through C12 such as terpenes, and oxygenated hydrocarbons (EPA-IV, 1998). Therefore, the concentrations of the lumped species such as PAR, OLE, TOL, XYL, and NR, estimated from only 55 species measured at PAMS sites, may be lower than actual concentrations of these lumped species in ambient air. For example, dodecane, not included in the 55 PAMS species, may be in a measurement of TNMOC, and 1 ppb of this species is converted to 12 ppb of PAR (12 ppbC) in terms of modeling species. Hence, a concentration of PAR converted from only 55 PAMS species may under-represent the actual concentration of PAR in the ambient air. Therefore, the concentrations of PAR, OLE, TOL, and XYL obtained from the 55 PAMS observed species are considered a lower limit of the actual concentrations in ambient air.

4.3 Approach

Two types of comparisons between observation and estimation were performed. One is the comparison of CB-IV VOC groups both in an absolute and a relative

manner. The other is a ratio comparison of each VOC source contribution, obtained from a source apportionment model, relative to NOx (or CO for the Camden PAMS site). As far as the ratio comparisons are concerned, they are based on NOx or CO rather than VOC, because NOx or CO likely has less uncertainty in both measurement and emissions modeling than VOC (Funk et al., 2001; Watson et al., 2001). In addition, the definitions of VOC categories in modeling and measurements are not the same. As described above, TNMOC observations include nonmethane hydrocarbons and oxygenated hydrocarbons, while the calculated total VOC from the emissions model stands for total organic gas (TOG) including methane. The morning time period from 6:00 a.m. to 9:00 a.m. was investigated to minimize the impact of chemical reactions and transport on comparisons with ambient measurements.

When it comes to comparing absolute concentrations of CB-IV VOC groups by employing the CMAQ photochemical model, there are some additional issues to be noted. The photochemical air quality model is a complicated system composed of a meteorological modeling system for the description of atmospheric states and motions, emission models for man-made and natural emissions injected into the atmosphere, and a chemistry-transport modeling system. Hence, the results from an air quality model reflect uncertainties in the meteorology and chemistry, in addition to uncertainty in the emission estimation. Even though the comparisons are performed during the morning period from 6:00 a.m. to 9:00 a.m. when the impacts of chemistry and transport are minimized, there still exists a possibility of errors in concentration predictions originating from meteorological parameters such as mixing height.

4.4 Results and discussion

4.4.1 Comparison of CB-IV VOC categories

ETH (ethene), TOL (toluene group), and XYL (xylene group) were considered for this comparison. Isoprene was excluded because this species is not appropriate for this comparison - short-lived isoprene is at a minimum in early morning hours, the time frame in which we focus. Considering the limitations mentioned earlier, TOL and XYL were included in this comparison, as toluene and xylenes are known as tracer species for both vehicle exhaust and solvent sources. Ethene is known as a tracer species for vehicle exhaust (Wadden et al., 1994; Fujita et al., 1994; Kenski et al, 1995; Scheff et al., 1996; Lawrimore and Aneja, 1997; Vega et al., 2000). Even though this comparison is limited to a few species group, the result is expected to give insight into the emissions inventories of sources such as vehicle exhaust and solvent usage – major VOC sources in urban and suburban areas (Placet et al., 2000; Lawrimore and Aneja, 1997; Mukund et al., 1996).

Figure 4.3 shows the comparison of the estimated and observed average ratios of each species to NOx between 6:00 a.m. and 9:00 a.m. at Essex, Maryland (MD). Here, the estimated ratios from SMOKE were calculated for five different grid areas surrounding the monitoring site including: the cell containing the monitoring site with 16 km^2 area, extended areas of 3 x 3 cells, 5 x 5 cells, 7 x 7 cells, and 9 x 9 cells. That is because the estimates from SMOKE do not incorporate the impact of transport and chemistry, and comparing only at a corresponding grid cell to the monitoring site may be misleading. The ratios from CMAQ were the average values at the site cell

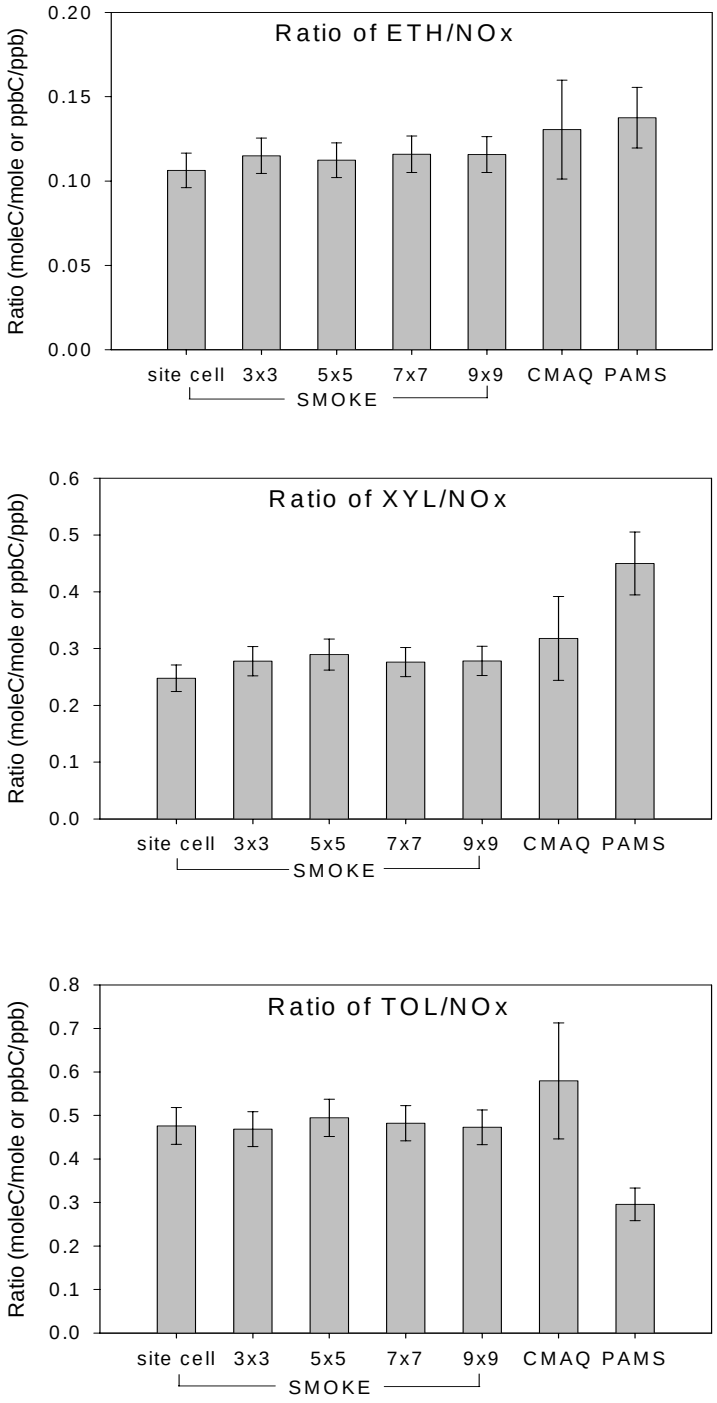

Figure 4.3: Comparison of average ratios between the estimated (SMOKE or CMAQ) and the observed values in the morning from 6:00 a.m. to 9:00 a.m. for Essex, MD. The error bars indicate the two-sigma standard errors of the means (95% confidence interval).

corresponding to the location of the PAMS monitoring station. The emission estimates from SMOKE show little diversity with respect to spatial distribution. The ratios from CMAQ and SMOKE show good agreement with each other for all species, suggesting that processes such as chemical evolution, transport, and deposition of pollutants during the morning period of 6:00 a.m. to 9:00 a.m. are relatively unimportant in the CMAQ simulation.

The estimated ratios of ETH to NOx from SMOKE and CMAQ are within an acceptable range of the corresponding observed ratio, taking into account the uncertainties associated with the averages. However, the model XYL/NOx ratio appears to be somewhat underestimated, while TOL/NOx seems considerably overestimated by a factor of 1.5 to 2.

Figure 4.4 compares the average concentration predicted by CMAQ to the observed values in the morning period from 6:00 a.m. to 9:00 a.m. at Essex, MD. The concentration of NOx predicted by CMAQ is a little higher than the observed NOx concentration. In addition, ETH and TOL show a trend similar to the ratio comparisons in Figure 4.3. On the other hand, the predicted XYL concentration is in good agreement with observed XYL.

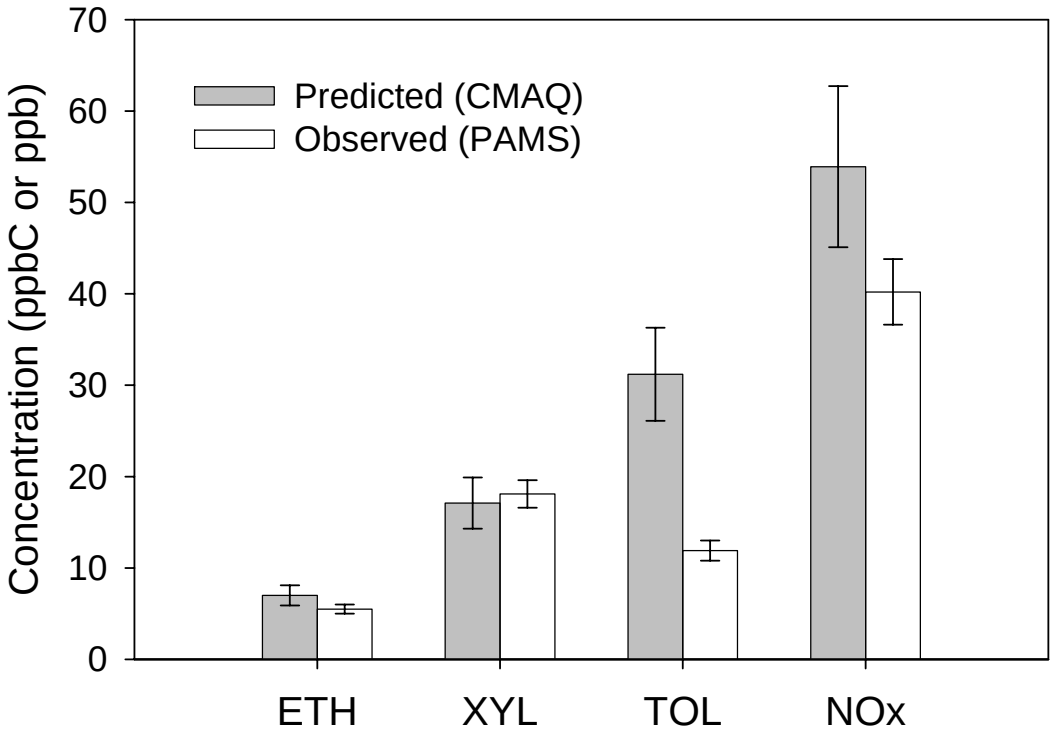

Figure 4.4: Comparison of average concentrations between the predicted (CMAQ) and the observed values in the morning from 6:00 a.m. to 9:00 a.m. for Essex, MD. The error bars indicate the two-sigma standard errors of the means (95% confidence interval).

To identify the major sources of TOL, XYL, and ETH in the estimates, SMOKE was run with only solvent and vehicle exhaust emissions. Table 4.2 shows the average percentage contribution of both emission sources to emission estimates of each modeling species in the morning period around the three observation sites. As indicated in Table 4.2, around 60% of estimated TOL in the vicinity of the Essex site is emitted from solvent sources, and 30% from vehicle exhaust. If the estimates of vehicle exhaust emissions are assumed to be acceptable as indicated by the favorable comparison between observed and estimated ETH/NOx ratios, an overestimate of emissions from solvent sources would be the likely cause for the overestimated TOL/NOx ratio.

Table 4.2: Average percentage contribution of sources to emission estimates of each species in the morning period by SMOKE

	Essex, MD		McMillan Reservoir, DC		Camden, NJ	
Grid cells	Solvent	Vehicle	Solvent	Vehicle	Solvent	Vehicle
			ETH (%)			
Site cell	3	62	1	88	5	93
3x3	5	62	2	70	8	68
5x5	5	62	5	74	11	53
7x7	5	56	6	76	12	49
9x9	5	56	6	78	11	50
			TOL (%)			
Site cell	63	31	58	37	54	42
3x3	60	34	58	35	57	36
5x5	63	34	58	34	63	31
7x7	59	30	57	35	65	28
9x9	59	31	55	36	64	29
			XYL (%)			
Site cell	35	57	28	61	29	64
3x3	33	56	29	54	32	57
5x5	35	54	30	51	37	50
7x7	33	52	29	53	37	45
9x9	32	53	28	54	38	47

At the McMillan reservoir site in Washington District of Columbia (DC), there is little variability in the spatial distribution of emission estimates of ETH/NOx, and TOL/NOx from SMOKE, as shown in Figure 4.5. For the XYL/NOx ratio, there is some spatial variability, but this is not a remarkable change. Also, the ratios from CMAQ and SMOKE show good agreement with each other for all species. While the XYL/NOx ratio shows good agreement with observation, ETH/NOx is slightly underestimated, and TOL/NOx is overestimated with statistical significance at 95% confidence interval. In Figure 4.6, the predicted NOx at the McMillan site is three times higher than observed NOx, and other species show similar patterns of overestimations. However, considering that the ratios from CMAQ in Figure 4.5 are similar to those from SMOKE, the consistent overestimation of concentrations from CMAQ implies that the incorrect estimates originated from a miscalculated mixing height rather than a problem with the ratios of emissions, and therefore the emissions inventory. From Table 4.2, more than 70% of the estimated ETH comes from vehicle exhaust. About 50% of the estimated XYL is emitted from vehicle exhaust with 30% from solvent sources. On the other hand, around 60% of the estimated TOL around this site is emitted from solvent sources while 35% comes from vehicle exhaust. The data suggest that solvent sources are significantly overestimated in this area.

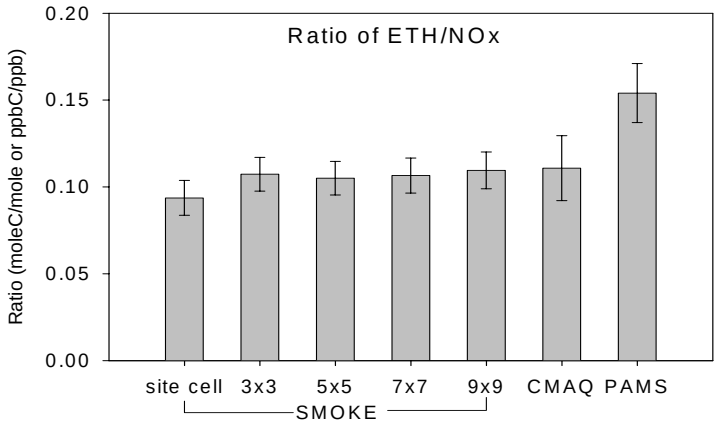

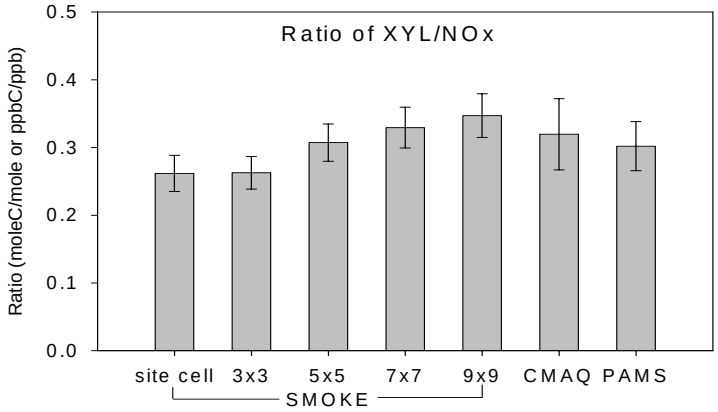

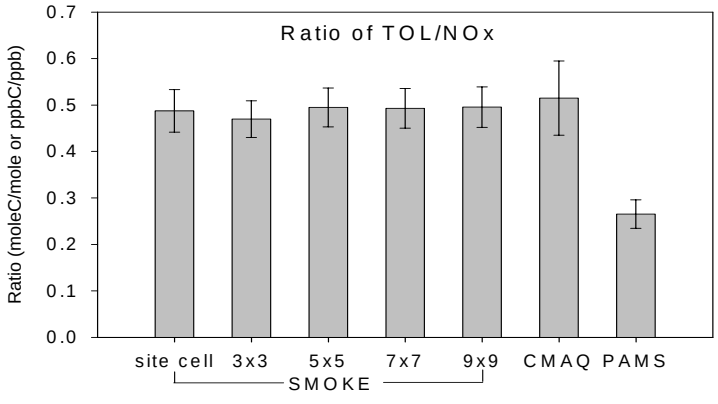

Figure 4.5: Comparison of average ratios between the estimated (SMOKE or CMAQ) and the observed values in the morning from 6:00 a.m. to 9:00 a.m. for McMillan reservoir, DC. The error bars indicate the two-sigma standard errors of the means (95% confidence interval).

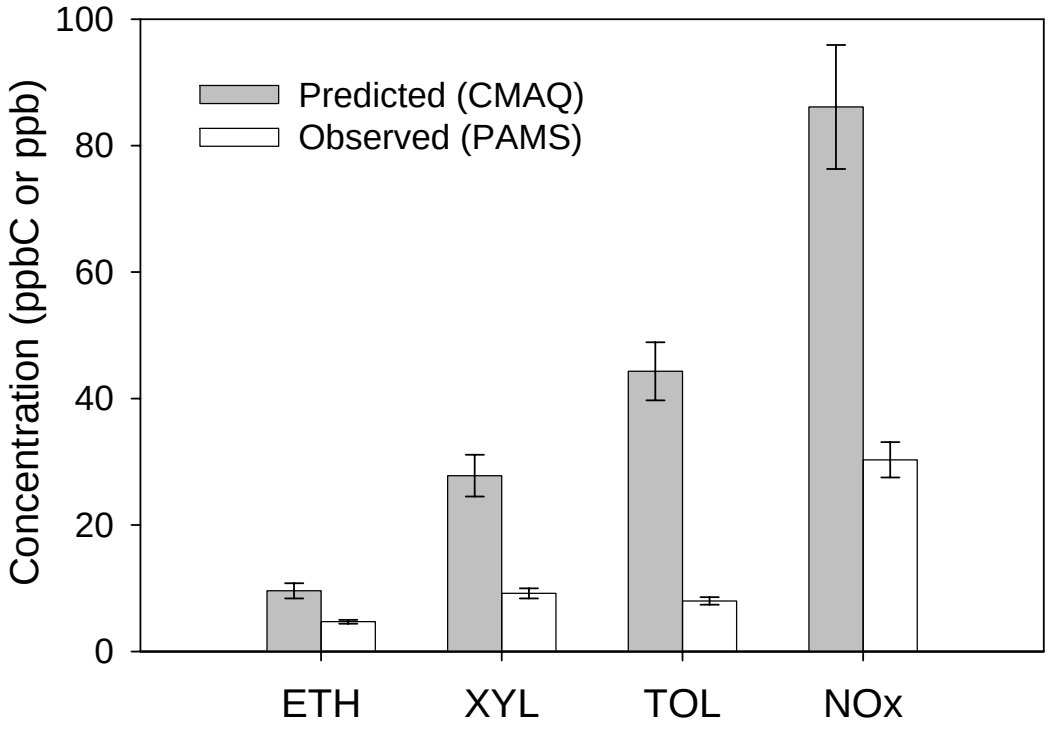

Figure 4.6: Comparison of average concentrations between the predicted (CMAQ) and the observed values in the morning from 6:00 a.m. to 9:00 a.m. for McMillan reservoir, DC. The error bars indicate the two-sigma standard errors of the means (95% confidence interval).

At the Camden site in New Jersey (NJ), the estimated emission ratios for the grid cells surrounding the site are spatially non-homogeneous with large emissions gradients observed among grid cells in the inventory. As shown in Figure 4.7, the ratios of all three species from CMAQ and SMOKE show overestimation. In particular, the estimated TOL/NOx ratio is two to three times higher than the observed ratio. The comparison of concentrations shows the same trend of overestimation, as indicated in Figure 4.8. Also, the relative contributions of sources to emission estimates are very similar to those at the other two PAMS sites.

In addition, we adjusted NOx or CO in the ratios in accordance with the comparison of CMAQ outputs and observations in order to look at whether the result would be affected if the NOx or CO estimations were wrong. Figure 4.9 shows the ratio comparison of TOL to adjusted NOx or CO for Essex, MD and Camden, NJ sites. The McMillan reservoir site in DC was excluded because of concern that the mixing height was wrong so that the estimated concentrations at this site did not reflect real values. As shown in Figures 4.4 and 4.8, NOx or CO is slightly overestimated. We can expect that the extent of overestimation in the ratios with the adjustment of NOx or CO to the ambient value will be larger than without adjustment. Hence, Figure 4.9 reveals the overestimate of TOL becomes larger after adjusting NOx or CO.

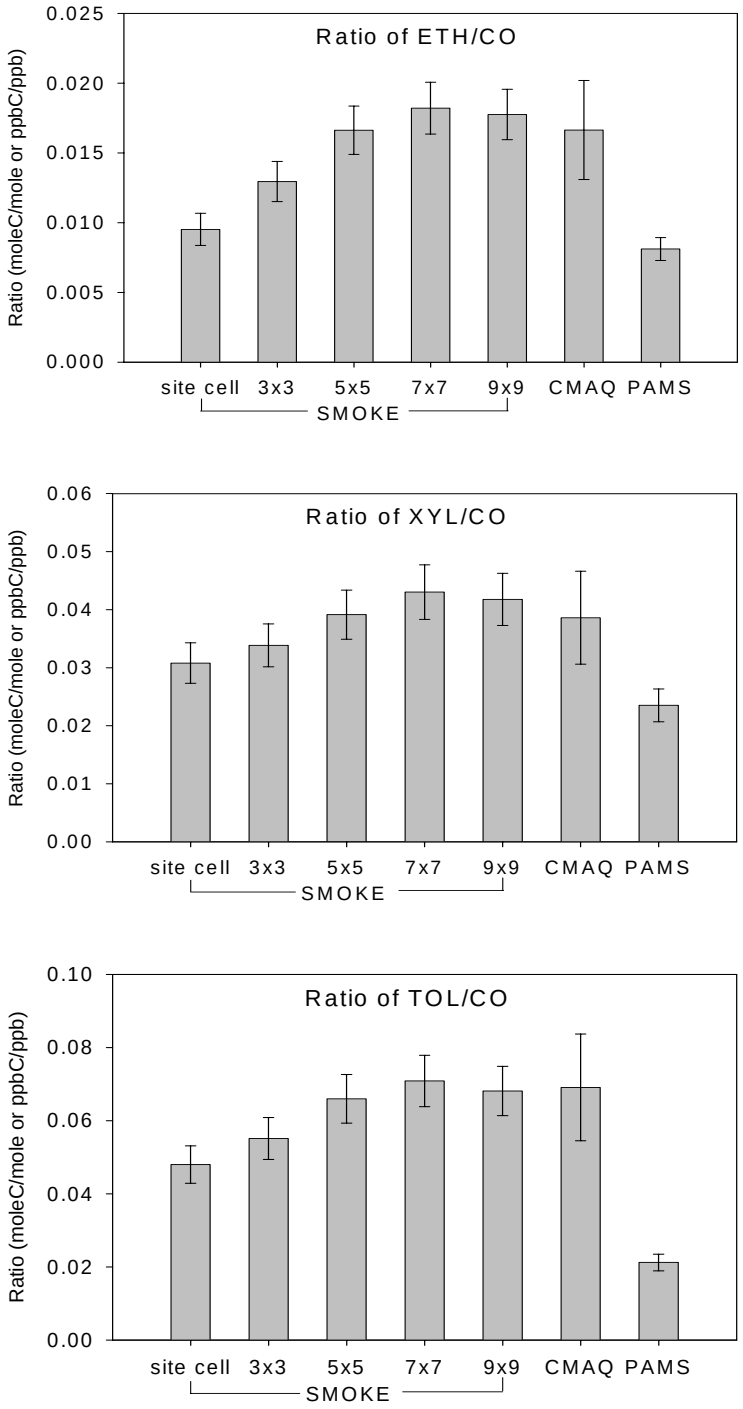

Figure 4.7: Comparison of average ratios between the estimated (SMOKE or CMAQ) and the observed values in the morning from 6:00 a.m. to 9:00 a.m. for Camden, NJ. The error bars indicate the two-sigma standard errors of the means (95% confidence interval).

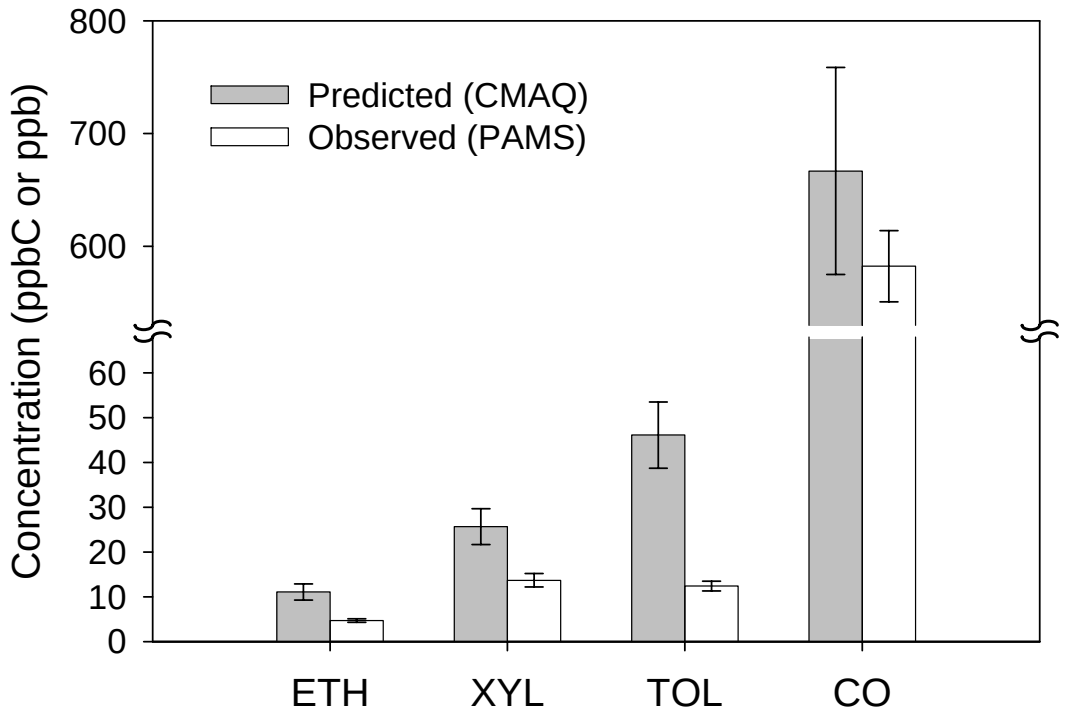

Figure 4.8: Comparison of average concentrations between the predicted (CMAQ) and the observed values in the morning from 6:00 a.m. to 9:00 a.m. for Camden, NJ. The error bars indicate the two-sigma standard errors of the means (95% confidence interval).

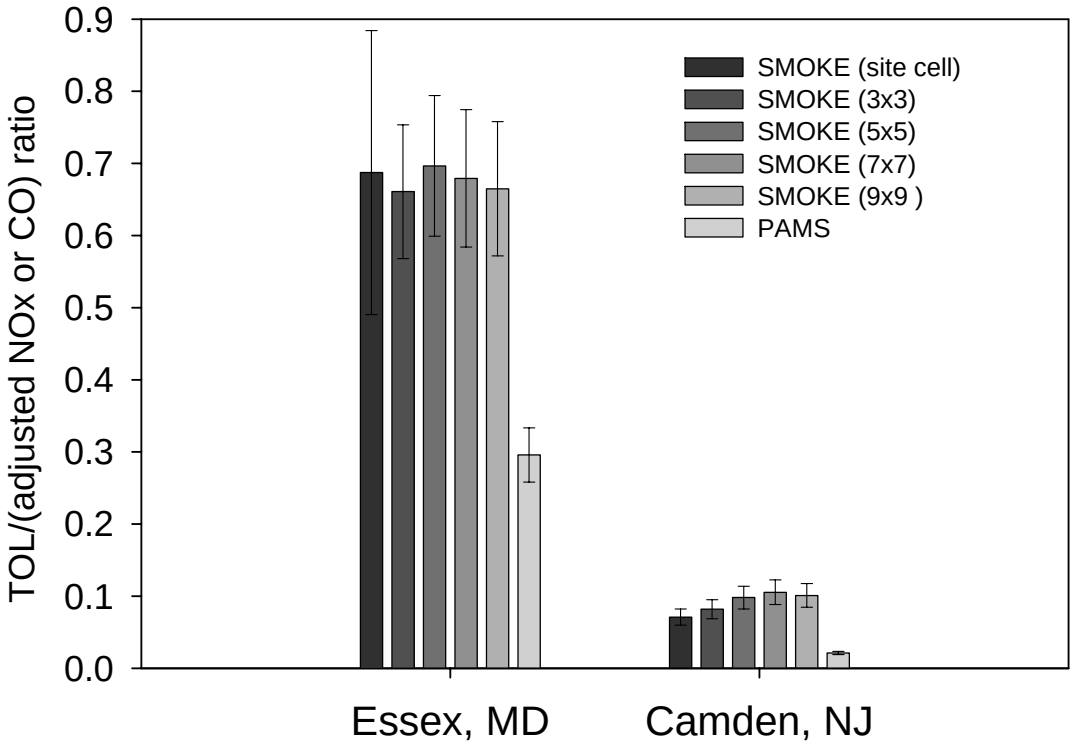

Figure 4.9: Comparison of average ratios of TOL to adjusted NOx or CO between the estimated (SMOKE) and the observed values in the morning period of 6:00 a.m. to 9:00 a.m. The error bars indicate the two-sigma standard errors of the means (95% confidence interval).

As stated above, the results for all three sites suggest a significant overestimate of solvent emissions while the estimates of emissions from vehicle exhaust differ depending on location. However, the observed TOL might under-represent the actual concentration because of the unidentified portion in PAMS observations as mentioned earlier; this result is very dependent upon the VOC speciation step in SMOKE. If the speciation of VOC does not represent reality, this comparison might lead to an erroneous conclusion. Therefore, we implemented another method of evaluation of emissions estimates from vehicle exhaust and solvent sources, a source apportionment technique. The next section describes the method and the results.

4.4.2 Comparison of ratios of VOC source categories using a source apportionment model

To identify and apportion VOC sources, the UNMIX 2.4 receptor model was used. The details about the UNMIX were described in the Chapter 3.

Using PAMS measurements from Essex, MD, six possible VOC emission sources were identified: vehicle exhaust, gasoline vapor, liquid gasoline, solvent, natural gas, and biogenics. The procedure of identification of source categories is described in the study of VOC emissions sources in the Baltimore area using PAMS measurements by Choi and Ehrman (2004). As for the DC and NJ measurements, we could not identify distinct solvent sources of VOC using UNMIX. The unexplained source categories, which may represent real sources or mixtures of real sources, were extracted by using UNMIX at the two sites. The composition of each of these source

categories showed a high portion of toluene, suggesting a possibility that a solvent source category may be mixed into other source categories instead of being separated out as a distinct category. Refer to Appendix 2 regarding source apportionment results. Hence, we focus here on the source apportionment results from the Essex site, MD, only.

Figure 4.10 shows a comparison of the average ratios of VOC source contributions to total NOx estimated from SMOKE and UNMIX at Essex, MD. The ratios for vehicle exhaust are underestimated. In contrast, the SMOKE solvent source contribution from SMOKE is three times higher than for the source apportionment. This overestimate of solvent sources is consistent with the results for the comparison of individual VOC species in the previous section. We could not perform the same comparison using the DC and NJ measurements, but the consistency of the results between VOC species comparison and VOC source contribution comparison at the Essex site suggests that the overestimate of emissions from solvent sources may also occur at the McMillan Reservoir in DC and the Camden in NJ sites.

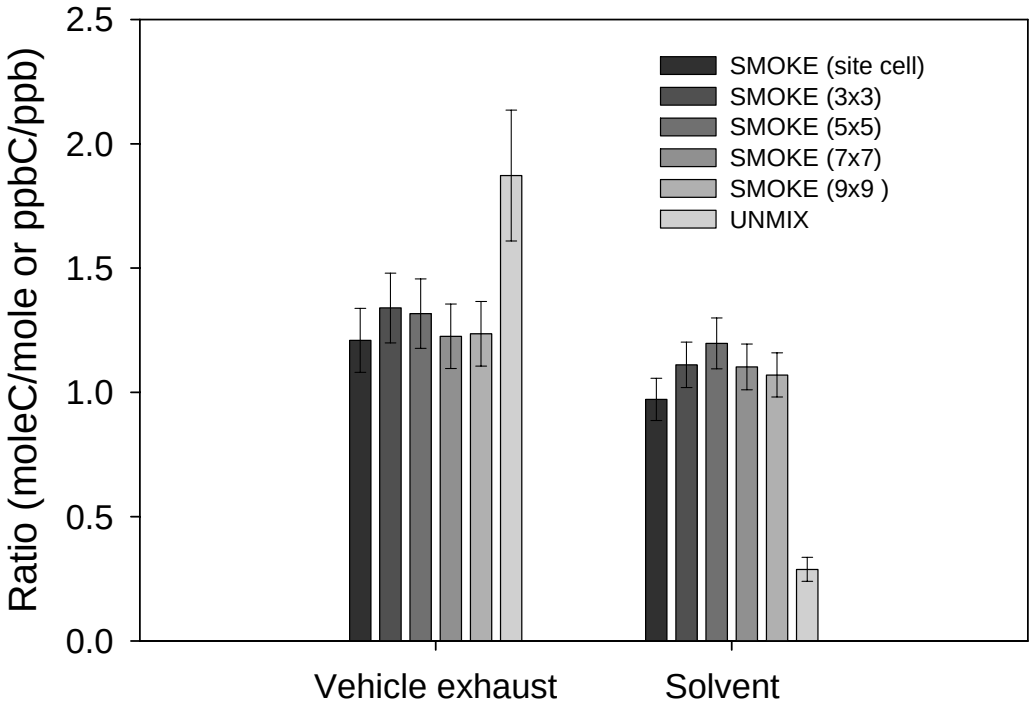

Figure 4.10: Comparison of average ratio of each VOC source contribution to NOx between estimates from SMOKE and UNMIX for Essex, MD in the morning from 6:00 a.m. to 9:00 a.m. The error bars indicate the two-sigma standard errors of the means (95% confidence interval).

4.4.3 Modeling the impact of VOC solvent source emissions reduction on ozone and anthropogenic secondary organic aerosol (SOA) concentrations

Parrish et al. and Demerjian pointed out the uncertainties associated with PAMS measurements (Parrish et al., 1998, 2000; Demerjian, 2000). According to an internal consistency test of PAMS measurements at several observation sites by Parrish et al. (1998), poor precision and systematic measurement errors were present in the PAMS measurements. Our study was based on PAMS measurements, and a certain degree of uncertainty may exist in the results. Nevertheless, there are several studies suggesting a result for solvent emissions similar to this study. Mannschreck et al. evaluated an emissions inventory for the city of Augsburg in Germany using an extensive comparison between individual hydrocarbons (HC_i) to total measured hydrocarbons (HC_{sum}), HC_i/CO, HC_{sum}/CO, and HC_{sum}/NO emission ratios from measured concentrations and modeled emissions (Mannschreck et al., 2002). Their results showed a possible overestimate of emissions from solvent sources. Mannschreck et al. suggested a further analysis from measurements including oxygenated and halogenated VOC, which are important solvent components, and implementation of a source apportionment model. In addition, Watson et al. reviewed VOC source apportionment using the CMB method in more than 20 urban areas, mainly in the United States, and pointed out that coatings and solvent contributions were much lower than the proportions attributed to these sources in current emissions inventories (Watson et al., 2001).

Even though we cannot perform further analysis using oxygenated and halogenated VOCs, use of two different approaches at the Essex, MD PAMS site - relative and absolute comparison of individual species, and relative comparison of source contribution to NOx - leads to a similar conclusion about the estimate of solvent source emissions. The other two sites also showed patterns of overestimates of TOL like those at the Essex site, suggesting that overestimation of solvent sources in urban and suburban areas may be a general phenomenon, as Watson et al. pointed in their review (Watson et al., 2001).

Based on the findings of this study and other studies, the impact of a reduction of solvent source VOC emissions on ozone and anthropogenic SOA concentrations in the study domain was investigated using a photochemical air quality model. VOC emissions from solvent sources throughout the study domain were reduced by 50 %, in line with the average overestimation at the three PAMS sites. This reduction corresponds to 16% reduction of total VOC emissions. A CMAQ simulation was performed with this modified emissions inventory. Figure 4.11 compares the frequency distributions of hourly surface ozone and anthropogenic SOA concentrations for the base case and the 50% reduction in solvent VOC emissions case. As for ozone, there is little difference between these cases. The maximum difference in ozone concentration between the two cases when time and space are paired was less than 10 ppb. The solvent emissions around the three PAMS sites are roughly speciated to 55% PAR, 25% TOL, 11% NR, and 8% XYL. According to a study of photochemical ozone creation potential (POCP) for organic compounds by Derwent et al. and a study of ozone reactivity scales for VOCs by Carter, TOL (toluene group)

shows one third to a half of the ozone forming potential of XYL (xylene group), which has approximately as high an ozone forming potential as isoprene (Derwent et al., 1998; Carter, 1994). Hence, the undetectable change of ozone after a solvent emissions reduction may result from solvent emissions being dominated by VOC species that do not have high ozone forming potentials. As another reason, it is speculated that this region has NOx-sensitive characteristics, such that VOC control does not result in a remarkable change of ozone concentration. When it comes to anthropogenic SOA, the difference between two cases is not substantial. However, we can see a noticeable decrease of SOA concentrations in with 50% solvent emissions reduction. TOL and XYL have been studied as precursors of secondary organic aerosol, and their aerosol yields are approximately similar (Bowman et al., 1995; Apndis et al., 1992).

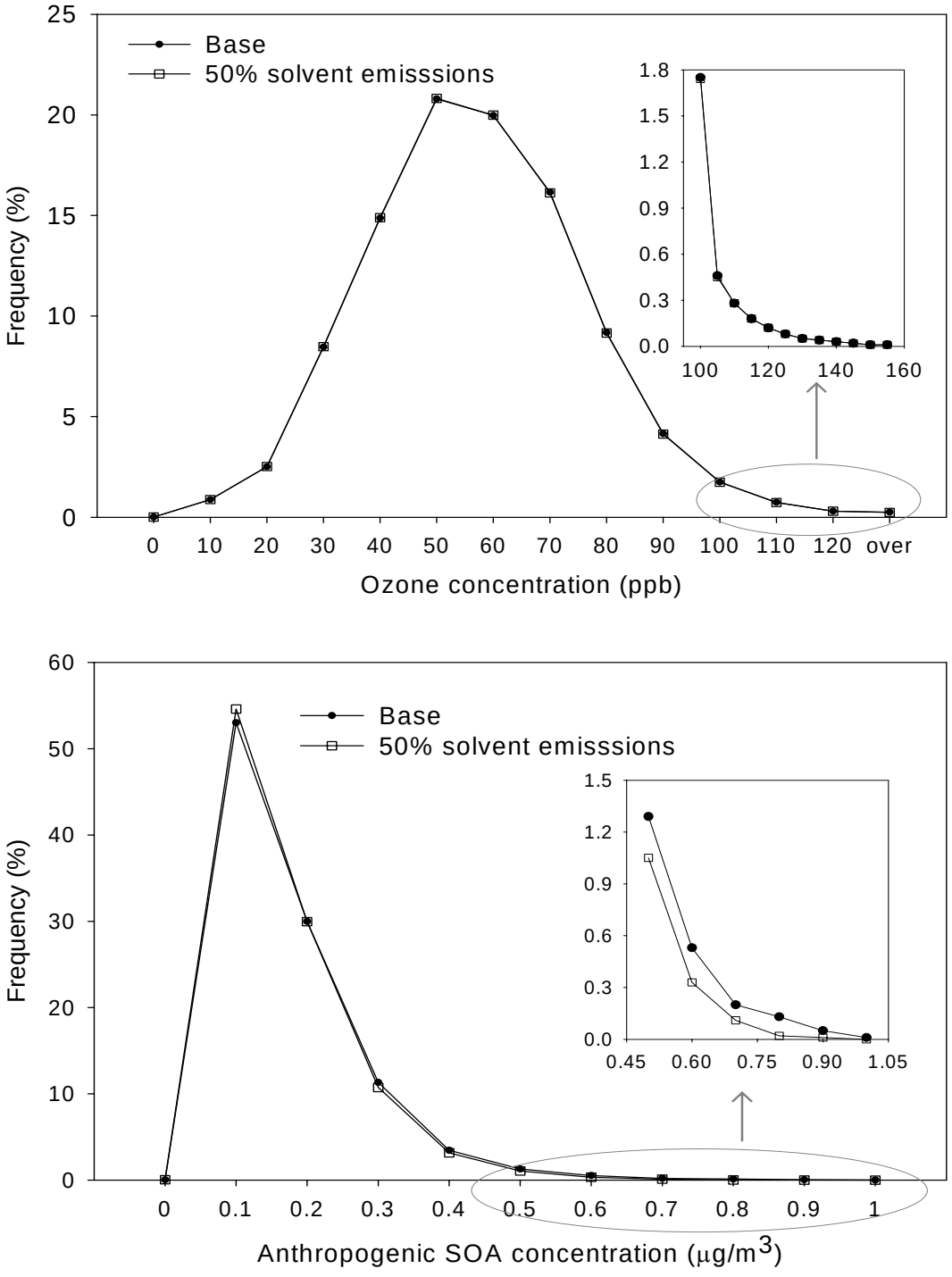

Figure 4.11: Comparison of the frequency distributions of hourly surface ozone and anthropogenic SOA concentrations between the base case and the case with 50% of the total solvent VOC emissions from July 8 to July 20, 1997, based on all grids in the modeling domain.

4.5 Conclusions

At the Essex, MD and McMillan reservoir, DC sites the comparisons of ETH/NOx and XYL/NOx ratios between estimates and measurements, and the comparisons of predicted ETH and XYL concentrations to the corresponding observed concentrations showed some differences between methods. However, the results for the Camden, NJ site demonstrated consistent results between comparison methods, implying a possible overestimate of vehicle exhaust. In terms of TOL, which is mainly emitted from solvent sources, the ratio of TOL to NOx as well as absolute concentrations of TOL and NOx revealed overestimates of solvent sources by a factor of 1.5 to 3 at all three sites. In addition, overestimates of solvent source emissions were corroborated by comparing ratios of VOC solvent source contribution to NOx to the ratio from SMOKE at the Essex, MD PAMS site. Other investigators also proposed that solvent sources were overestimated, implying the possibility of inaccurate emission factors in estimating VOC emissions from solvent sources. Hence, we recommend further investigation of the emissions inventory of solvent sources and their emission factors.

The photochemical model simulations did not show a perceptible change in ozone concentrations after the reduction of solvent VOC emissions, possibly because this region is NOx-sensitive, or because the solvent chemical species do not readily form ozone. However, a noticeable decrease of high SOA concentrations with 50% solvent emissions reduction was observed.

Chapter 5: Regional-scale Ozone Air Quality Modeling over the Baltimore/Washington Ozone Non-attainment Area: Characteristics of a Multi-day Ozone Event and Development of an Optimal Control Strategy

5.1 Introduction

The lifetime of ozone is longer in the free troposphere than near the surface, and meteorological processes play a critical role in transport and diffusion as well as chemical transformation (Jonson et al., 2001). Additionally, transport of pollutants on the order of 100 km-500 km across state boundaries has been reported within the northeastern U.S. (Samson and Shi, 1988; NRC, 1991; Solomon et al., 2000). Therefore, local emissions of ozone precursors cannot be entirely responsible for the ozone events in individual urban areas exceeding National Ambient Air Quality Standard (NAAQS).

Horizontal transport within the PBL is described in detail by Hidy (2000) and Solomon et al. (2000). For example, the PBL can be separated into three layers: a nocturnal surface boundary layer from the ground to about 400 m, an intermediate layer from 400-1000 m, and a sub-synoptic layer above 1000 m to the free atmosphere around 1.5 km. Note that the height of each layer varies greatly depending on time and geographical location. At night, the lower two layers are often decoupled, while

during daytime these two layers become mixed. Furthermore, all three layers are frequently well blended in the middle of the day. In the surface boundary layer, local dynamic processes such as surface friction are predominant. In the intermediate layer, local scale and mesoscale phenomena coexist. In the upper layer, synoptic scale phenomena dominate. Hence, the origins of winds in these three layers are most likely to be different. In the upper two layers of the PBL, usually called the nocturnal residual layer, pollutants can be transported during the night over long distances with faster winds than at the surface. In the morning as the ground starts to heat up, warm air above the ground ascends, forcing the growth of the mixing layer. As the mixing layer grows, pollutants trapped aloft in the nocturnal residual layer can be entrained downward into the mixing layer (Zhang and Rao, 1999). Based on this characteristic of the diurnal variation of the PBL, and subsequent vertical distribution of pollutant concentrations, most ozone events are a product of both long distance transport of pollutants and in-situ photochemical production.

There are several areas in the Northeastern United States with elevated ozone levels often exceeding the NAAQS. In particular, the highest ozone concentrations in the Northeastern U.S. occur across the Northeast Corridor of the United States, a relatively concentrated string of urban centers extending from Washington D.C. to Boston (Kumar and Russell, 1996). With a focus on the Baltimore-Washington (B-W) ozone non-attainment area, the extreme ozone events occur during multi-day episodes. These events can be regional in scale, with ozone concentrations exceeding the NAAQS at numerous locations along the East Coast. According to an analysis in the mid-Atlantic by Ryan et al. (2000), high ozone events are typically associated with a

slow moving, high-pressure system overhead or just west of the region and an upper air ridge to the west or northwest. The ridge maximizes the local potential for ozone formation by causing subsidence downstream of the ridge axis. The subsidence inhibits cloud formation and strengthens the low level inversion so that photochemistry is maximized and vertical mixing of low-level emissions is minimized. In addition, the upper air ridge to the west of the region leads to transport of air from heavily industrialized areas west and northwest of the Baltimore/Washington region (NRC, 1991; Ryan et al., 1998).

Ryan et al. (1998) showed the impact of significant regional scale transport of ozone and its precursors on an ozone event in July 1995 in this region through an analysis of observations and calculation of back trajectories. However, with only an observational analysis, we cannot reach a conclusion as to the relative impacts of long-range transport of ozone and its precursors versus local emissions on the ozone events in the region. For that reason, we employed a three dimensional photochemical model in order to study an ozone episode during July 1997, which showed a similar synoptic meteorological pattern to historically typical ozone events.

The focus of this modeling study is three-fold:1) to investigate the relative impact of long-range transport of ozone and precursors versus local emissions on high ozone occurrences in the Baltimore/Washington ozone non-attainment area, 2) to investigate the relative contribution of biogenic VOC emissions and anthropogenic VOC emissions to local ozone production during ozone events, and 3) to identify and apply control strategies leading towards ozone reduction. As stated earlier, ozone events are combinations of long-range transport and local generation. Hence, in order

to come to an effective control strategy for ozone reduction, it is necessary to identify the relative importance of long-range transport and local emissions. After that, we can focus on the dependence of ozone formation on local emissions. In this study, in particular, the relative impact of biogenic VOC emissions versus local anthropogenic VOC emissions on local ozone production was compared. Our motivation is that only anthropogenic emissions can be controlled, and a significant role of biogenic VOC in rural areas as well as in many urban and suburban locations in ozone formation has been reported based upon several observation-based studies (Chameides et al., 1988, 1992; Cardelino and Chameides, 1995, 2000; Morales-Morales, 1998; Choi and Ehrman, 2004). Several modeling studies have suggested that in general, VOC controls might be effective in reducing ozone levels in urban and suburban areas, which are most strongly impacted by anthropogenic emissions (McKeen et al., 1991; Possiel and Cox, 1993; Hanna, 1996). However, the biogenic emissions used in modeling studies in the past are now considered most likely underestimated (Guenter et al., 2000; Russell et al., 2000). Consequently, VOC control for certain urban and suburban areas might not lead to sufficient ozone reductions. Thus, modeling-based as well as observation-based studies of the importance of biogenic VOC emissions in ozone events for the region of interest are warranted, and the results should be consistent with each other. With this information, reliable control strategies for anthropogenic emissions for urban and suburban areas can be developed.

Morales-Morales (1998) and Choi and Ehrman (2004) suggested a significant contribution of biogenic VOC emissions to local ozone production in the Baltimore area based upon observed measurements. The second focus of this modeling study is

to investigate the relative contributions of local biogenic VOC emissions versus local anthropogenic VOC emissions on high ozone events. Finally, several local control scenarios were applied to identify a possible control strategy for reducing high ozone events in the Baltimore/Washington ozone non-attainment area.

5.2 Methods

5.2.1 Description of the modeling system

In this study, we implemented a three-dimensional modeling system that consists of MM5 version 3.3, the SMOKE version 1.4 and the CMAQ version 4.3. MM5 is used to provide meteorological input fields for the model simulation in SMOKE and CMAQ. The MM5 simulations, consisting of the two nested grid domains with resolutions of 36 km, and 12 km, were conducted with a modified Blackadar PBL scheme and standard nudging process by the Department of Meteorology, University of Maryland (Sistla et al., 2002; Zhang and Zheng, 2004). The meteorological variables were extracted using MCIP version 2.2. This program was also used to provide meteorological variables at the 4 km grid resolution by interpolating 12 km grid results. Figure 5.1 shows the modeling domain for three nested grids with 36 km, 12 km, and 4 km resolution. The detailed study domain, nested within the outer domains, covers the entire state of Maryland, and parts of Virginia, West Virginia, Delaware, New Jersey, and Pennsylvania. The detailed domain has 108 columns by 78 rows with 4 km horizontal grid cell resolution.

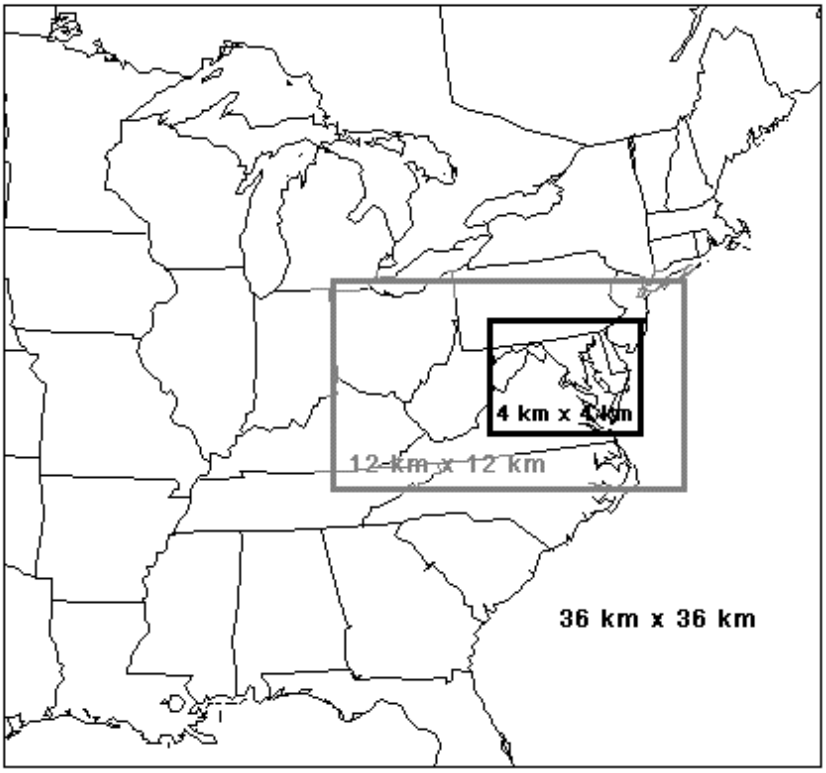

Figure 5.1: Map of CMAQ modeling domain.

There are 16 vertical layers extending from the surface to approximately 20 km above the ground. The vertical layers are unevenly distributed with higher resolution at lower levels to better resolve boundary layer phenomena. The total height of the lowest 8 layers is around 1.5 km, and the surface layer height is about 30 m.

In this study, an aggregated emissions inventory was obtained from the Mid-Atlantic Regional Air Management Association (MARAMA). SMOKE processing using this emissions inventory was described in the Chapter 4.

In the CMAQ chemistry and transport model, the Modified Euler Backward Iterative (MEBI) chemistry solver was used (Dolwick et al., 2001). The chemistry mechanism employed by CMAQ is based on CB-IV, a chemical kinetic mechanism for urban and regional photochemistry, and contains 37 species and 96 reactions (EPA-III, 1999).

5.2.2 Modeling period

Our simulation period begins on July 5 and ends on July 20 1997. This period includes the most extensive episode of 1997, which occurred from July 12 to July 17. The weather pattern associated with this episode was very similar to the July 1995 episode. Aloft, a ridge formed over the region, resulting in decreased vertical motion, limited cloud formation, and strong photochemistry. In addition, a surface high-pressure system with widely spaced isobars created weak winds and limited horizontal ventilation. Also, the clear skies led to radiational cooling at night, which produced a surface inversion, and caused an even greater buildup of pollutants near the surface.

At the beginning of the July 12 to July 17, 1997 episode, a ridge moved into position west of the region, and ozone exceedances were reported on July 12 in Pennsylvania and Maryland, and spread into New York and New Jersey on July 13. Region-wide exceedances (from Virginia to Connecticut) were reported on July 14 and 15 (NESCAUM, 1998).

5.3 Organization of simulations

In this study, the simulations were divided into three main categories based on different objectives. Firstly, five simulations including the base case were conducted with the objective of investigating the contribution of long-range transport of pollutants versus local emissions to ozone episodes in the Baltimore/Washington ozone non-attainment region. The simulations were performed mainly by controlling output variables from the Boundary Condition (BCON) processor in CMAQ. BCON is used to generate species concentrations for the cells immediately surrounding the modeling domain from the existing three dimensional, gridded, time-variant concentration files of a coarser grid (Ching and Byun, 1999). In this case, the boundary condition files for the base case, with 4 km grid resolution, were obtained from the concentration files with 12 km grid resolution. Table 5.1 lists the identification (RUN) code, which will be referred to in the subsequent discussion, and the conditions of operation for each simulation. The "NoEmis" case has no emissions from both anthropogenic and biogenic sources within the modeling domain with 4 km grid resolution, but the boundary conditions are the same as the base case. This case

Table 5.1: Simulation details

Run Code	Operation Conditions	
	Emissions	Boundary conditions
Base	Normal emissions (biogenic & anthropogenic pollutants)	Normal B.C. (obtained from the runs with 12 km rid resolution)
NoEmis	No emissions	Normal B.C.
CleanBC	Normal emissions	Without O_3 and precursors
CleanOZ	Normal emissions	Without O_3 but with precursors
CleanPRE	Normal emissions	Without precursors but with O_3
CleanBC_woAVOC	Without anthropogenic VOC emissions but with other emissions	Without O_3 and precursors
CleanBC_woBVOC	Without biogenic VOC emissions but with other emissions	Without O_3 and precursors
Half_Anox	With 50 % reduction of anthropogenic NOx emissions	Normal B.C.
Half_Avoc	With 50 % reduction of anthropogenic VOC emissions	Normal B.C.
Half_Anox_Avoc	With 50 % reduction of both anthropogenic NOx and VOC emissions	Normal B.C.
HalfozBC_baseEMI	Normal emissions	With 50% reduction of ozone in B.C.
HalfozBC_halfAnox	With 50 % reduction of anthropogenic NOx emissions	With 50% reduction of ozone in B.C.

was included to probe how transported pollutants would evolve in the modeling domain. The clean boundary conditions or "CleanBC" case has the same emissions as the base case, but there are no pollutants such as ozone and its precursors in the boundary conditions. Here, the precursors denote NOy and VOC in terms of the CB-IV chemical mechanism as listed in Table 5.2. From this case, we expect to get insight into the impact of local contributions on an ozone episode in the modeling domain. The clean ozone precursors in the boundary condition or "CleanPRE" case have the same emissions as the base case. However, the boundary conditions do not include ozone precursors, NOy and VOC, but do include transported ozone. This simulation can provide insight into the impact of transported ozone on the ozone episode in the modeling domain. The clean ozone in the boundary conditions or "CleanOZ" case has the same emissions as the base case, while the boundary conditions include not ozone, but ozone precursors, NOy and VOC. This simulation can provide insight into the impact of transported ozone precursors on an ozone episode within the modeling domain.

Secondly, two additional simulations were carried out in order to test the relative contributions of biogenic VOC and anthropogenic VOC to local ozone production. The first one, the clean boundary conditions without anthropogenic VOC emissions or "CleanBC_woAVOC" case, has the same boundary conditions as the "CleanBC" case, and the anthropogenic VOC emissions are excluded, but the biogenic VOC emissions and both anthropogenic and biogenic NOx emissions are included.

Table 5.2: NOy, and VOC species list in terms of CB-IV chemical mechanism (Ching and Byun, 1999)

Symbol		Description
NOy	NO	Nitric oxide
	NO2	Nitrogen dioxide
	HONO	Nitrous acid
	NO3	Nitrogen trioxide
	N2O5	Nitrogen pentoxide
	HNO3	Nitric acid
	PNA	Peroxynitric acid
	PAN	Peroxyacyl nitrate
	NTR	Organic nitrate
VOC	PAR	Paraffin carbon bond
	ETH	Ethene
	OLE	Olefinic carbon bond
	TOL	7 carbon aromatics
	XYL	8 carbon aromatics
	ISOP	Isoprene
	FORM	Formaldehyde
	ALD2	Acetaldehyde and higher aldehydes
	MGLY	Methyl glyoxal
	CRES	Cresol and higher molecular weight phenols

The clean boundary conditions without biogenic VOC emissions or "CleanBC_woBVOC" case is different in that it excludes only biogenic VOC emissions with the same boundary conditions as the "CleanBC" case.

Lastly, five simulations were performed in order to investigate possible control strategies towards ozone mitigation for the Baltimore/Washington ozone non-attainment area. A 50% reduction of anthropogenic NOx emissions or "Half_Anox" case is the same as the Base case except that the anthropogenic NOx emissions in the domain were reduced to 50% of their original emissions. The "Half_Avoc" case has 50% reduction of anthropogenic VOC emissions, and the "Half_Anox_Avoc" case has 50% reduction of both anthropogenic NOx and VOC emissions, with the other conditions the same as the Base case. In the remaining two simulations, ozone concentrations in the boundary conditions were reduced by 50% in order to look at a reduction effect of long-range transport of ozone on ozone concentrations in this area. In one simulation, normal emissions in the modeling domain were used (HalfozBC_baseEMI), while in the other a 50% reduction of anthropogenic NOx emissions in the modeling domain was incorporated (HalfozBC_halfAnox).

5.4 Results and discussion

5.4.1 Model performance

CMAQ model performance was evaluated based on 1-hr surface ozone measurements for 56 observation sites in the modeling domain for July 8-July 20, 1997, and aircraft data measured during University of Maryland (UM) research flights

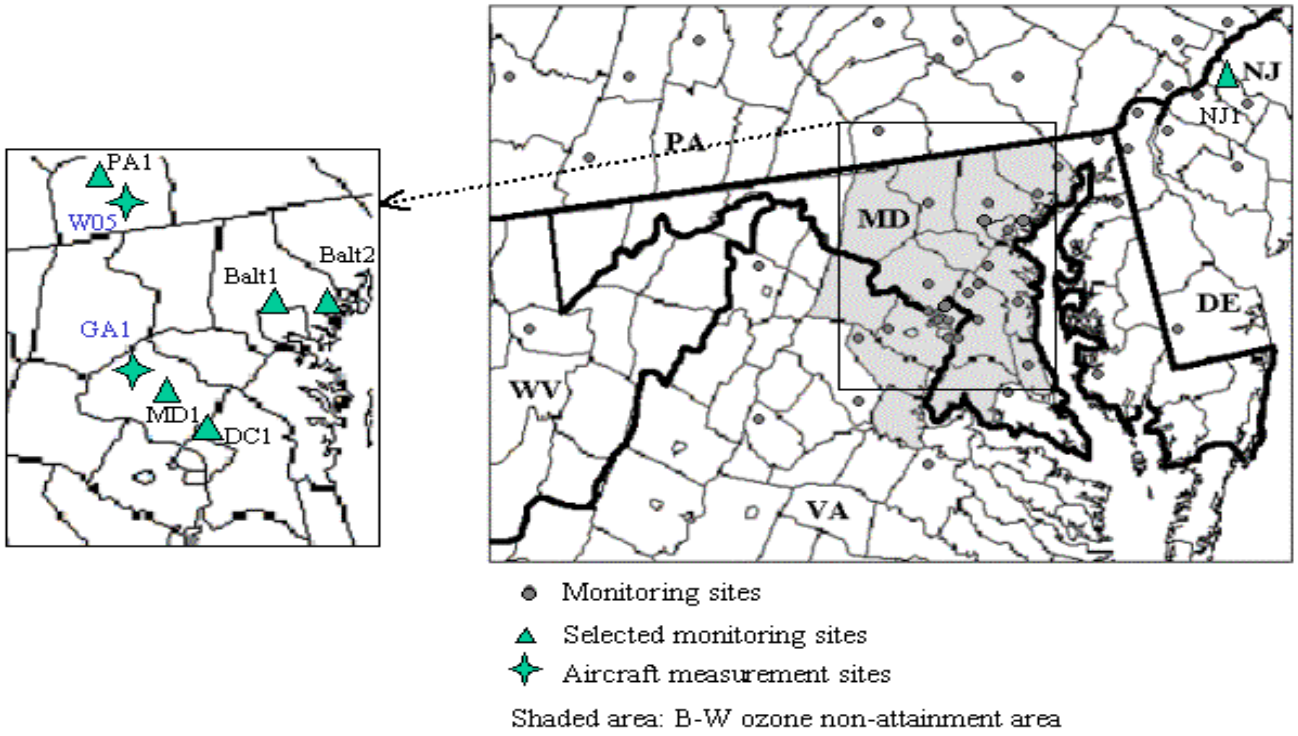

Figure 5.2: Map of the ozone monitoring sites. DE (Delaware), MD (Maryland), NJ (New Jersey), PA (Pennsylvania), VA (Virginia), and WV (West Virginia). Balt2 (Essex PAMS site), NJ1 (Camden PAMS site), and DC1 (McMillan reservoir PAMS site).

for July 12-July 17, 1997. Figure 5.2 shows the locations of the monitoring sites. The first three days are not included in the performance evaluation, and are considered model "spin-up" days.

Modeled ozone levels were statistically evaluated using measures, which are recommended by the U. S. EPA (EPA-V, 1991), for both a grid cell corresponding to the location of the observation sites and nine grid cells surrounding the observation sites. The statistical values for a grid cell and nine grid cells do not show a significant difference. The normalized bias is computed as the mean residual, where the residual is the predicted minus the observed concentration, divided by the corresponding observed concentration before averaging. Therefore, negative bias implies underprediction of observations by the model. Gross error is computed in the same manner as bias except that the absolute values of the residuals are used, so gross error is always positive. Note that underpredictions and overpredictions may offset one another in computing bias statistics. Whenever the observed ozone concentration is below the specified cutoff level of 60 ppb, the observed and predicted concentrations for that hour and location are not used in computing the performance statistics (McNair et al., 1996). It should be noted that even though the statistics have been extensively used for model evaluation, there is a concern that such statistical measures do not reveal model weaknesses. These recommendations were based on previous modeling studies, in which the models were tuned to improve the model performance. As such, use of these guidelines may not be appropriate for evaluation of more recently developed models (Russell and Dennis, 2000).

As shown in Table 5.3, the negative values of unpaired peak and normalized bias suggest a slight tendency toward underprediction, while normalized bias is somewhat over the EPA's guideline (Sistla et al., 2001; Yarwood et al., 2003). Figure 5.3 compares time series of modeled ozone to observed ozone at selected monitoring sites marked in Figure 5.2. The model prediction shows different results depending on the location of monitoring station. However, the model simulates well the times of the ozone peak within 2-3 hours during the ozone event days of July 12 to July 15 (Yarwood et al., 2003). In addition, we compared vertical ozone profiles observed and estimated at two aircraft measurement sites shown in Figure 5.2.

Table 5.3: Statistical analysis of model performance for ozone

Statistical measure	Model		Guidelines
	Site cell	Avg. for nine cells	
Unpaired peak (%)	-2.2	-5.4	$< \pm 20$
Normalized bias (%)	-21	-20	$< \pm 15$
Normalized gross error (%)	24	23	< 35
Correlation coefficient	0.75	0.76	

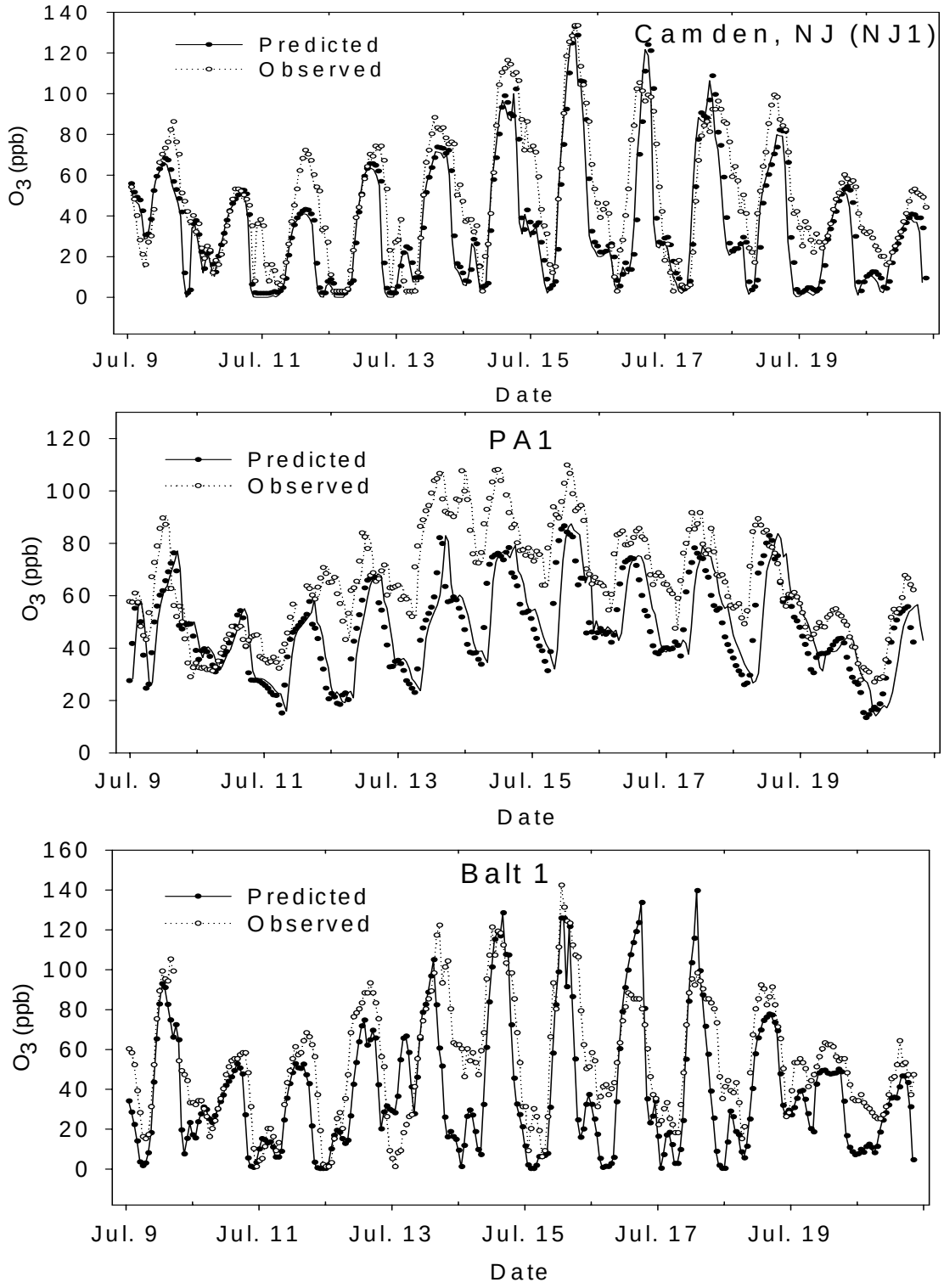

Figure 5.3: Time series of predicted (site grid cell) and observed ozone concentration for the selected sites for July 9 ~ 20, 1997.

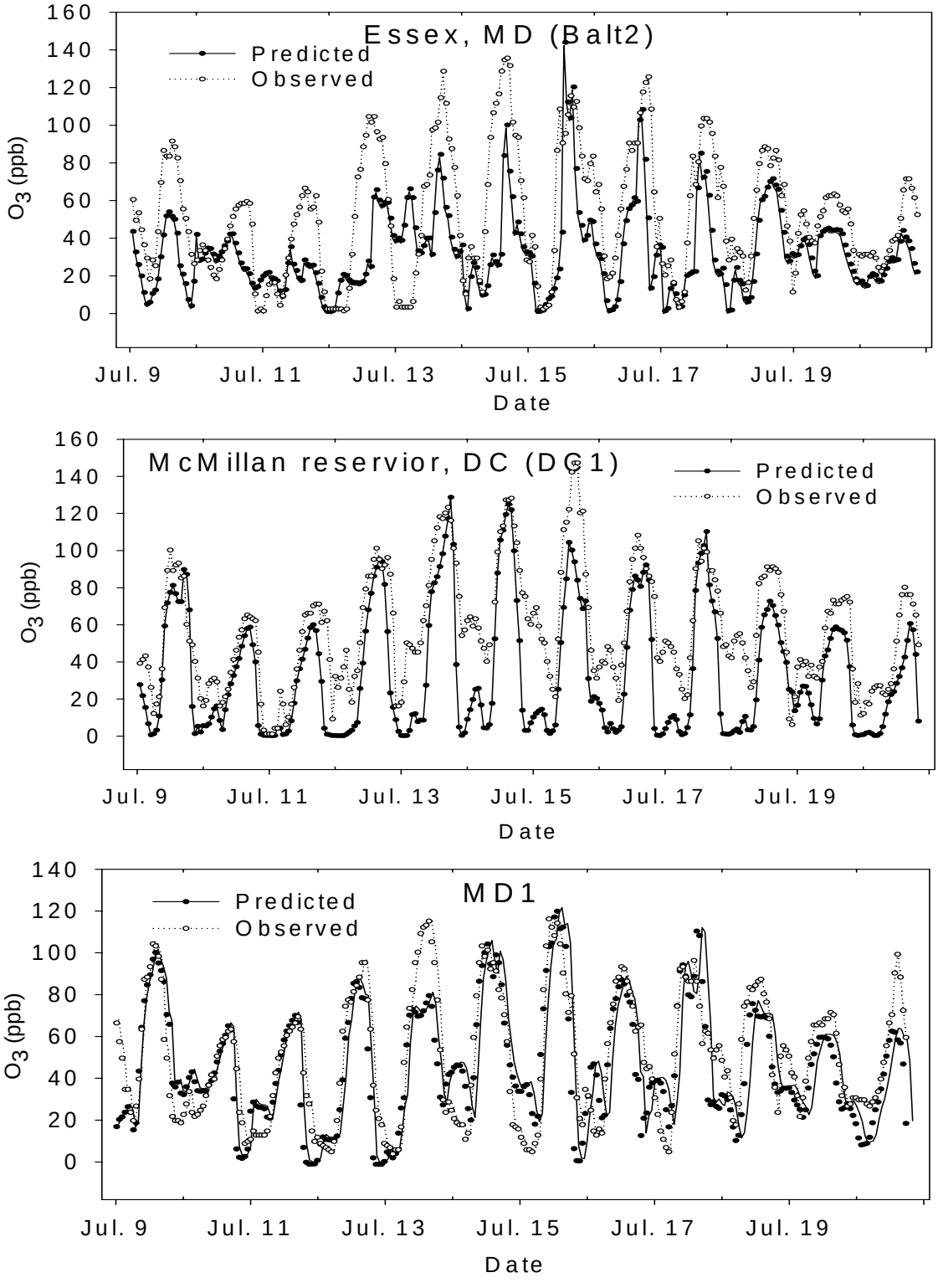

Figure 5.3: (continued)

Figures 5.4 and 5.5 show the comparison of predicted and observed vertical ozone profiles at two aircraft sites indicated in Figure 5.2. The CMAQ simulation of the morning of July 13 appears to underpredict the extraordinarily high ozone at about 0.8-1.5 km above the ground, which is within the nocturnal residual layer. Ozone contained in this layer can be a combination of the previous day's ozone by local photochemical generation and regional transport of ozone. Even under stagnant conditions at night near the surface, ozone can be transported by the nocturnal jet aloft (Aneja et al., 2000). Synoptic scale or mesoscale flow at this elevation is dominant during nighttime and just after sunrise, so that the underprediction of ozone at this elevation in the morning may suggest underprediction of long-range transport during the day. Hence, this seems linked to the negative normalized bias mentioned earlier, since the under-prediction of ozone aloft in the morning affects the surface ozone concentration after the mixing layer is fully developed. However, the measurements aloft are limited at these two sites, and the vertical ozone profiles on two later days (July 16 and 17) showed relatively good agreement between prediction and observation. Therefore, we cannot conclude that the CMAQ simulations in this study did not reproduce the long-range transport. Nevertheless, we should keep the possibility of under-prediction of long-range transport in mind in further analysis of the CMAQ simulation results. In particular, the significant underestimation of ozone concentrations in July 12 and 13 at the W05 site in Gettysburg, PA, is thought to be a combined result of underestimated emissions and underestimated transport. The two days are weekend days, and the SMOKE emission model allocates fewer emissions on weekends than weekdays.

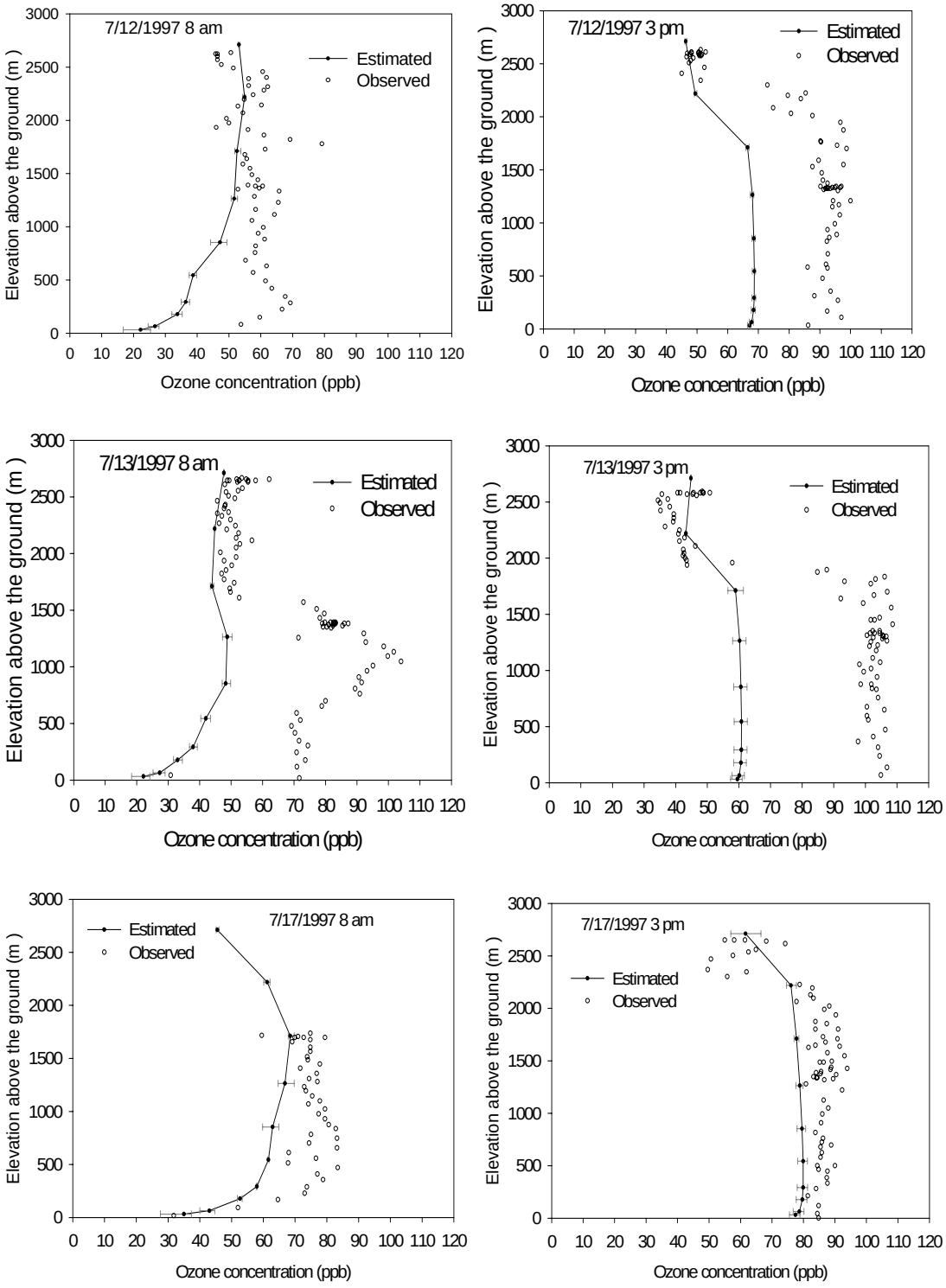

Figure 5.4: Comparison of estimated ozone (average of nine grid cells surrounding the observation site) with aircraft measurements at W05 (Gettysburg, PA). The horizontal bars indicate the minimum and maximum values in nine grid cells.

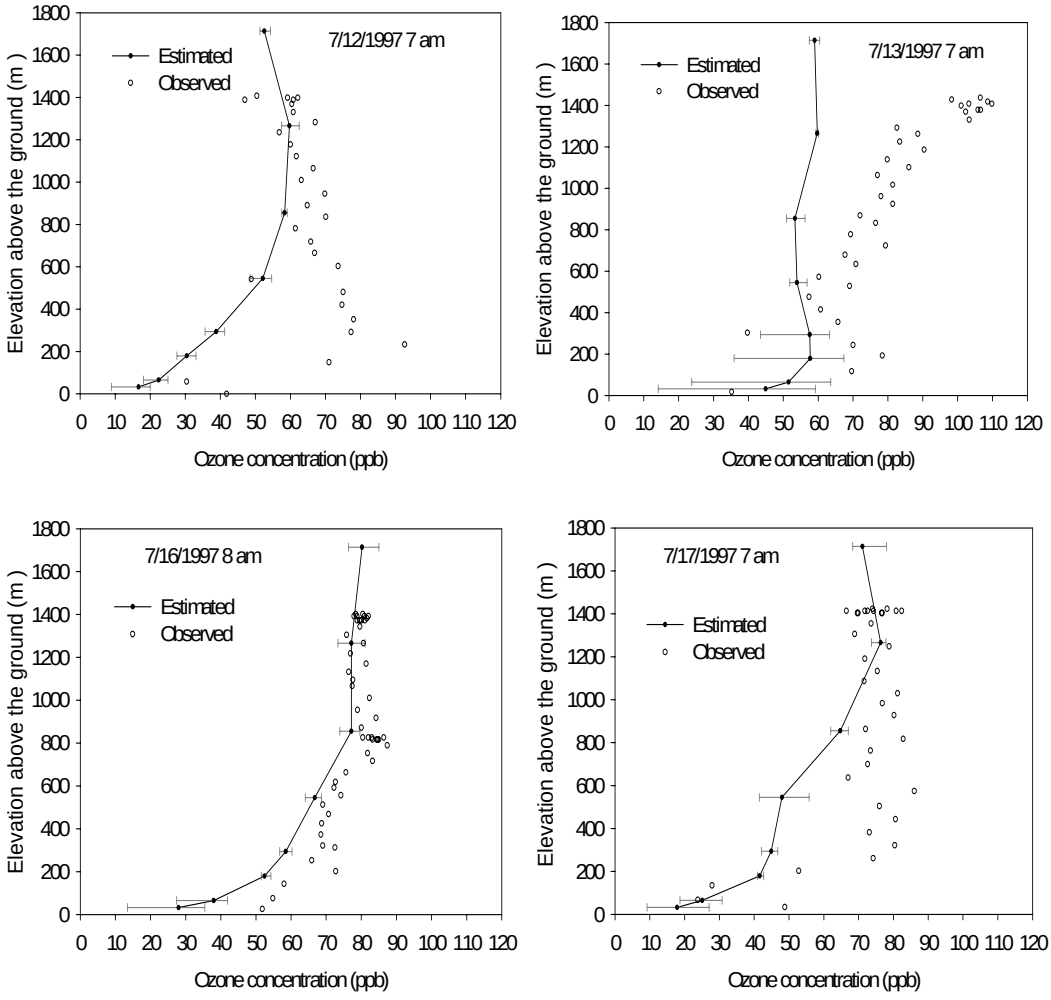

Figure 5.5: Comparison of estimated ozone (average of nine grid cells surrounding the observation site) with aircraft measurements at GAI (Montgomery, MD). The horizontal bars indicate the minimum and maximum values in nine grid cells.

The location is one of high weekend tourist activity in the summer, and SMOKE did not incorporate all possible extra activities at a specific location and a specific period with currently available temporal and spatial allocation factors.

The uncertainty of biogenic estimation remains an essential subject in the continuing debate on NOx versus VOC control, and we made a rough comparison of the estimated and observed isoprene at three PAMS sites located in urban/suburban areas that are shown in Figure 5.2. Taking into account that short-lived isoprene emissions are much more spatially heterogeneous than long-lived species, the comparison was done using the values at a site cell with 16 km^2 area and the average values for 3 cells x 3 cells surrounding the observation site. Figure 5.6 shows box plots of observed and estimated isoprene at the Essex site, MD for the site cell and 3 cells x 3 cells surrounding the Essex site. The black line across the box denotes the mean value, and the gray line across the box denotes the median value. The estimated isoprene concentrations agree with measured values better during the mid-day hours, when the atmosphere is well mixed and biogenic emissions are greatest, than during night. These differences during night are likely to be associated with problems with the modeled mixing height, nighttime chemistry representation, and/or deposition, rather than with emissions (Trainer et al., 2000; Pierce et al., 1998).

The isoprene emissions rates estimated using BEIS2, not shown here, were very small at night. When we take a closer look at the difference between the site cell comparison and nine cells comparison during daytime, the predictions show different behavior.

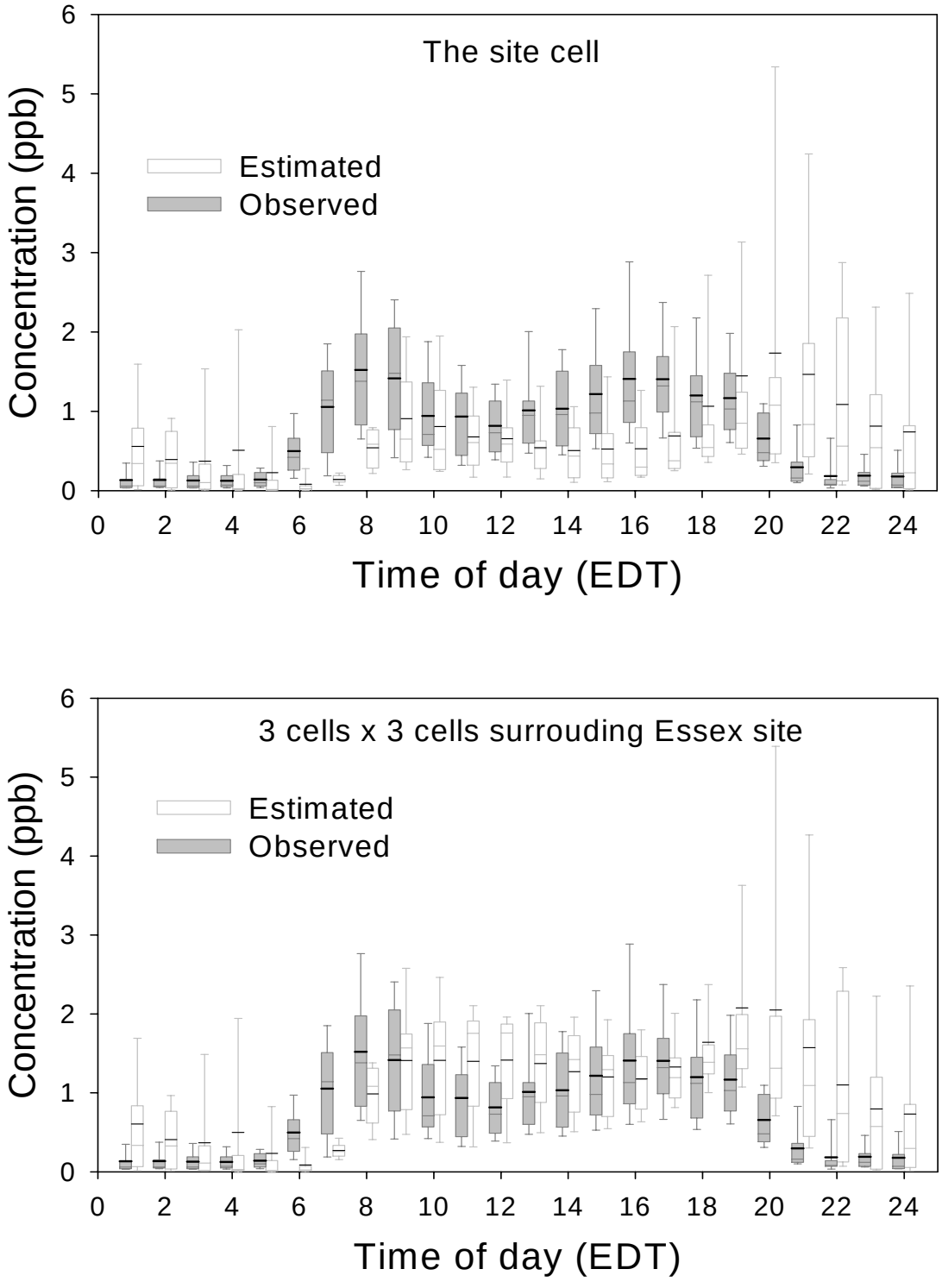

Figure 5.6: Comparison of observed and estimated isoprene during July 8 to July 20, 1997 at Essex site, MD for the site grid cell and 3 cells x 3 cells surrounding the Essex site (Balt2).

The predictions for the site cells are somewhat underpredicted, while those from the nine cells are slightly overestimated. In addition, the normalized bias using measured and predicted isoprene concentrations during daytime from 9 am to 6 pm at three PAMS sites was about + 40% for the nine cells comparison, and about –22% for the site cell comparison. Goldstein et al. (1998) found that BEIS2 underestimated the summer midday isoprene emission flux by at least 40% at Harvard forest, and Geron et al. (1997) pointed out that BEIS2 isoprene flux estimates are accurate to within about 50% from an analysis of published field flux studies. Our result seems consistent with those published studies.

There exist a wide variety of factors that could be responsible for isoprene overprediction or underprediction. These factors include chemical destruction rates, and horizontal advection, deposition, or vertical mixing in this modeling system (Pierce et al., 1998), as well as limitations associated with BEIS2. Andronache et al. (1994) recommended the use of measurements of isoprene concentration above at least 40 m rather than measurements near the surface because of the difficulties attributed to rapid and spatially heterogeneous processes of emissions, vertical diffusion, and surface chemistry (Pierce et al., 1998). Here, it is difficult to separate shortcomings originating from the complex modeling system from shortcomings from measurements. Since this analysis is limited to a few surface measurements located at urban/suburban sites, we are not confident about drawing conclusions regarding biogenic emissions modeling. However, assuming that land-use is well projected onto these fine grid cells, the site cell comparison might be more representative than the average of nine grid

cells. The underprediction of isoprene from the site cell comparison might be connected to the tendency for underprediction of ozone as mentioned earlier.

5.4.2 Investigation of transport vs. local contributions to ozone occurrences

Figures 5.7 through 5.10 show the surface ozone concentrations simulated for the ozone episode of July 1997, starting from July 12 to July 15 at the peak time of each day. From a comparison of the Base case, the NoEmis case and the CleanBC case (a, b, and c in Figures 5.7-5.10), it is seen that long-range transported pollutants, including ozone and its precursors (boundary conditions), have a significant influence on the ozone concentrations near the boundary cells, and the impact of long-range transport becomes less significant towards the center of the domain.

The Base case and the CleanPRE case (a and e in Figures 5.7-5.10) each show a similar distribution of ozone over the domain, while the CleanBC case and the CleanOZ case (c and d in Figures 5.7-5.10) look alike. These results imply that long-range transport of ozone has a more immediate influence on ozone concentration in the domain than transported ozone precursors. In addition, the contribution of transported ozone amounts to 40-90 ppb ozone for the area surrounding the Baltimore/Washington D.C ozone non-attainment area, while its contribution is less than 40 ppb for the Baltimore/Washington D.C. ozone non-attainment area.

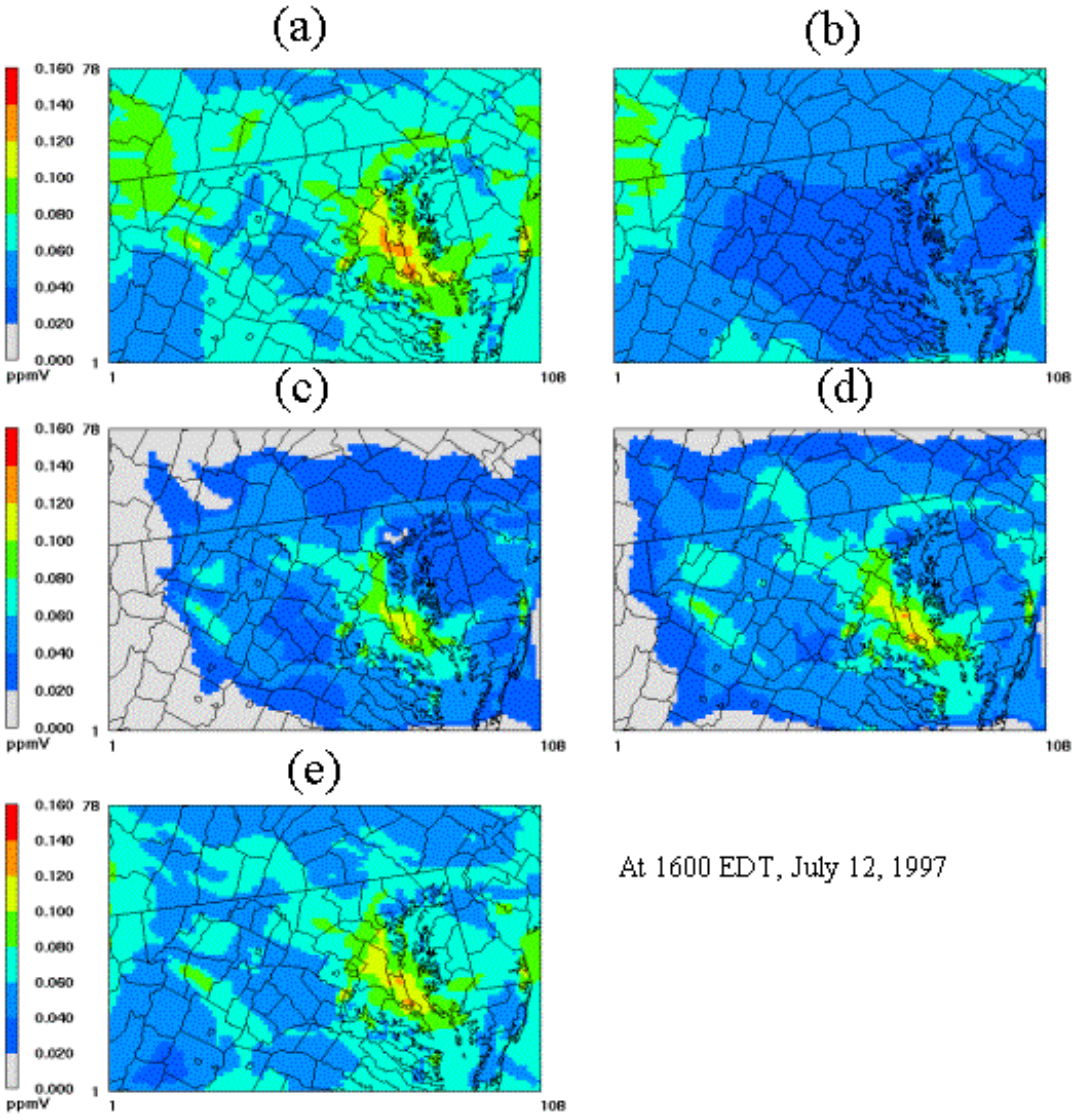

Figure 5.7: Surface ozone concentrations at 1600 EDT, July 12, 1997: (a) Base case, (b) NoEmis case, (c) CleanBC case, (d) CleanOZ case, and (e) CleanPRE case.

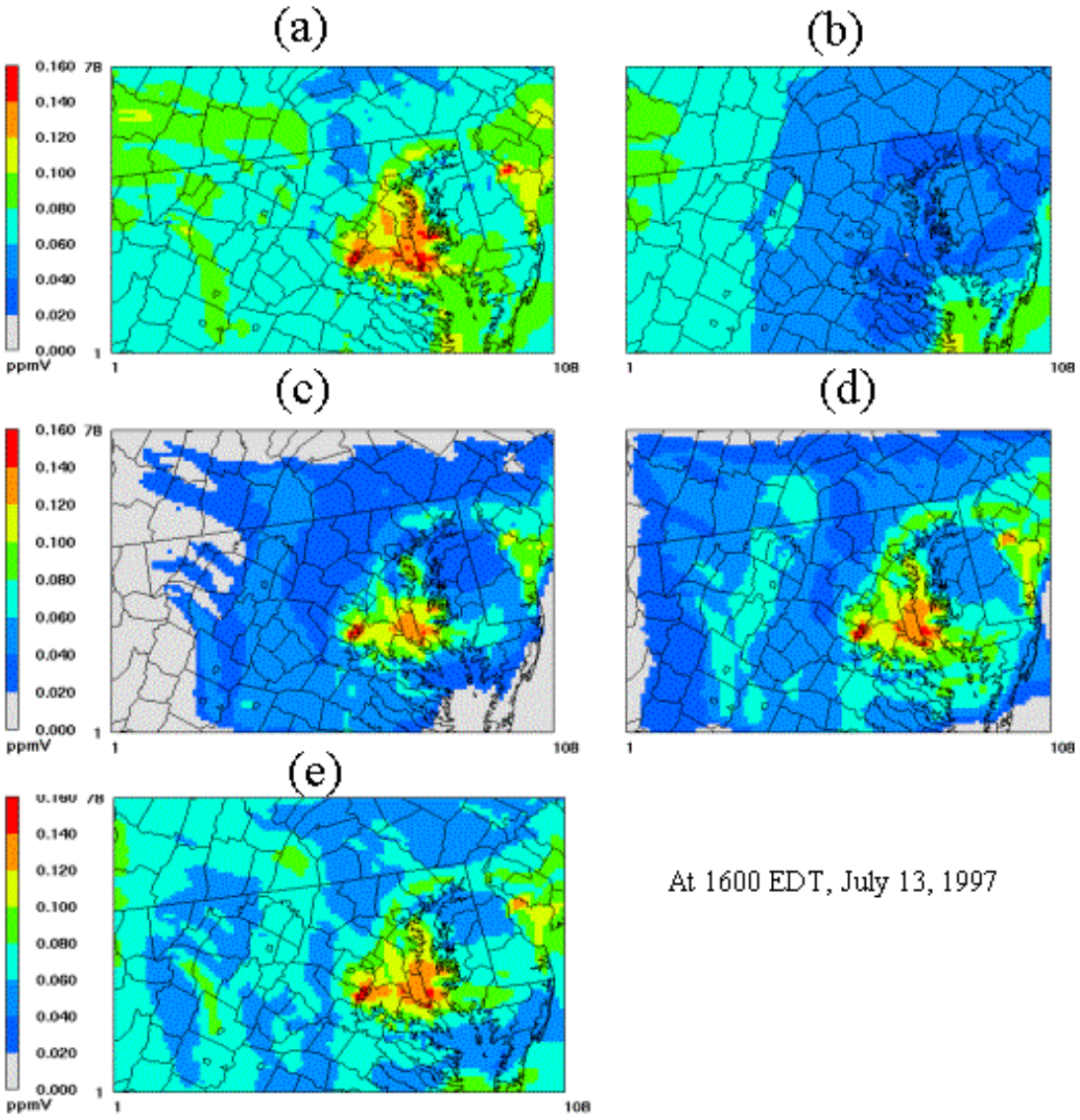

Figure 5.8: Surface ozone concentrations at 1600 EDT, July 13, 1997: (a) Base case, (b) NoEmis case, (c) CleanBC case, (d) CleanOZ case, and (e) CleanPRE case.

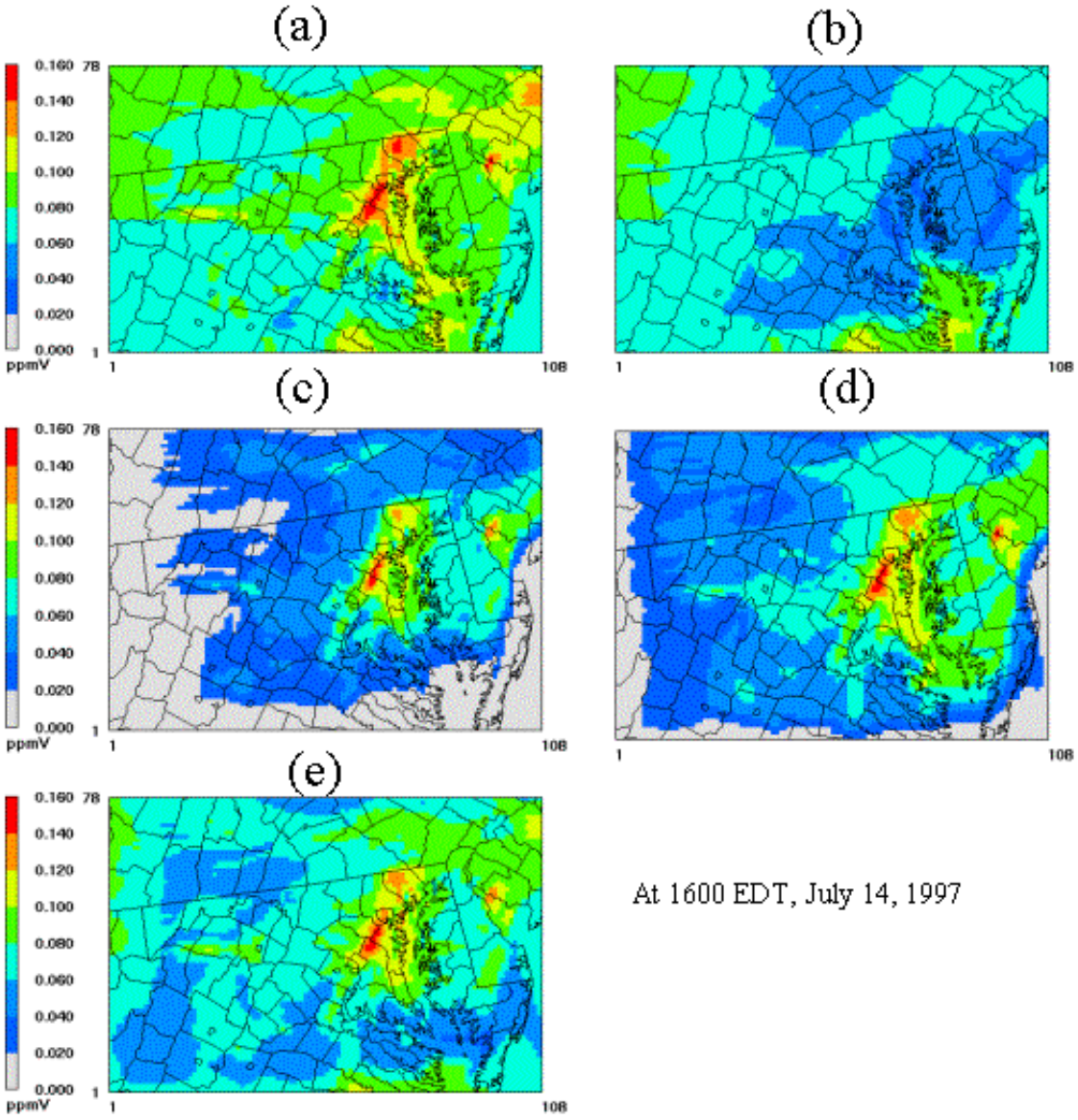

Figure 5.9: Surface ozone concentrations at 1600 EDT, July 14, 1997: (a) Base case, (b) NoEmis case, (c) CleanBC case, (d) CleanOZ case, and (e) CleanPRE case.

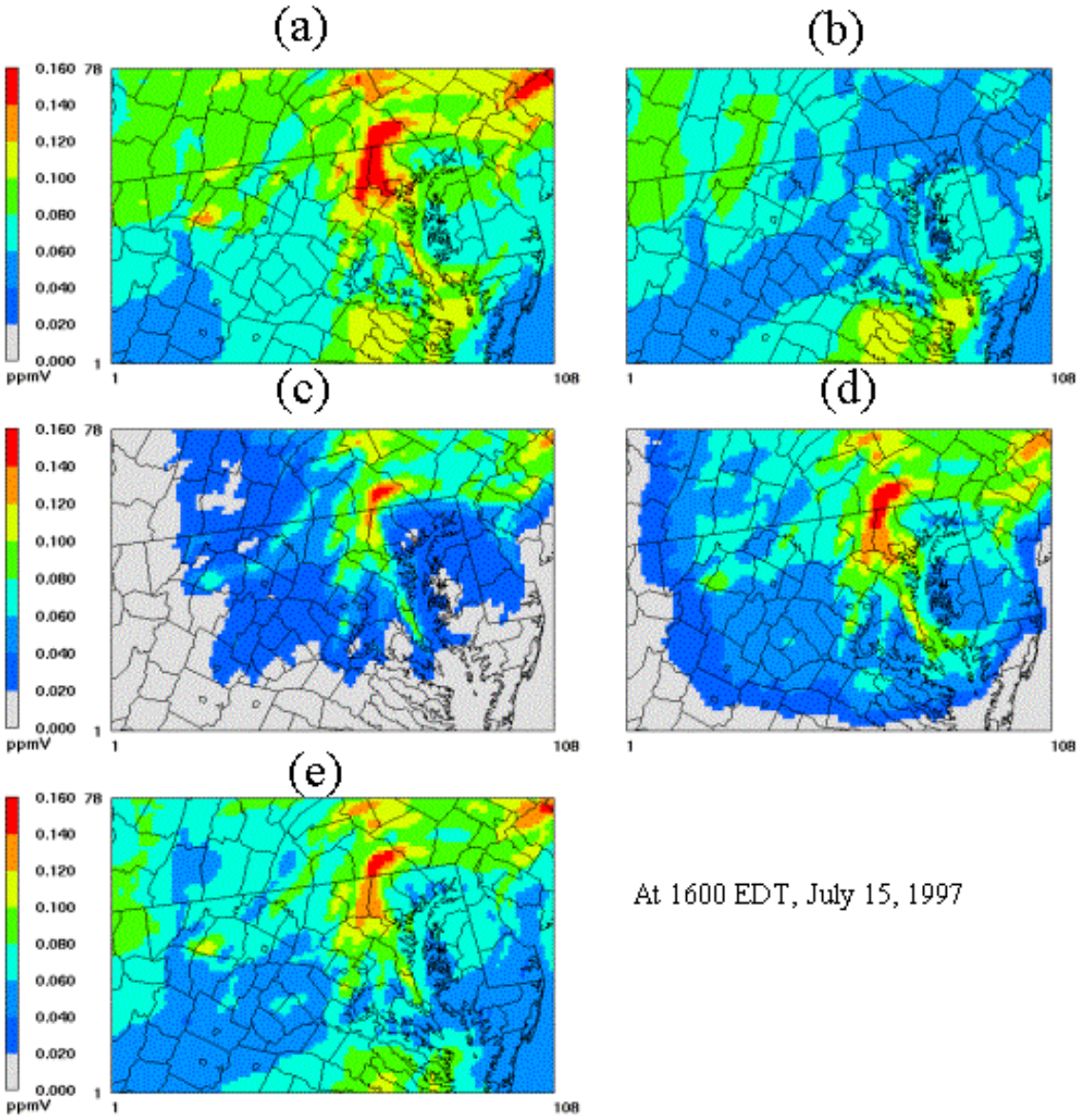

Figure 5.10: Surface ozone concentrations at 1600 EDT, July 15, 1997: (a) Base case, (b) NoEmis case, (c) CleanBC case, (d) CleanOZ case, and (e) CleanPRE case.

The remarkable point in these figures is that hot spots, areas with more than 100 ppb of ozone concentration, are seen in all cases but the NoEmis case. For each day, the peak concentration of ozone in the CleanBC case is less than the Base case by 10-20 ppb. In particular, on July 14 more than 120 ppb of ozone along the I-95 corridor connecting Washington D.C. and Baltimore is observed in the CleanBC case, while the NoEmis case shows lower concentration in this area than in the surrounding area. This suggests that local emissions contribute significantly to this high ozone episode in the Baltimore/Washington D. C. ozone non-attainment area. In general, transported pollutants appear to strengthen the intensity of ozone by about 10-20 ppb for the Baltimore/Washington D.C. area.

Figure 5.11 compares the frequency distributions of hourly surface ozone concentrations for the five cases. The CleanBC and the CleanOZ cases show very different characteristics from the other cases. More than half of the simulated grid hours show ozone concentrations less than 20 ppb. As shown in Figures 5.7 through 5.10, this results from effect of the boundary conditions on the grid cells near the boundaries. The NoEmis case and the CleanPRE case show a similar distribution with slightly increased occurrences of high ozone. As indicated earlier, transported pollutants seem to play a role, enhancing ozone by about 40-70 ppb in this area.

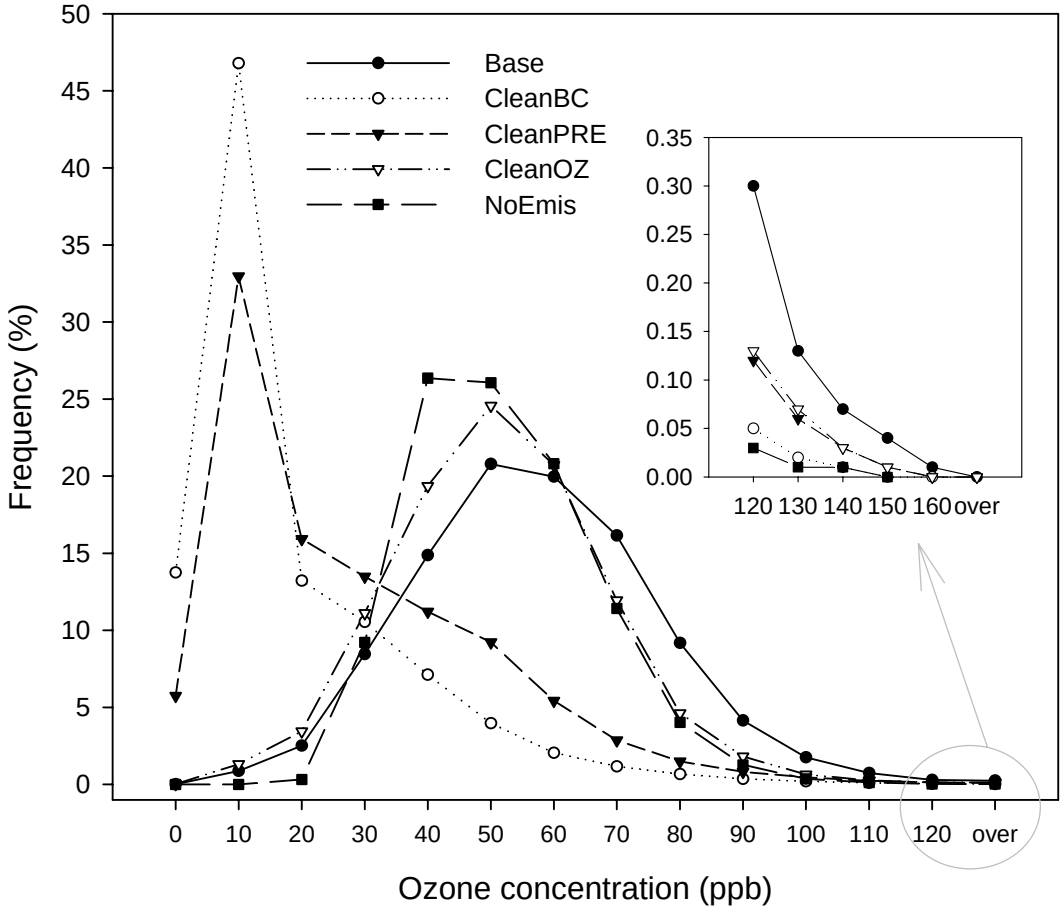

Figure 5.11: Comparison of frequency distributions of hourly surface ozone concentrations between July 8 and July 20, 1997, based on all grids in the modeling domain for the Base, the CleanBC, the CleanOZ, the CleanPRE, and NoEmis cases.

In summary, local emissions are mainly responsible for the 1 hour ozone standard exceedance in Baltimore/Washington D.C. area, while the long-range transport of ozone and/or precursors are most likely to contribute to the 8 hr ozone standard exceedance by adding to local emissions, leading to the occurrence of elevated concentrations over a wider area.

5.4.3 Investigation of the contribution of biogenic vs. anthropogenic VOC to local ozone production

Most NOx emissions are from combustion-related sources such as motor vehicles and fossil-fueled power plants in urban and suburban areas. On the other hand, VOCs are emitted from a wide variety of sources, both anthropogenic and biogenic. In the United States, it is estimated that the total amount of reactive VOC emissions from biogenic sources is approximately 1.4 times greater than emissions from anthropogenic VOC when it is averaged by land use over the continental US (Solomon et al., 2000). However, there are large variations of this ratio on a region-to region basis. According to the study by Guenther et al. (2000), over 98% of total biogenic VOCs in North America are from vegetation, and isoprene, with high ozone forming potential, accounts for 35% of the total VOCs emitted from vegetation.

In this section, we compare the relative contribution of anthropogenic VOC emissions versus biogenic VOC emissions to local ozone production. Figures 5.12 and 5.13 are the surface ozone distribution from the model at 1600 EDT, on July 13 and July 14, 1997. Compared to the CleanBC case with both anthropogenic and

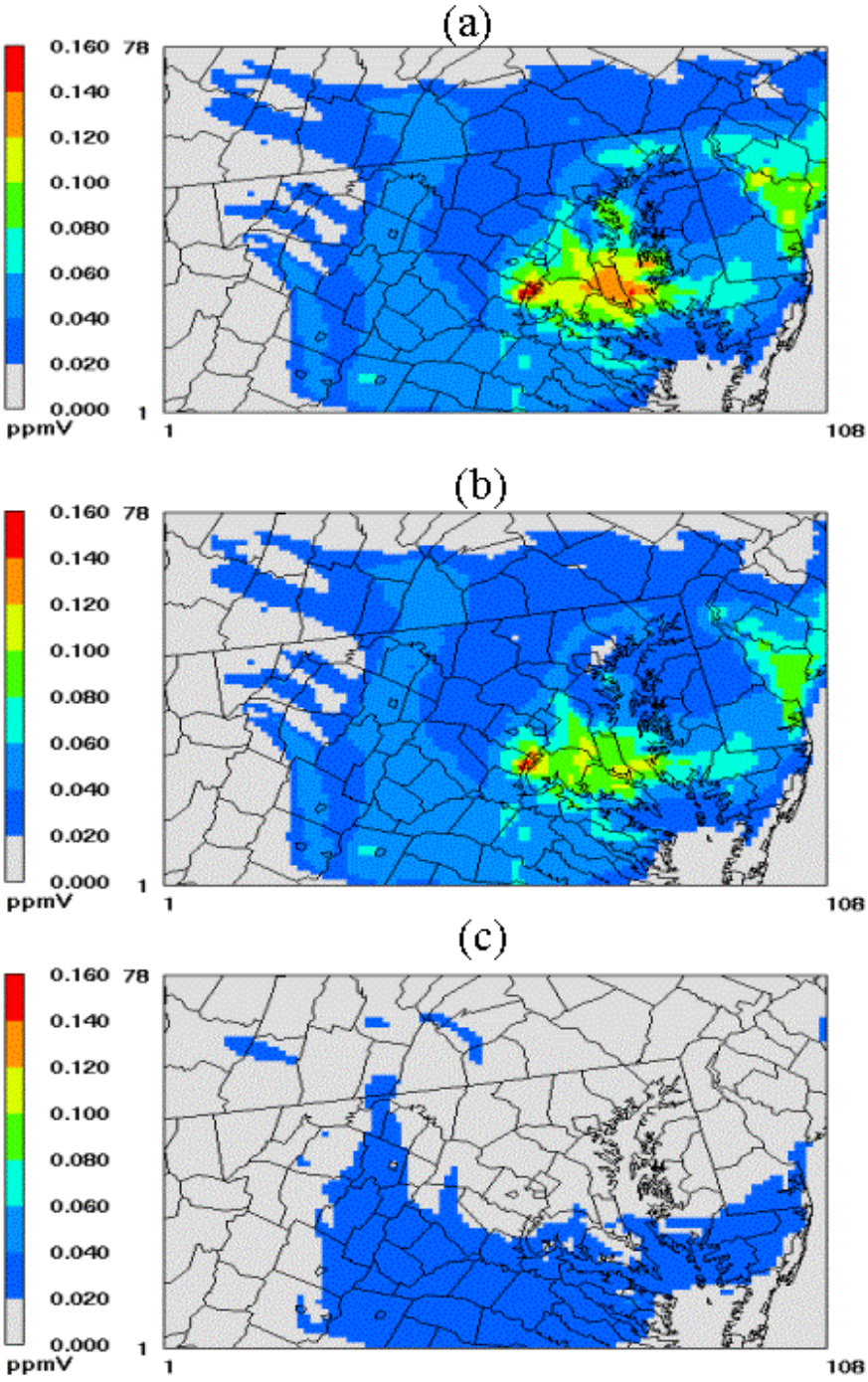

Figure 5.12: Surface ozone concentrations at 1600 EDT, July 13, 1997: (a) CleanBC case, (b) woAVOC case, and (c) woBVOC case.

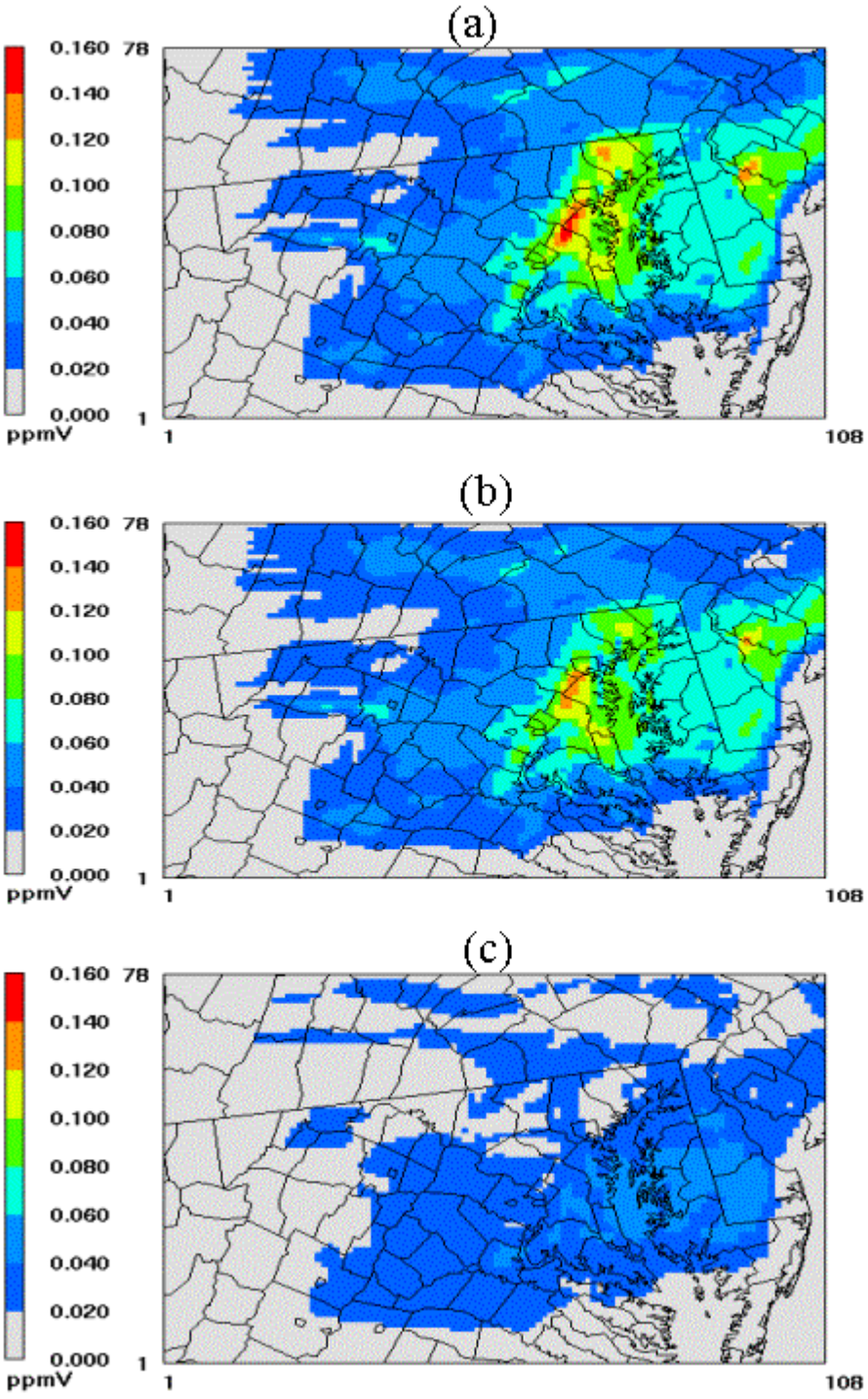

Figure 5.13: Surface ozone concentrations at 1600 EDT, July 14, 1997: (a) CleanBC case, (b) woAVOC case, and (c) woBVOC case.

biogenic emissions, the woAVOC case, which includes biogenic VOC emissions and not anthropogenic VOC emissions, displays a similar distribution of surface ozone. On the other hand, the woBVOC case, which has anthropogenic VOC emissions but not biogenic VOC emissions, shows a nearly homogeneous distribution of ozone below 60 ppb over the domain, except for the grid cells near the boundary. Moreover, the frequency distribution of surface ozone concentration shown in Figure 5.14 exhibits the same consequences. Hence, the results suggest that biogenic VOC emissions play a critical role in formation of local ozone in Baltimore/Washington D.C. region. These results are also in agreement with findings from observation-based analyses for the Baltimore area by Morales-Morales (1998) and in Chapter 3 of this dissertation.

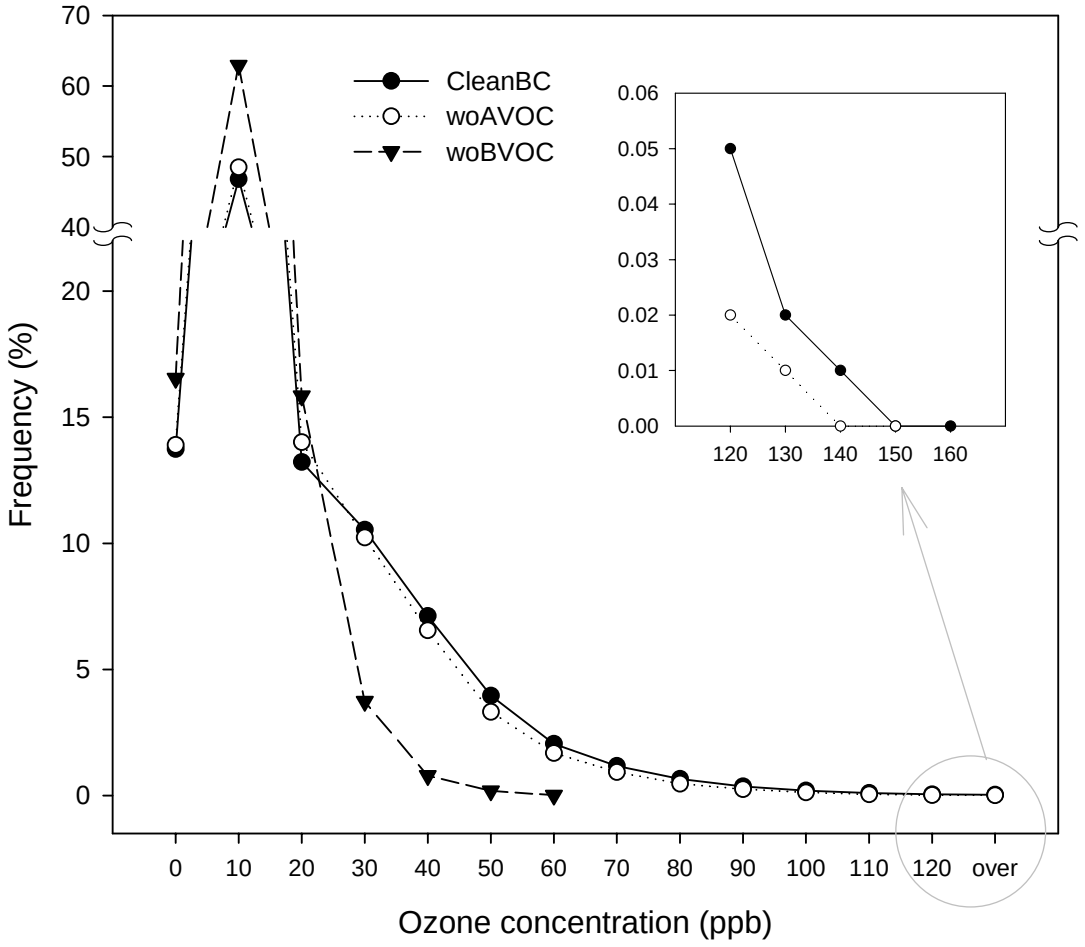

Figure 5.14: Comparison of frequency distribution of hourly surface ozone concentrations between July 8 and July 20, 1997, based on all grids in the modeling domain for the CleanBC, the woAVOC, and woBVOC cases.

5.4.4 Application of control scenarios

Three control scenarios were simulated: 50% anthropogenic NOx reduction (Half_Anox), 50% anthropogenic VOC reduction (Half_Avoc), and 50% anthropogenic NOx and VOC reduction (Half_Anox_Avoc) with the same boundary conditions as the Base case. Two additional scenarios with 50% reduction of ozone in the boundary conditions were performed. One was with normal emissions (HalfozBC_baseEMI), and the other was with 50% anthropogenic NOx reduction (HalfozBC_halfAnox).

The frequency distribution of ozone concentrations for the five control scenarios and the base case are compared in Figure 5.15. While the Half_Avoc case and the Base case show approximately the same distribution of ozone concentrations, the Half_Anox case and the Half_Anox_Avoc case show a similar pattern. Figures 5.16 and 5.17, which give the ozone distribution at selected times during the episode, show the same trend of ozone concentrations as was seen in the frequency comparison. These results suggest that anthropogenic NOx emissions control in the domain is more likely to lead to alleviation of high ozone occurrences, in contrast to anthropogenic VOC emissions control that rarely affects ozone reduction. As mentioned in the previous section, the contribution of transport is not negligible. When local NOx reduction accompanying reduced transport of ozone was simulated, we could observe improved results as indicated in Figures 5.16 and 5.17.

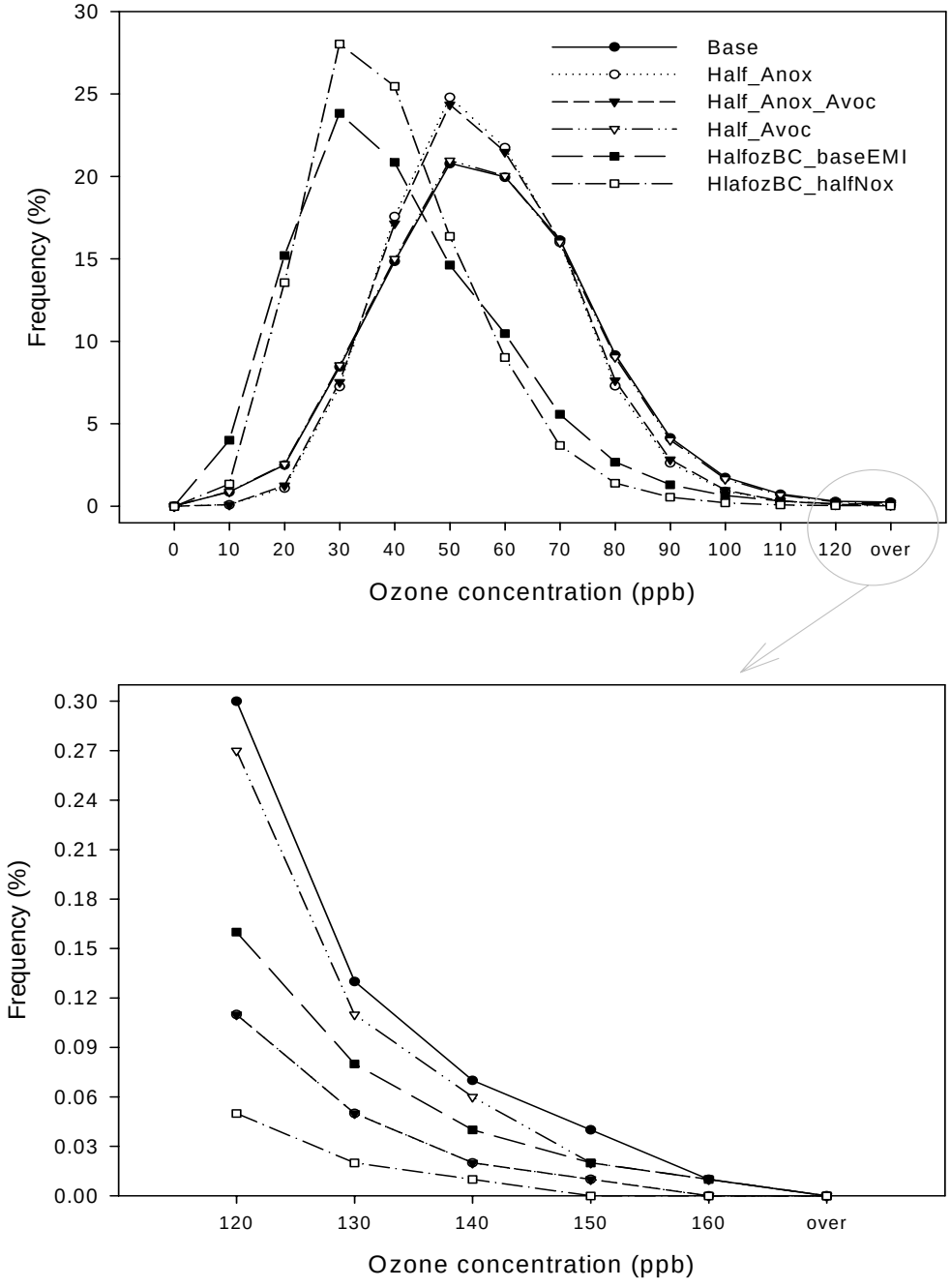

Figure 5.15: Comparison of frequency distribution of hourly surface ozone concentrations between July 8 and July 20, 1997, based on all grids in the modeling domain for the Base, Half_Anox, the Half_Anox_Avoc, the Half_Avoc, the HalfozBC_baseEMI, and the HalfozBC_halfAnox cases.

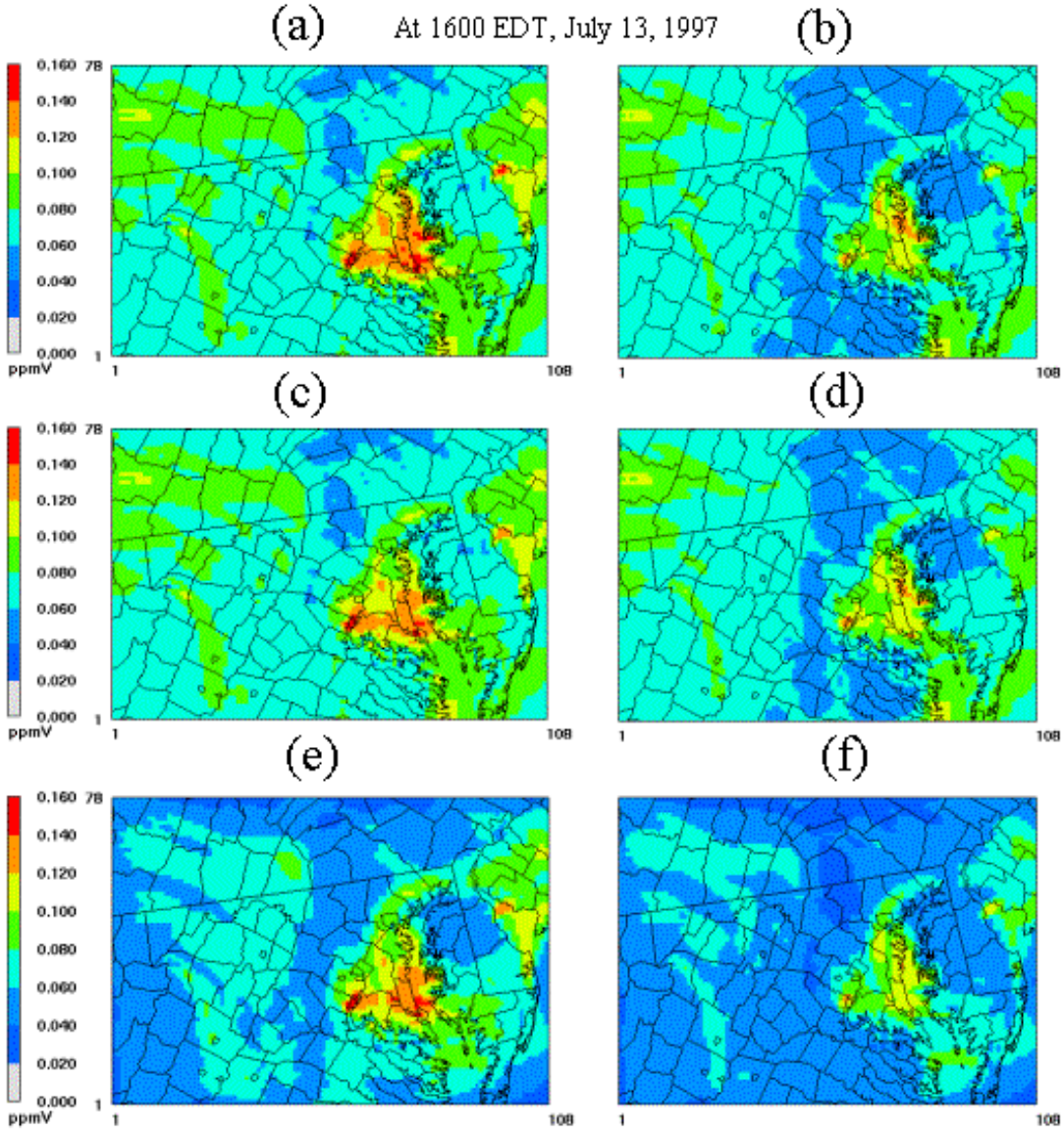

Figure 5.16: Surface ozone concentrations at 1600 EDT, July 13, 1997: (a) Base case, (b) Half_Anox case, (c) Half_Avoc case, (d) Half_Anox_Avoc case, (e) HalfozBC_baseEMI case, and (f) HalfozBC_halfAnox case.

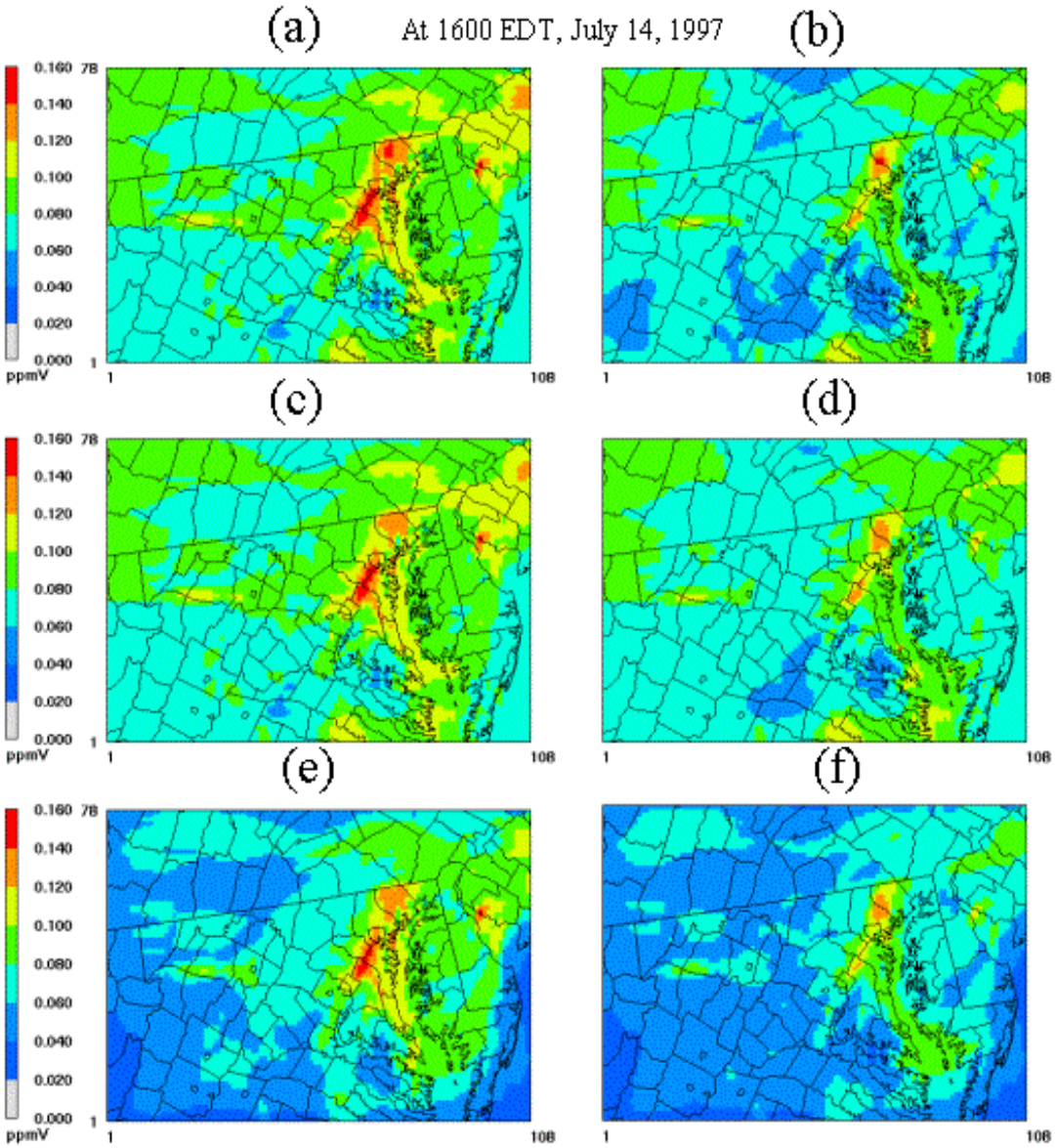

Figure 5.17: Surface ozone concentrations at 1600 EDT, July 14, 1997: (a) Base case, (b) Half_Anox case, (c) Half_Avoc case, (d) Half_Anox_Avoc case, (e) HalfozBC_baseEMI case, and (f) HalfozBC_halfAnox case.

5.5 Summary and conclusions

Photochemical simulations were performed of an ozone event in July 1997 to investigate both the relative contribution of long-range transport versus local emissions, and the relative impact of biogenic VOC emissions versus anthropogenic VOC emissions on local ozone production. Even though the simulations were limited to a single ozone event, the synoptic weather pattern was typical of high ozone occurrences. Therefore, the conclusions drawn from these simulations are more general.

From the first set of simulations, it appears that transported pollutants may be responsible for 20-90 ppb of ozone concentration in the domain, displaying a decreasing contribution as they pass through the Baltimore/Washington D.C. ozone non-attainment area. Simulations without including long-range transport of pollutants show a significant contribution of local emissions to high ozone occurrences in this region. Hence, the results imply that local emissions are mainly responsible for 1 hour ozone standard exceedances in the Baltimore/Washington D.C. area. However, transported ozone and its precursors play an important role in the violation of the 8 hr ozone standard, by adding to the local contribution and resulting in elevated concentrations over a wider area.

In the second set of simulations, the relative contribution of anthropogenic VOC emissions versus biogenic VOC emissions to local ozone production was investigated. The simulations suggest that biogenic VOC emissions in this region are responsible, to a great extent, for local ozone production. This conclusion is similar to

those obtained from observation based studies of the Baltimore area described in Chapter 3.

Finally, three control scenarios were applied to the region: 50% anthropogenic NOx reduction, 50% anthropogenic VOC reduction, 50% anthropogenic NOx and VOC reduction. The results show the potential for NOx emissions reduction for the mitigation of high ozone occurrences around the Baltimore/Washington area. This result supports a significant role for biogenic VOC emissions in ozone formation in this region, identified in the second set of simulations. That is, the role of biogenic VOCs in ozone formation will be limited due to a reduced concentration of NOx. On the other hand, the reduction of only anthropogenic VOCs, which has much less ozone-forming potential than biogenic VOCs, might not be able to effectively limit ozone formation as compared to NOx reduction. In addition, we observed an enhanced reduction when the contribution of ozone transported from outside the modeling domain was reduced, along with the reduction of local NOx emissions.

In conclusion, the simulations show significant roles for both transported and local emissions. Our results suggest controlling NOx emissions locally would be effective in alleviating extremely severe ozone events. However, considering that the 8 hr ozone standard needs to be attained as well, control of only local NOx emissions may not be satisfactory, because of the importance of long-range transport of ozone and its precursors. In the future, several emissions control scenarios for the upwind area outside the domain should be investigated through simulation, in order to determine the degree of ozone reduction that can be achieved through control of transported ozone and its precursors.

Chapter 6: Conclusions and Recommendations

6.1 Summary and conclusions

The Baltimore/Washington area has experienced severe ozone episodes in the past. In order to find a strategy for ozone reduction in a given area, it is essential to understand the complex chemistry between the precursors of ozone, VOC and NOx, to identify the role of biogenic VOC in local ozone formation, and to identify the impact of long-range transport on the ambient ozone concentration. Hence, three studies of ozone for Baltimore/Washington area were undertaken to identify and evaluate control strategies towards ozone alleviation for effectiveness.

The first study was to investigate sources of VOC emissions in the Baltimore area using highly time resolved measurements, and to investigate possible relationships between each VOC source category and episodes of elevated ozone concentrations. In this work, hourly ambient concentrations of 55 VOC species, measured at the Essex PAMS site in Baltimore County in the state of Maryland during the summer months of 1996 ~ 1999, were analyzed to investigate the relationships between ozone and its natural and anthropogenic precursors using the UNMIX receptor model. Gasoline-related sources such as vehicle exhaust, gasoline vapor, and liquid gasoline accounted for more than half of the total VOC mixing ratio, which is a typical result for VOC in urban/suburban areas in the United States. Natural gas, surface coatings, and biogenic source categories each explained 13, 12 and 11 % of the

total VOC, respectively. Even though the hourly average contribution of biogenic sources in quantity did not appear to be significant, comparisons of diurnal patterns of high-ozone days with those of low-ozone days and rough reactivity-weighted daytime source apportionment results implied that biogenic emissions might contribute considerably to local ozone production for episodes in which the National Air Quality 8-hour standard for ambient ozone was violated at this site.

The second part of this study consisted of an evaluation of an emissions inventory, an essential input to a photochemical air quality model. Emissions inventories significantly affect photochemical model performance, and thus development of effective control strategies. In this study, in order to evaluate a VOC emissions inventory, the ratios of CB-IV VOC groups to NOx or CO, and the ratios of VOC source contributions from a source apportionment technique to NOx or CO were compared with the corresponding ambient ratios at three observation sites located in Maryland, District of Columbia, and New Jersey. Furthermore, a photochemical air quality model was introduced to compare ratios of CB-IV VOC groups to NOx or CO, and the absolute concentrations of CB-IV VOC groups with the same ratios and concentrations from observations.

The comparisons of ETH(ethene)/NOx ratio, XYL(xylenes)/NOx ratio, ETH and XYL concentrations between estimates and measurements showed some differences, depending on the comparison approach, at the MD and DC sites. On the other hand, the consistent results at the NJ site were observed, implying a possible overestimation of vehicle exhaust. However, in the case of TOL(toluenes), which are emitted mainly from solvent sources, the ratios of TOL to NOx or CO as well as the

absolute concentrations revealed an overestimate of solvent sources by a factor of 1.5 to 3 at the three sites. In addition, the overestimate of solvent sources agreed with the comparisons of solvent source contributions relative to NOx from a source apportionment technique to the corresponding value of estimates at the MD site. Other researchers have also proposed the overestimation of solvent sources, implying a possibility of inaccurate emission factors in estimating VOC emissions from solvent sources.

The photochemical model simulations with 50% reduction of solvent VOC emissions did not show a perceptible change in ozone concentrations, possibly because this region is NOx-sensitive, or because the solvent chemical species do not readily form ozone. However, a noticeable decrease of secondary organic aerosol (SOA) concentrations with 50% solvent emissions reduction was observed.

The last part of this dissertation was to develop an effective control strategy for the Baltimore/Washington ozone non-attainment area, which requires an understanding of the relative impact of long-range transport of ozone and precursors versus local emissions on ozone events, and the contribution of biogenic VOC emissions to ozone production during ozone events in the area. In this study, ozone simulations for the Baltimore/Washington ozone non-attainment area were performed in order to investigate both the relative contribution of long-range transport versus local emissions to an ozone event which occurred in July 1997, to identify the relative impact of biogenic VOC emissions versus anthropogenic VOC emissions on local ozone production, and finally to test a possible control strategy for this area.

The simulation results showed that long-range transport of ozone was responsible for 20-90 ppb of ozone concentration in the state of Maryland, Northern Virginia, and D.C. area, displaying a decreasing contribution as it passed through the Baltimore/Washington D.C. area. Local emissions contributed considerably to high ozone occurrences in the Baltimore/Washington D.C. ozone non-attainment area. In particular, the contribution of biogenic VOC emissions in this region was responsible for the local ozone production to a great extent, which was consistent with the past studies based on observations for the Baltimore area including a result from the first part of my study. Accordingly, the results suggested that NOx emissions reduction rather than VOC emissions reduction might mitigate high ozone occurrences in the Baltimore/Washington ozone non-attainment area, and it was confirmed through several simulations with emissions reductions. However, our results suggested that a control of only local NOx emissions might not be sufficient to comply with the 8 hr ozone standard because of the importance of long-range transport of ozone and its precursors.

In conclusion, both observational-based and emissions-based air quality modeling studies consistently suggested a significant role of biogenic VOC emissions in high ozone formation over the Baltimore/Washington region. Also, control of anthropogenic NOx emissions may possibly lead to a decrease in high ozone occurrences.

6.2 Recommendations for future work

In this study, we employed a receptor model, UNMIX, to analyze observations and to induce meaningful conclusions from the analyses. As mentioned in the Chapter 3, in addition to the UNMIX receptor model, there are several receptor models such as PMF and Chemical Mass Balance (CMB) 8, recently refined and developed. In particular, it is important to obtain reliable results for topics related to policy-making, based on scientific findings and analyses. For that reason, we recommend introducing other well-evaluated receptor models to analyze the same observations in future.

In addition, the analysis here was limited to a single sampling site. However, there are a couple of observation stations with high time resolution around the study domain, and we can apply the same analysis approach to the observations. Since the stations are not close to each other, we can get some insight into atmospheric conditions over the sampling sites, and compare the characteristics between sites. Considering that the meteorological information such as wind speeds and wind directions are usually available at the sampling sites, we may be able to identify possible connections between emission source categories at upwind observation areas and those at downwind observation areas.

When it comes to air quality modeling studies, the simulations were based on a multi-day ozone episode and the synoptic weather during the episode followed a pattern typical of high ozone formation. Therefore, the transport from outside the region and biogenic emissions, which are highly dependent on meteorological parameters, and significant factors during high ozone occurrences over this region,

may not be considerably different from ozone episode to episode. However, the conclusions we drew in this study will be more reliable if simulations for other ozone episodes over this area are performed, and similar results are obtained. Hence, we recommend gathering reliable inputs into the modeling system and observations for evaluations for other ozone episodes, and following the same practice.

Appendix 1: CB-IV representations of PAMS 55 hydrocarbons

	ALD2	ETH	FORM	ISOP	OLE	PAR	TOL	XYL	NR
ethane						0.4			1.6
ethene		1							
propane						3			
propene					1	1			
i-butane						4			
butane						4			
acetylene						1			1
t-2-butane	2								
1-butene					1	2			
c-2-butane	2								
cyclopentane						5			
isopentane						5			
pentane						5			
t-2-pentene	2					1			
1-pentene					1	3			
c-2-pentene	2					1			
2,2-dimethylbutane						6			
2,3-dimethrylbutane						6			
2-methylpentane						6			
3-methylpentane						6			
isoprene				1					
2-methyl-1-pentene					1	4			
hexane						6			
methylcyclopentane						6			
2,4-dimethylpentane						7			
benzene						1			5
cyclohexane						6			
2-methylhexane						7			
2,3-dimethylpentane						7			
3-methylhexane						7			
2,2,4-trimethylpentane						8			
heptane						7			
methylcyclohexane						7			
2,3,4-trimethylpentane						8			
toluene							1		
2-methylheptane						8			
3-methylheptane						8			
octane						8			
ethylbenzene						1	1		
m&p-xylene								1	
styrene					1	1			5
o-xylene								1	
nonane						9			
isopropylbenzene						2	1		
propylbenzene						2	1		

	ALD2	ETH	FORM	ISOP	OLE	PAR	TOL	XYL	NR
1-ethyl-3-methylbenzene						1		1	
1-ethyl-4-methylbenzene						1		1	
1,3,5-trimethylbenzene						1		1	
1-ethyl-2-methylbenzene						1		1	
1,2,4-trimethylbenzene						1		1	
decane						10			
1,2,3-trimethylbenzene						1		1	
m-diethylbenzene						2		1	
p-diethylbenzene						2		1	
undecane						11			

Appendix 2: Source compositions (mass fraction) and apportionment results using UNMIX

A. Essex site, MD for 1996 summer measurements

Estimated source category	Source 1 Liquid gasoline	Source 2 Surface coatings	Source 3 biogenic	Source 4 Natural gas	Source 5 Vehicle exhaust	Source 6 Gasoline vapor
Species						
Ethane	0.0295	0.0086	0.0313	**0.1584**	**0.0628**	0.0295
Ethylene	0.0221	0.0117	0.0150	0.0187	**0.0723**	0.0200
Propane	**0.0856**	0.0193	0.0230	**0.1261**	**0.0719**	0.0006
Propylene	0.0136	0.0078	0.0086	0.0117	0.0372	0.0077
Acetylene	0.0013	0.0075	0.0215	0.0149	0.0467	0.0104
n-butane	0.0169	0.0047	0.0288	**0.0509**	0.0324	0.0209
iso-butane	0.0178	0.0040	0.0057	0.0323	0.0244	0.0089
n-pentane	**0.2794**	0.0048	0.0162	0.0227	0.0277	0.0189
iso-pentane	0.0715	0.0487	0.0534	0.0943	**0.0590**	**0.0932**
3-methylpentane	0.0149	-0.0004	0.0055	0.0149	0.0156	0.0166
n-hexane	0.0209	-0.0018	0.0026	0.0166	0.0129	0.0240
Isoprene	0.0051	0.0026	**0.2115**	0.0001	0.0026	0.0015
3-methylhexane	0.0094	0.0014	0.0073	0.0075	0.0086	0.0164
2,2,4-trimethylpentane	0.0102	-0.0014	0.0004	0.0110	0.0271	0.0261
2,3,4-trimethylpentane	0.0047	-0.0004	-0.0034	0.0042	0.0119	0.0108
Methylcyclopentane	0.0090	-0.0002	0.0019	0.0082	0.0084	0.0115
2-methylhexane	0.0078	-0.0016	0.0053	0.0057	0.0062	0.0133
2,3-dimethylbutane	0.0062	0.0005	0.0076	0.0095	0.0111	0.0089
2-methylpentane	0.0244	-0.0007	0.0078	0.0251	0.0275	0.0260
2,3-dimethylpentane	0.0048	-0.0000	-0.0038	0.0046	0.0116	0.0096
M&p xylene	0.0263	0.0126	0.0053	0.0162	0.0228	**0.0531**
Benzene	0.0169	0.0036	0.0114	0.0139	0.0305	0.0168
Toluene	**0.0573**	0.0120	0.0590	0.0427	**0.0556**	**0.0851**
o-xylene	0.0080	0.0042	0.0055	0.0068	0.0087	0.0175
1,2,4-trimethylbenzene	0.0176	**0.5004**	0.0034	0.0102	0.0284	0.0112
Total NMOC(ppbc)	10.3	8.9	11.3	40.4	38.7	57.6
% of total NMOC	6	5	7	24	23	34

B. Essex site, MD for 1997 summer measurements

Estimated source category	Source 1 Liquid gasoline	Source 2 biogenic	Source 3 Surface coatings	Source 4 Natural gas	Source 5 Vehicle exhaust	Source 6 Gasoline vapor
Species						
Ethane	0.0397	0.0434	0.0007	**0.2138**	**0.0542**	0.0267
Ethylene	0.0213	0.0194	0.0080	0.0109	**0.0553**	0.0247
Propane	**0.0636**	0.0382	-0.0046	**0.2344**	0.0408	0.0013
Propylene	0.0129	0.0116	0.0022	0.0171	0.0270	0.0089
Acetylene	0.0056	0.0115	0.0009	0.0089	0.0284	0.0091
n-butane	0.0077	0.0333	0.0248	**0.0674**	0.0163	0.0275
iso-butane	0.0090	0.0066	0.0074	0.0492	0.0168	0.0135
n-pentane	**0.3366**	0.0175	0.0127	0.0198	0.0223	0.0223
iso-pentane	**0.0521**	0.0495	**0.0607**	0.0472	**0.0610**	**0.1007**
3-methylpentane	0.0066	0.0082	0.0115	0.0055	0.0169	0.0213
n-hexane	0.0097	0.0107	0.0162	0.0130	0.0225	0.0261
Isoprene	0.0024	**0.1582**	0.0011	-0.0026	0.0032	0.0023
3-methylhexane	0.0055	0.0097	0.0106	0.0050	0.0128	0.0164
2,2,4-trimethylpentane	0.0038	0.0112	0.0210	-0.0031	0.0241	0.0348
2,3,4-trimethylpentane	0.0025	0.0028	0.0086	-0.0014	0.0106	0.0140
Methylcyclopentane	0.0040	0.0045	0.0080	0.0037	0.0102	0.0130
2-methylhexane	0.0042	0.0060	0.0086	0.0019	0.0108	0.0139
2,3-dimethylbutane	0.0030	0.0082	0.0062	0.0052	0.0087	0.0114
2-methylpentane	0.0102	0.0130	0.0187	0.0082	0.0255	0.0337
M&p xylene	0.0170	0.0097	**0.1671**	0.0022	0.0334	0.0278
Benzene	0.0092	0.0141	0.0081	0.0101	0.0268	0.0172
Toluene	0.0197	0.0317	**0.0808**	0.0439	**0.0658**	**0.0919**
Ethylbenzene	0.0054	0.0059	0.0495	0.0015	0.0108	0.0081
o-xylene	0.0086	0.0059	0.0466	0.0016	0.0139	0.0116
1,2,3-trimethylbenzene	0.0115	0.0142	0.0063	0.0105	0.0089	0.0074
Total NMOC(ppbc)	7.9	13.2	12.2	20.0	47.1	41.2
% of total NMOC	6	9	9	14	33	29

Bold values indicate mass fractions > 0.05.

C. Essex site, MD for 1998 summer measurements

Estimated source category Species	Source 1 biogenic	Source 2 Liquid gasoline	Source 3 Natural gas	Source 4 Gasoline vapor	Source 5 Vehicle exhaust
Ethane	0.0309	**0.0574**	**0.2293**	**0.0554**	0.0168
Ethylene	0.0142	0.0228	0.0143	0.0247	**0.0517**
Propane	0.0240	**0.0853**	**0.1842**	0.0133	0.0411
Propylene	0.0092	0.0128	0.0126	0.0092	0.0258
Acetylene	0.0194	0.0083	0.0108	0.0136	0.0253
n-butane	0.0359	0.0296	0.0483	0.0380	0.0185
iso-butane	0.0137	0.0188	0.0461	0.0166	0.0172
n-pentane	0.0175	**0.1903**	0.0175	0.0158	0.0186
iso-pentane	**0.0690**	**0.0910**	0.0330	**0.1189**	0.0483
3-methylpentane	0.0087	0.0163	0.0052	0.0231	0.0142
n-hexane	0.0045	0.0202	0.0074	0.0244	0.0166
Isoprene	**0.1899**	0.0017	0.0009	-0.0007	0.0026
3-methylhexane	0.0046	0.0102	0.0044	0.0148	0.0126
2,2,4-trimethylpentane	0.0094	0.0120	-0.0049	0.0357	0.0196
2,3,4-trimethylpentane	0.0030	0.0054	-0.0026	0.0146	0.0086
Methylcyclopentane	0.0038	0.0096	0.0033	0.0128	0.0086
2-methylhexane	0.0025	0.0085	0.0016	0.0127	0.0103
2,3-dimethylbutane	0.0108	0.0077	0.0037	0.0135	0.0072
2-methylpentane	0.0156	0.0258	0.0078	0.0371	0.0221
M&p xylene	-0.0076	0.0239	0.0176	0.0374	**0.0515**
Benzene	0.0103	0.0145	0.0128	0.0174	0.0240
Toluene	0.0288	**0.0594**	0.0205	**0.0882**	**0.0747**
Ethylbenzene	0.0016	0.0.079	0.0064	0.0119	0.0163
o-xylene	0.0009	0.0094	0.0048	0.0147	0.0184
1,2,4-trimethylbenzene	-0.0075	0.0129	0.0026	0.0145	0.0180
Total NMOC(ppbc)	10.6	12.5	19.2	33.0	33.2
% of total NMOC	10	12	18	30	31

Bold values indicate mass fractions > 0.05.

D. McMillan reservoir, DC for 1997 summer measurements

Estimated source category	Source 1 Unidentified	Source 2 Unidentified	Source 3 Natural gas	Source 4 Diesel exhaust	Source 5 Gasoline (Vehicle exhaust & evaporization)
Species					
Acetylene	0.0124	0.0131	0.0072	**0.0836**	0.0127
Ethylene	-0.0145	0.0037	0.0173	**0.1748**	0.0437
Ethane	-0.0172	**0.1179**	**0.3109**	**0.0835**	0.0295
Propylene	0.0069	-0.0054	0.0149	**0.0543**	0.0253
Propane	0.0086	**0.0541**	**0.1946**	0.0137	0.0251
iso-butane	-0.0072	0.0248	**0.0569**	0.0171	0.0215
n-butane	0.0453	0.0347	**0.0834**	0.0237	0.0294
iso-pentane	0.3419	0.0284	**0.1757**	**0.0972**	**0.0736**
n-pentane	**0.0707**	0.0120	**0.0534**	0.0339	0.0262
Isoprene	**0.4340**	0.0009	-0.0116	0.0058	0.0015
2,3-dimethylbutane	0.0167	0.0035	0.0124	0.0157	0.0111
2-methylpentane	**0.0240**	0.0080	0.0279	0.0358	0.0296
3-methylpentane	0.0156	0.0065	0.0158	0.0205	0.0191
n-hexane	-0.0001	0.0176	0.0019	0.0010	0.0203
Benzene	0.0071	0.0106	-0.0054	0.0246	0.0301
3-methylhexane	-0.0018	0.0097	-0.0055	-0.0008	0.0145
2,2,4-trimethylpentane	0.0014	0.0157	-0.0084	0.0280	0.0365
2,3,4-trimethylpentane	-0.0005	0.0059	-0.0054	0.0129	0.0158
Toluene	0.0319	**0.0594**	0.0199	**0.0657**	**0.0931**
Ethylbenzene	0.0109	0.0145	-0.0020	0.0084	0.0149
M&p xylene	0.0187	0.0437	-0.0076	0.0313	0.0479
o-xylene	0.0108	0.0169	-0.0031	0.0137	0.0185
1,2,4-trimethylbenzene	-0.0004	0.0220	-0.0047	0.0381	0.0174
n-decane	-0.0009	**0.0854**	-0.0028	-0.0063	0.0025
Total NMOC(ppbc)	4.4	9.4	14.5	9.4	47.9
% of total NMOC	5	11	17	11	56

Bold values indicate mass fractions > 0.05.

E. Camden, NJ for 1997 summer measurements

Estimated source category	Source 1 Unidentified	Source 2 Unidentified	Source 3 Biogenic	Source 4 Refinery	Source 5 Natural gas	Source 6 Vehicle exhaust	Source 7 Gasoline vapor
Species							
Acetylene	-0.0008	0.0013	0.0028	0.0018	0.0012	0.0221	-0.0030
Ethylene	0.0059	0.0136	0.0145	0.0110	0.0038	0.0482	0.0162
Ethane	0.0165	0.0435	0.030	0.0281	**0.0649**	**0.0890**	-0.0061
Propylene	0.0151	0.0058	-0.0030	**0.2443**	0.0077	0.0099	0.0033
Propane	**0.0811**	0.0462	0.0094	**0.1225**	**0.2260**	0.0430	-0.0338
iso-butane	0.0487	0.0096	0.0127	0.0447	**0.0879**	0.0254	-0.0225
n-butane	**0.0996**	0.0002	0.0078	**0.2032**	**0.1839**	0.0052	-0.0104
iso-pentane	-0.0667	**0.0677**	0.0292	**0.0860**	**0.1063**	**0.0812**	**0.0808**
n-pentane	-0.0784	0.0431	0.0139	0.0222	**0.0914**	0.0323	0.0065
Isoprene	-0.0032	-0.0012	**0.0754**	-0.0015	-0.0002	-0.0008	0.0001
Cyclopentane	**0.1649**	0.0000	-0.0001	-0.0003	-0.0007	-0.0000	0.0002
2-methylpentane	0.0217	-0.0063	0.0077	0.0225	0.0178	0.0265	0.0429
3-methylpentane	-0.0035	0.0161	0.0046	0.0076	0.0150	0.0136	0.0266
n-hexane	0.0290	0.0160	0.0042	0.0119	0.0261	0.0181	0.0250
Methylcyclopentane	0.0109	0.0029	-0.0015	0.0077	0.0109	0.0104	0.0131
Benzene	0.0136	0.0275	0.0086	0.0439	0.0047	0.0182	0.0195
2-methylhexane	0.0180	0.0082	0.0017	0.0052	0.0044	0.0046	0.0342
3-methylhexane	0.0336	0.0110	-0.0014	0.0028	0.0035	-0.0027	**0.0685**
2,2,4-trimethylpentane	0.0104	0.0114	0.0117	0.0096	0.0043	0.0290	0.0272
Toluene	0.0306	**0.0580**	0.0180	0.0128	0.0086	**0.0873**	**0.0683**
M&p xylene	0.0141	0.0238	0.0001	0.0102	0.0054	0.0499	0.0339
Isopropylbenzene	-0.0035	**0.1244**	-0.0002	-0.0002	0.0002	-0.0003	0.0000
1,2,3-trimethylbenzene	0.0005	0.0053	-0.0011	0.0011	0.0015	0.0149	0.0035
Total NMOC(ppbc)	5.0	5.7	21.3	16.9	60.4	39.8	25.3
% of total NMOC	3	3	12	10	35	23	15

Bold values indicate mass fractions > 0.05.

Bibliography

Anderson, M. J., Daly E. P., Miller, S. L., Milford, J. B., Source apportionment of exposures to volatile organic compound: II. Application of receptor models to TEAM study area. Atmospheric Environment 36, 3643-3658, 2002.

Andronache, C., Chameides, W., Rodgers, M., Martinez, J., Zimmerman, P., Greenberg, J., Vertical distribution of isoprene in the lower boundary layer of the rural and urban southern United States. Journal of Geophysical Research 99,16989-16999, 1994.

Aneja, V. P., Mathur, R., Arya, S. P., Li, Y., Murray, G. C., Manuszak, T. L., Coupling the vertical distribution of ozone in the atmospheric boundary layer. Environmental Science and Technology 34, 2324-2329, 2000.

Apndis, S. N., Harley, R. A., Cass, G. R., Seinfeld, J. H., Secondary aerosol formation and transport. Atmospheric Environment 26A, 2269-2282, 1992.

Arunachalam, S., Adelman, Z., Mathur, R., Olerud, D., Holland A., A comparison of Models3/CMAQ and MAQSIP modeling system for ozone modeling in North Carolina. 94th Annual meting of the Air and Waste Management Association, Orlando, Florida. Paper #989, 2001.

Atkinson, R., Atmospheric chemistry of VOCs and NOx. Atmospheric Environment 34, 2063-2101, 2000.

Baumann, K., Williams, E.J., Angevine, W.M., Roberts, J. M., Norton, R. B., Frost, G. J., Fehsenfeld, F. C., Springston, S. R., Bertman, S. B., Hartsell, B., Ozone production and transport near Nashville, Tennessee: Results from the 1994 study at New Hendersonville. Journal of Geophysical Research 105, 9137-9153, 2000.

Billford, P.D.E., Meeker, G. O., A factor analysis model of large scale pollution. Atmospheric Environment 1, 147-157, 1967.

Bowman, F. M., Pilinis, C., Seinfeld, J. H., Ozone and aerosol productivity of reactive organics. Atmospheric Environment 29, 579-589, 1995.

Cardelino, C. A., Chameides, W. L., An observation-based model for analyzing ozone precursor relationships in the urban atmosphere. Journal of Air & Waste Management Association 45, 161-180, 1995.

Cardelino, C. A., Chameides, W. L., The application of data from photochemical assessment monitoring stations to the observation-based model. Atmospheric Environment 34, 2325-2332, 2000.

Carter, W. P., Development of ozone reactivity scales for volatile organic compounds. Journal of Air and Waste Management Association 44, 881-899, 1994.

Carter, W.P.L., Documentation on the SAPRC-99 chemical mechanism for VOC reactivity assessment. Final Report to California Air Resources Board Contract No. 92-329 and 95-308, 2000.

Chameides, W. L., Lindsay, R. W., Richardson, J., Kiang, C. S., The role of biogenic hydrocarbons in urban photochemical smog: Atlanta as a case study. Science 241, 1473-1475, 1988.

Chameides, W. L., Fehsenfekd, D., Rodgers, M. O., Cardelino, C., Martinez, J., Parrish, D., Lonneman, W., Lawson, D. R., Ramussen, R. A., Zimmerman, P., Greenberg, J., Middleton, P., Wang, T., Ozone precursor relationships in the ambient atmosphere. Journal of Geophysical Research 97, 6037-6055, 1992.

Chen, L. W. A., Doddridge, B. G., Dickerson, R. R., Chow, J. C., Henry, R. C., Origins of fine aerosol mass in the Baltimore-Washington corridor: implications from observation, factor analysis, and ensemble air parcel back trajectories. Atmospheric Environment 36, 4541-4554, 2002.

Ching, J. K., Byun, D. W., Science algorithms of the EPA Models-3 Community multiscale Air Quality (CMAQ) modeling system.; U.S. EPA; Office of Research and Development; Washington D. C., EPA-600/R-99/030, 1999.

Choi, Y., Ehrman, S. H., Investigation of sources of volatile organic carbon in the Baltimore area using highly time resolved measurements. Atmospheric Environment 38, 775-791, 2004.

Cooter, E. J., Hutzell, W. T., A regional atmospheric fate and transport model for Atrazine. 1. Development and implementation. Environmental Science & Technology 36, 4091-4098, 2002.

Dennis, R. L, Byun, D. W., Nocak J. H., Galluppi, K. J., Coats, C. J., The next generation of integrated air quality modeling: EPA's models-3. Atmospheric Environment 30, 1925-1938, 1996.

Demerjian, K. L., A review of national monitoring networks in North America. Atmospheric Environment 34, 1861-1884, 2000.

Department of Energy (DOE) Document, Historical natural gas annual 1930 through 2000. DOE/EIS-E-0110(00), 2001.

Derwent, R. G., Middleton, D. R., Field, R. A., Goldstone, M. E., Lester, J. N., Perry, R., Analysis and interpretation of air quality data from an urban roadside location in central London over the period from July 1991 to July 1992. Atmospheric Environment 29, 923-946, 1995.

Derwent, R. G., Jenkin, M. E., Saunders, S. M., Pilling, M. J., Photochemical ozone creation potentials for organic compounds in Northwest Europe calculated with a master chemical mechanism. Atmospheric Environment 32, 2429-2441, 1998.

Dillon, W. R., Goldstein, M., Multivariate analysis, John Wiley & Sons Inc., 1984.

DNREC home page, http://www.dnrec.state.de.us. 2001

Dolwick, P., Jang, C., Possiel, N., Timin, B., Gipson, G. L., Godowitch, J., Summary of results from a series of Models-3/CMAQ simulations of ozone in the Western United States. Proceedings of the 94th Annual Meeting of the Air and Waste Management Association, Orlando, FL, June 24-28, 2001. Paper #957, 2001.

Elkins, J. B., Hemby J., Rao V., Mintz D., National air quality and emissions trends report, 1999. 94th Annual meting of the Air and Waste Management Association, Orlando, Florida. Paper #466, 2000.

EPA Document I, Technical Assistance Document (TAD) for Sampling and Analysis of Ozone Precursors. EPA/600-R-98/161, 1998.

EPA Document II, Evaluating emissions factors, models, and inventories with PAMS data. EPA-454/R-96-006, 1996.

EPA Document III, Science algorithms of the EPA Models-3 Community Multi-scale Air Quality (CMAQ) modeling system. EPA/600/R-99/030, 1999.

EPA Document IV, Technical assistance document for sampling and analysis of ozone precursors. EPA/600-R-98/161, 1998.

EPA Document V, Guideline for regulatory applications of the Urban Airshed Model. EPA-450/4-91-013, 1991.

Finlayson-Pitts, B. J., Pitts, J. N., Upper and lower atmosphere. Academic press, 2000.

Fiore, A., Holloway T., Hastings, M. G., A global perspective on air quality. EM December, 13-22, 2003.

Fujita, E. M., Croes, B. E., Bennerr C. L., Lawson, D. R., Comparison of emissions inventory and ambient concentration ratios of CO, NMOG, and NOx in California's south coast air basin. Journal of Air & Waste Management Association 42, 264-276, 1992.

Fujita, E. M., Watson, J. G., Chow, J. C., Lu, Z., Validation of the chemical mass balance receptor model applied to hydrocarbon source apportionment in the Southern California air quality study. Environmental Science and Technology 28, 1633-1649, 1994.

Fujita, E. M., Waston, J. G., Chow, J. C., Magliano, K. L., Receptor model and emissions inventory source apportionments of nonmethane organic gases in California's San Joaquin valley and San Francisco bay area. Atmospheric Environment 29, 3019-3035, 1995.

Fujita, E. M., Hydrocarbon source apportionment for the 1996 Paso del Norte ozone study. The Science of the Total Environment 276, 171-184, 2001.

Funk, T. H., Chinkin, L. R., Roberts, P. T., Saeger, M., Mulligan, S., Paramo Figueroa, V. H., Yarbrough, J., Compilations and evaluation of a Paso del Norte emission inventory. The Science of the Total Environment 276, 135-151, 2001.

Geron, C. D., Nie, D., Arnts, R. R., Sharkey, T. D., Singsaas, E. L., Vanderveer, P. J., Guenther, A., Sickles II, J. E., Kleindienst, T. E., Biogenic isoprene emissions: Model evaluatin in a southeastern Unites States bottomland deciduous forest. Journal of Geophysical Research 102, 18889-18901, 1997.

Gery, M.W.,m Whitten, G. Z., Killus, J. P., Dodge, M.C., A photochemical kinetics mechanism for urban and regional scale computer modeling. Journal of Geophysical Research, 94, 12925-12956, 1989.

Goldstein, A. H., Goulden, M. L., Munger, J. W., Wofsy, S. C., Geron, C. D., Seasonal course of isoprene emissions from a midlatitude deciduous forest. Journal of Geophysical Research 103, 31045-31056, 1998.

Guentehr, A., Geron, C., Pierce, T., Lamb, B., Harley, P., Fall, R., Natural emissions of non-methane volatile organic compounds, carbon monoxide, and oxides of nitrogen from North America. Atmospheric Environment 34, 2205-2230, 2000.

Haagen-Smit, A. J., Fox, M. M., Photochemical ozone formation with hydrocarbons and automobile exhaust. Journal of Air Pollution Control Association 4, 105-109, 1954.

Hanna, S.R., Moore, G.E., Fernau, M. E., Evaluation of photochemical grid models (UAM-IV, UAM-V, and the ROM/UAM-IV couple) using data from the Lake Michigan Ozone Study (LMOS). Atmospheric Environment 30, 3265-3279, 1996.

Hanna, S. R., Chang, J.C., Fernau, M.E., Monte Carlo estimates of uncertainties in predictions by photochemical grid model (UAM-IV) due to uncertainties in input variables. Atmospheric Environment 32, 3619-3628, 1998.

Harley, R. A., Hannlgan, M. P., Cass, G. R., Respeciation of organic gas emissions and detection of excess unburned gasoline in the atmosphere. Environmental Science & Technology 26, 2395-2408, 1992.

Henry, R. C., UNMIX version 2.4 Manual, 2001.

Henry, R. C., Multivariate receptor modeling by N-dimensional edge. Submitted to Journal of Chemometrics and Intelligent laboratory Systems, 2002..

Hidy, G. M., Ozone process insights from field experiments Part I: Overview. Atmospheric Environment 34, 2001-2022, 2000.

Hopke, P. K., Receptor modeling for air quality management, Elsevier Science Publishing Company Inc., 1991.

Houyoux, M.R., Vukovich, J. M., Coats, C. J., Emission inventory development and processing for the Seasonal Model for Regional Air Quality (SMRAQ) project. Journal of Geophysical Research 105, 9079-9090, 2000.

Irwin, J. S., A historical look at the development of regulatory air quality models. EM January, 22-29, 2003.

Isidorov, V., Jdanova, M., Volatile organic compounds from leaves litter. Chemosphere 48, 978-979, 2002.

Jacobson, M. Z., Fundamentals of Atmospheric Modeling, Cambridge University Press, 1999.

Jacobson, M. Z., Atmospheric pollution, Cambridge University Press., 2002.

Jenkin, M. E., Clemitshaw, K. C., Ozone and other secondary photochemical pollutants: Chemical processes governing their formation in the planetary boundary layer. Atmospheric Environment 34, 2499-2527, 2000.

Jonson, J. E., Sundet, J. K., Tarrason, L., Model calculations of present and future levels of ozone and ozone precursors with a global and a regional model. Atmospheric Environment 35, 525-537, 2001.

Jimenez, P, Baldasano, J. M., Dabdub, D., Comparison of photochemical mechanisms for air quality modeling. Atmospheric Environment 37, 4179-4194, 2003.

Jonson, J. E., Sundet, J. K., Tarrason, L., Model calculations of present and future levels of ozone and ozone precursors with a global and a regional model. Atmospheric Environment 35, 525-537, 2001.

Kavouras, I. G., Koutrakis, P., Tsapakis, M., Lagoudki, E., Stephanou, E. G., Baer, D. V., Oyola, P., Source apportionment of urban particulate aliphatic and polynuclear aromatic hydrocarbons (PAHs) using multivariate methods. Environmental Science and Technology 35, 2288-2294, 2001.

Kenski, D. M., Wadden, R. A., Scheff, P. A., Lonneman, W. A., Receptor modeling approach to VOC emissions inventory validation. Journal of Environmental Engineering 121, 483-491, 1995.

Kuhlwein, J., Wickert, B., Trukenmuller, A., Theloke, J., Friedrich, R., Emission-modeling in high spatial and temporal resolution and calculation of pollutant concentrations for comparisons with measured concentrations. Atmospheric Environment 36, S7-S18, 2002.

Kumar, N., Russell A. G., Multiscale air quality modeling of the northeastern United States Atmospheric Environment 30, 1099-1116, 1996.

Kumar, A. V., Patil, R. S., Nambi, K. S. V., Source apportionment of suspended particulate matter at two traffic junctions in Mumbia, India. Atmospheric Environment 35, 4245-4251, 2001.

LADCO report I, Comparison of ambient and emissions VOC and NOx data in the Lake Michigan region. (Available at http://www.ladco.org), 1998.

Lawrimore, J. H., Aneja, V. P., A chemical mass balance analyses of nonmethane hydrocarbon emissions in North Carolina. Chemosphere 35, 2751-2765, 1997.

Lewis, C. W., Henry, R. C., Shreffler, J. H., An exploratory look at hydrocarbon data from the photochemical assessment monitoring stations network. Journal of Air and Waste management Association 48, 71-76, 1998.

Mannschreck, K., Klemp, D., Kley, D., Friedrich, R., Huhlwein, J., Wickert, B., Matuska, P., Habram, M., Slemr, F., Evaluation of an emission inventory by comparisons of modeled and measured emission ratios of individual HCs, CO and NOx. Atmospheric Environment 36, S81-S94, 2002.

McKeen, S. A., Hsie, E. Y., Liu, S. C., A study of the dependence of rural ozone on ozone precursors in the Eastern United States. Journal of Geophysical Research 96, 15377-15394, 1991.

McNair, L. A., Harley, R. A., Russell, A. G., Spatial inhomogeneity in pollutant concentrations, and their implications for air quality model evaluation. Atmospheric environment 30, 4291-4301, 1996.

Milford, J. B., Gao D., Sillman S., Blossy P., Russell A.G., Total reactive nitrogen (NO_y) as an indicator of the sensitivity of ozone to reductions in hydrocarbon and NO_x emissions. Journal of Geophysical Research 99, 3533-3542, 1994.

Miller, M. S., Friedlander, S. K., Hidy, G. M., A chemical element balance for the Pasadena aerosol. Journal of Colloid and Interface Science 39, 165-176, 1972.

Miller, S. L., Anderson, M. J., Daly, E. P., Milford, J. B., Source apportionment of exposures to volatile organic compounds. I. Evaluation of receptor models using simulated exposure data. Atmospheric Environment 36, 3629-3641, 2002.

Miller, S. L., Anderson, M. J., Daly, E. P., Milford, J. B., Source apportionment of exposures to volatile organic compounds. II. Application of receptor models to REAM study data. Atmospheric Environment 36, 3643-3658, 2002.

Morales-Morales, R., Carbon monoxide, ozone, and hydrocarbons in the Baltimore metropolitan area. Ph.D. Thesis, University of Maryland, College Park, MD, USA, 1998.

Mukund, R., Kelly, T. J., Spicer, C. W., Source attribution of ambient air toxic and other VOCs in Columbus, Ohio. Atmospheric Environment 30, 3457-3470, 1996.

Na, K., Kim, Y. P., Moon, K. C., Diurnal characteristics of volatile organic compounds in the Seoul atmosphere. Atmospheric Environment 37, 733-742, 2003.

National Research Council (NRC), Rethinking the ozone problem in urban and regional air pollution. National Academy Press. Washington D.C., 1991.

NESCAUM, 1997 summer ozone season in the NESCAUM region. (http://www.nescaum.org/pdf/o3rpt_8a.PDF), 1998.

Parrish, D. D., Trainer, M., Young, V., Goldan, P. D., Kuster, W. C., Jobson, B. T., Fehsenfeld, F. C., Lonneman, W. A., Zika, R. D., Farmer, C. T., Riemer, D. D., Rodgers, M. O., Internal consistency tests for evaluation of measurements of anthropogenic hydrocarbons in the troposphere. Journal of Geophysical Research 103, 22339-22359, 1998.

Parrish, D. D., Fehsenfeld, F. C., Methods for gas-phase measurements of ozone, ozone precursors and aerosol precursors. Atmospheric Environment 34, 1921-1957, 2000.

Pierce, T., Geron, C., Bender, L., Dennis, R., Tonnesen, G., Guenther, A., Influence of increased isoprene emissions on regional ozone modeling. Journal of Geophysical Research 103, 25611-25629, 1998.

Placet, M., Mann, C. O., Gilbert, R. O., Niefer, M. J., Emissions of ozone precursors from stationary source: a critical review. Atmospheric Environment 34, 2183-2204, 2000.

Poirot, R. L., Wishinski, P. R., Hopke, P. K., Polissar, A.V., Comparative application of multiple receptor methods to identify aerosol sources in Northern Vermont. Environmental Science and Technology 35, 4622-4636, 2001.

Possiel, N.C., Cox, W. M., The relative effectiveness of NO_x and VOC strategies in reducing northeast US ozone concentrations. Water, Air and Soil Pollution 67, 161-179, 1993.

Rappengluck, B., Fabian, P., Kalabokas, P., Viras, L. G., Ziomas, I. C., Quasi-continuous measurements of non-methane hydrocarbons (NMHC) in the greater Athens area during MEDCAPHOT-TRACE. Atmospheric Environment 32, 2103-2121, 1998.

Roselle, S. J., Pierce, T. E., Schere, K. L., The sensitivity of regional ozone modeling to biogenic hydrocarbons. Journal of Geophysical Research 96, 7371-7394, 1991.

Roselle S. J., Schere K. L., Modeled response of photochemical oxidants to systematic reductions in anthropogenic volatile organic compound and NO_x emissions. Journal of Geophysical Research 100, 22929-22941, 1995.

Russell, A., Dennis, R., NARSTO critical review of photochemical models and modeling. Atmospheric Environment 34, 2283-2324, 2000.

Ryan, W. F., Doddridge, B. G., Dickerson, R. R., Morales, R. M., Hallock, K. A., Roberts, R. T., Blumenthal, D. L., Anderson, J.A., Civerolo, K. L., Pollutant transport during a regional O3 episode in the Mid-Atlantic States. Journal of Air and Waste Management Association 48, 786-797, 1998.

Ryan, W. F., Piety C. A., Luebehusen, E. D., Air quality forecasts in the mid-Atlantic region: Current practice and benchmark skill. Weather and Forecasting 15, 46-60, 2000.

Samson, P. J., Shi, B., A meteorological investigation of high ozone values in American cities. Report prepared for the United States Congress, Office of Technology assessment. Washington, D. C. : U.S. Government Printing Office, 1988.

Scheff, P. A., Wadden, R. A., Kenski, D. M., Chung, J., Receptor model evaluation of the southeast Michigan ozone study ambient NMOC measurements. Journal of Air and Waste Management Association 46, 1048-1057, 1996.

Seinfeld, J., Pandis, S. N., Atmospheric Chemistry and Physics, John Wiley & Sons, Inc., 1998.

Sillman, S., The relation between ozone, NO(x) and hydrocarbons in urban and polluted rural environments. Atmospheric Environment 33, 1821-1845, 1999.

Sistla, G., Hao W., Ku J., Kallos G., An operational evaluation of two regional scale ozone air quality modeling systems over the eastern United States. Bulletin of the American Meteorological Society 82, 945-964, 2001.

Sistla, G., Ku, M., Hao, W., An assessment of an MM5 simulation of July 6 to 19, 1997, in the Eastern United States. New York Department of Environment Conservation. (Available at http://www.otcair.org), 2002.

Slemr, F., Baumbach, G., Blank, P., Corsmeier, U., Fiedler, F., Fridrich, R., Habram, M., Kalthoff, N., Klemp, D., Kuhlwein, J., Mannschreck, K., Mollmann-coers, M., Nester, K., Pannitz, H.-J., Rabl, P., Slemr, J., Vogt, U., Wickert, B., Evaluation of modeled spatially and temporarily highly resolved emission inventories of photosmog precursors for the city of Augsburg: The experiment EVA and its major results. Journal of Atmospheric Chemistry 42, 207-233, 2002.

Smith, J.H., Durrenberger, P.E., Garrett, C., Control strategy modeling for the Huston-Galveston ozone nonattainment area. 94th Annual meeting of the Air and Waste Management Association, Orlando, Florida. Paper #987, 2001.

Solomon, P., Cowling, E., Hidy, G., Furiness, C., Comparison of scientific findings from major ozone field studies in North America and Europe. Atmospheric Environment 34, 1885-1920, 2000.

Stockwell, W. R., Middleton, P., Chnag, J.S., The second generation regional acid deposition model chemical mechanism for regional air quality modeling. Journal of Geophysical Research, 95, 16343-16367, 1990.

Stoeckenius, T., Jimenez, M., Reconciliation of an emissions inventory with PAMS ambient monitoring data in the Mid-Atlantic region: Final Report prepared for MARAMA, ENVIRON International corporation. 2000. (Available at http://www.marama.org/report), 2000.

Thurston, G. D., Spengler, J. D., A Quantitative assessment of source contributions to inhalable particulate matter pollution in metropolitan Boston. Atmospheric Environment 19, 9-25, 1985.

Trainer, M., Parrish, D.D., Goldan, P.D., Roberts, J., Fehsenfeld, F.C., Review of observation-based analysis of the regional factors influencing ozone concentrations. Atmospheric Environment 34, 2045-2061, 2000.

UCAR MM5 home page, http://www.mmm.ucar.edu/mm5/mm5-home.html, 2003.

Vega, E., Mugica, V., Carmona, R., Valencia, E., Hydrocarbon source apportionment in Mexico City using the chemical mass balance receptor model. Atmospheric Environment 34, 4121-4129, 2000.

Wadden, R.A., Scheff, P. A., Uni, I., Receptor modeling of VOCs-II. Development of VOC control functions for ambient ozone. Atmospheric Environment 28, 2507-2521, 1994.

Wallace, J. M., Hobbs, P. V., Atmospheric science, Academic Press, 1977.

Watson, J. G., Chow, J. C., Fujita, E. M., Review of volatile organic compound source apportionment by chemical mass balance. Atmospheric Environment 35, 1567-1584, 2001.

Wierman, S. S., Will the 8-hr ozone standard finally get off the ground, EM September, 20-28, 2003.

Winner, D. A., Cass, G. R., Effect of emissions control on the long-term frequency distribution of regional ozone concentrations. Environmental Science & Technology. 34, 2612-2617

Wu, C. Y., Pratt, G. C., 2002. UNMIX modeling assessment of gaseous organic compounds. 95th Annual Meeting, Baltimore, MD. Air and Waste Management association, Pittsburgh, PA, 2000.

Yarwood, G., Stoeckeninus, T. E., Heiken, J. G., Dunker, A. M., Modeling weekday/weekend ozone differences in the Los Angeles region for 1997. Journal of Air and Waste Management Association 53, 864-875, 2003.

Zhang, D., Zheng, W., Diurnal cycles of surface winds and temperature as simulated by five boundary layer parameterizations. Journal of Applied Meteorology 43, 157-169, 2004.

Zhang, J., Rao, S. T., The role of vertical mixing in the temporal evolution of ground-level ozone concentrations. Journal of Applied meteorology 38, 1674-1691, 1999.